Expression of Pea3 Transcription Factor Genes in Frontonasal and Mandibular Mesenchyme of the Chick Embryo

A Thesis Submitted to the
College of Graduate
Studies and Research in
Partial Fulfilment of the
Requirements for the

Degree of Master of Science

in the

Department of Anatomy
and Cell Biology
University of
Saskatchewan
Saskatoon, Saskatchewan

Lindsay Diane Jacobi

PERMISSION TO USE

In presenting this thesis in partial fulfillment of the requirements for a Postgraduate degree from the University of Saskatchewan, I agree that the Libraries of this University may make it freely available for inspection. I further agree that permission for copying of this thesis/dissertation in any manner, in whole or in part, for scholarly purposes may be granted by the professor or professors who supervised my thesis work or, in their absence, by the Head of the Department or the Dean of the College in which my thesis work was done. It is understood that any copying or publication or use of this thesis or parts thereof for financial gain shall not be allowed without my written permission. It is also understood that due recognition shall be given to me and to the University of Saskatchewan in any scholarly use which may be made of any material in my thesis/dissertation.

DISCLAIMER

Reference in this thesis/dissertation to any specific commercial products, process, or service by trade name, trademark, manufacturer, or otherwise, does not constitute or imply its endorsement, recommendation, or favoring by the University of Saskatchewan. The views and opinions of the author expressed herein do not state or reflect those of the University of Saskatchewan, and shall not be used for advertising or product endorsement purposes.

Requests for permission to copy or to make other uses of materials in this thesis/dissertation in whole or part should be addressed to:

Head of the Department of Anatomy & Cell Biology
University of Saskatchewan, Saskatoon, Saskatchewan
Canada S7N 5E5

OR

Dean of the College of Graduate Studies and Research
University of Saskatchewan, Saskatoon, Saskatchewan
S7N 5A2 Canada

ABSTRACT

Fibroblast growth factors (FGFs) play an essential role in development and patterning of the vertebrate embryo. Despite extensive literature documenting the diverse roles of FGF signalling during craniofacial development, comparatively little is known about the specific downstream effectors through which FGFs influence gene expression. A previous study in our laboratory reported exogenous FGF elicited differential chondrogenic responses in frontonasal and mandibular mesenchyme (Bobick et al., 2007). Pea3 transcription factors are crucial components of the downstream effector pathway through which FGFs influence gene expression (Raible and Brand, 2001). Therefore, the purpose of my research was to examine whether differences in *pea3*, *erm*, and *er81* gene expression profiles underlie the distinct responses of the frontonasal and mandibular mesenchyme cells to FGF.

The present study demonstrates that FGF2 treatment differentially affects chondrogenesis in micromass cultures of frontonasal and mandibular mesenchyme isolated from stage 24/25 chick embryos. Whereas FGF2 inhibited chondrogenesis in frontonasal mesenchyme cultures, it had no effect on micromass cultures of mandibular mesenchyme. RT-qPCR and RNA dot blot analyses demonstrated that mRNA transcripts for the *pea3*, *erm*, and *er81* genes are expressed by mesenchyme cells of both frontonasal and mandibular processes of stage 24/25 and stage 28/29 chick embryos. In addition, western blot data demonstrated expression of the Pea3 and Er81 proteins in micromass and explant cultures of stage 24/25 frontonasal and mandibular mesenchyme.

The expression profiles of Pea3 genes were similar between the frontonasal and mandibular facial primordia prior to treatment with exogenous FGF2. However, these expression profiles were differentially altered in response to FGF2 exposure in both explant and micromass cultures. Specifically, whereas FGF2 treatment upregulated *pea3* mRNA levels in explants of frontonasal mesenchyme, it had no effect on *pea3* expression in mandibular explants. In micromass cultures, exogenous FGF2 elevated levels of *pea3 transcripts* in both frontonasal and mandibular mesenchyme. However, FGF2 treatment elevated *er81* expression in frontonasal, but not mandibular mesenchyme. Conversely, exogenous FGF2 elevated *erm* mRNA levels in mandibular, but not frontonasal mesenchyme.

Micromass cultures of mandibular mesenchyme from stage 28/29 chick embryos exhibited significantly lower levels of *pea3* expression than cultures of stage 24/25 mandibular mesenchyme. This stage-dependent change correlated with a reduction in the ability of the mandibular cells to undergo spontaneous chondrogenic differentiation in micromass culture. In contrast, no stage-dependent changes in *pea3* expression were observed in frontonasal mesenchyme cultures.

Collectively, my data indicate that the expression profiles of *pea3*, *erm*, and *er81* in frontonasal and mandibular mesenchyme become distinct only after exposure to exogenous FGF. This raises the possibility that the differences in Pea3 transcription factor expression patterns that arise in response to FGF stimuli may subsequently lead to distinct chondrogenic responses in the two facial mesenchyme populations.

ACKNOWLEDGEMENTS

I would like to thank my supervisors, Dr. William Kulyk and Dr. Nick Ovsenek, for sharing their knowledge and ideas with me. It has been a long journey. Your patience and guidance have been invaluable. Thank you, thank you, thank you.

I am also grateful for the advice, encouragement, and expertise offered from my committee members, Dr. David Cooper and Dr. Pat Krone, throughout my studies.

The College of Medicine, the Department of Anatomy and Cell Biology, and the provincial government along with and University of Saskatchewan through the Saskatchewan Innovation and Opportunity Scholarship program have supported me, and this research, through scholarships and bursaries.

To the many, many people who work (and play) in the Department of Anatomy & Cell Biology, a heartfelt thank you. Your smiles, friendship, and support have been welcome companions on my journey.

To my lab-mate (and favourite engineer), Chris Little: Sincere thanks for taking the time to explain all things mathematical. Your ability to smile and laugh in spite of the chaos and confusion that is so often science is a gift. Thanks for sharing it with me!

To my family (Lesley, Damien & Léandre, Clinton & Carlene, Marshall, and Wyatt, Allie & Nash): Thank you for caring enough about me to care about my research. Love you all long time! xxx

To Virgílio: It has been a such long and arduous journey. Thanks for sticking it out it with me. I needed your reminding to never lose sight of the forest for the trees. Everyday. xxx

Finally, to my parents, Mary and Ken Jacobi: Thanks for fostering my curiosity and nurturing my love of learning. You have always been offering unwavering support and encouragement, believing in me even when I didn't. I will always be grateful. Love and Thanks. xxx

TABLE OF CONTENTS

LIST OF TABLES

LIST OF FIGURES

LIST OF ABBREVIATIONS

AER	apical ectodermal ridge
BMK1	big map kinase 1
BMP	bone morphogenetic protein
cDNA	complimentary DNA
Cq	quantification cycle
DMEM	Dulbecco's modified Eagle's medium
DMMB	1,9-dimethylmethylene blue
dNTPs	deoxynucleotriphosphates
EGF	epidermal growth factor
Elk-1	Ets-like transcription factor 1
Er81	ETS-related protein 81
Erm	ETS-related molecule
ERK	extracellular signal regulated kinase
ESE-1	epithelial specific ETS-1
ETS	E-Twenty six transcription factors
ETS-DBM	ETS-DNA binding motif
FBS	fetal bovine serum
FGF	fibroblast growth factor
FGFR	fibroblast growth factor receptor
FN	frontonasal
GAG	glycosaminoglycan
Gapdh	glyceraldehyde3-phosphate dehydrogenase
gDNA	genomic DNA
Grb2	growth factor receptor-bound protein 2
HBSS	Hank's buffered saline solution
IGF-1	insulin-like growth factor-1
JNK	c-Jun N-terminal kinase K
LPCR	linear polymerase chain reaction
MAPK	mitogen kinase protein kinase
MAPKK	mitogen activated protein kinase kinase
MAPKKK	mitogen activated protein kinase kinase kinase
MD	mandible
MEK	mitogen activated protein kinase kinase 1/2
MIQE	Minimum Information Required for Publication of Quantitative Real-time PCR experiments
MOPS	3(n-morpholino)propane sulfonic acid
N-Cadherin	neural cadherin
N-CAM	neural cell adhesion molecule
NRT	no reverse transcription control
NTC	no-template control
PBS	phosphate buffered saline
PBST	phosphate buffered saline solution Tween-20
PCR	polymerase chain reaction
Pea3	polyoma enhancer activator 3
PIP2	PLCγ-phosphatidylinositol 4,5-bisphosphate

PKC	protein kinase C
PMSF	phenylmethylsulfonyl fluoride
REST™	relative expression software tool
RNA pol II b	RNA polymerase II b
RQI	relative quality indicator
RT-qPCR	real-time quantitative polymerase chain reaction
SDS	sodium dodecyl sulphate
SHC	src-homology 2 domain containing transforming protein
Shh	sonic hedgehog
STAT1	signal transducer and activator of transcription 1
T_a	annealing temperature
TGFβ	transforming growth factor beta
UDG	uracil-DNA glycosylase
VEGF	vascular angiogenic growth factor
ZPA	zone of polarizing activity

1 INTRODUCTION

1.1 Role of Cartilage in Skeletal Development

The majority of the vertebrate skeleton is derived from hyaline cartilage templates established during the embryonic period. This includes bones of the axial and appendicular skeleton, ribs and sternum, floor of the skull, and some portions of the facial skeleton (Cancedda et al., 1995). Therefore, clarifying mechanisms involved in the regulation of embryonic cartilage tissue formation (chondrogenesis) is crucial for understanding both normal skeletal development and the basis of many congenital skeletal malformations.

The vertebrate skeleton is comprised of cells from three distinct lineages: the somatopluere of the lateral plate mesoderm, the scleratome of the paraxial mesoderm, and the neural crest cells of the neural plate. During embryogenesis mesenchymal chondroprogenitor cells from these distinct lineages migrate to the prospective sites of skeletal elements (Hall and Miyake, 2000). Embryonic cartilage formation is ultimately derived from aggregates, or condensations, of mesenchymal chondroprogenitor cells within these sites. The origin of these mesenchymal chondroprogenitor cells varies within different regions of the body. The somatopleure of the lateral plate mesoderm gives rise to the cartilage templates of the long bones of the appendicular skeleton and sternum. The scleratome of the paraxial mesoderm yields the cartilage precursors of the axial skeleton (vertebrae and ribs), while neural crest cells that emerge from the margins of the neural plate give rise to the cartilaginous templates of the anterior portion of the base of the skull and some facial bones (Olsen et al., 2000).

In most anatomical locations, embryonic cartilage is a transient structure. During skeletogenesis, these transient structures are gradually replaced by bone through a process known as endochondral ossification (Mackie et al., 2008; Mackie et al., 2011; Olsen et al., 2000). However, cartilage persists postnatally in distinct locations including within the growth plate between the epiphyses and diaphyses of long bones where it allows for longitudinal bone growth during childhood/adolescence, and as a thin layer at the articular surfaces of diarthrodal joints (Ross and Pawlina, 2006).

Regardless of the embryonic lineage of the mesenchymal chondroprogenitor cells (mesoderm or neural crest derived) and their anatomical location, formation of the cartilaginous templates required for endochondral ossification proceeds along a common chondrogenic pathway (Lefebvre et al., 2001). Although a number of cell types are required for the step-wise progression of endochondral ossification, the process is ultimately driven by chondrocytes (Mackie et al., 2011).

The following section will summarize critical events in the various stages of cartilage formation. Emphasis will be placed on the early stages of chondrogenic differentiation, although subsequent stages of chondrocyte maturation, hypertrophy, and endochondral ossification will be briefly discussed.

1.2 Stages of Cartilage Differentiation, Chondrocyte Maturation, and Endochondral Ossification

1.2.1 Prechondrogenic mesenchymal condensation

Initiation of embryonic chondrogenesis involves the aggregation, or condensation of chondrogenic mesenchymal precursor cells within future regions of bone formation. The formation of high density, compact cellular aggregates serves to establish the size and position of each cartilage anlage (Goldring and Goldring, 1990). Aggregation also serves to permit crucial cell-cell interactions and signalling events that lead to overt chondrogenic differentiation (Hall and Miyake, 2000).

Initially, a transient extracellular matrix is produced by prechondrogenic mesenchymal cells at the sites of prospective cartilage formation. This transient extracellular matrix regulates both the aggregation and overt differentiation of mesenchymal cells into chondrocytes (Hall and Miyake, 2000). The unique composition of molecules present within the transient extracellular matrix provides insight into cellular progression throughout the distinct stages of chondrogenic differentiation (McAlinden et al., 2005).

In particular, the condensation of prechondrogenic mesenchyme is characterized by expression of type II collagen, the predominant collagen component of cartilage extracellular matrix in both adult and embryonic tissues (Kosher et al., 1986a; Nah et al., 1988). Type II collagen is first synthesized as pro-collagen polypeptides consisting of three identical α1 (II) chains, each of which contains both amino and carboxyl terminal pro-peptide sequences (Ala-Kokko et al., 1995). Within the endoplasmic reticulum, pro-collagen α1 (II) chains assemble into heterotrimers.

Hydroxylation of proline and lysine residues of the α1 (II) chains results in the formation of triple helical pro-collagen molecules which are transported to the golgi apparatus where glycosylation occurs. The triple pro-collagen molecules are then secreted from the cells where the amino and carboxy terminal propeptide sequences are excised. Within the extracellular spaces, the resulting tropocollagen molecules undergo cross linking to form mature type II collagen fibrils (McAlinden et al., 2005). These collagen fibrils, which contain primarily type II collagen but also small amounts of type IX and XI collagens, function to provide tensile strength and assist in the organization of the extracellular matrix (McAlinden et al., 2005).

The gene transcripts of the *col2a1* gene are alternatively spliced, generating two distinct mRNA isoforms, type IIA and IIB pro-collagens. Stages of chondrocyte differentiation are distinguishable on the basis of which type II collagen isoform predominates. Specifically, condensations of mesenchymal chondroprogenitor cells express type IIA pro-collagen mRNA transcripts, whereas expression of type IIB collagen is characteristic of differentiated chondrocytes (Ryan and Sandell, 1990).

Another collagen present within the transient extracellular matrix of aggregating prechondrogenic mesenchyme cells is Type I collagen. Although type I collagen is not present within mature hyaline cartilage extracellular matrix, it is thought to be involved in regulating condensation of prechondrogenic mesenchyme and overt chondrogenic differentiation (Bobick et al., 2009). In immunohistochemical studies of embryonic chick limb mesenchyme micromass cultures, Dessau et al. (1980) demonstrated the extracellular matrix of mesenchymal chondroprogenitor cells is rich in type I collagen prior to overt chondrogenesis (Dessau et al., 1980). Moreover, during condensation of these cells, type I collagen expression increases (DeLise et al., 2000).

In addition to the type II collagen fibrils, a large keratan sulphate/chondroitin sulphate rich proteoglycan known as aggrecan is the second major constituent of the cartilage extracellular matrix (Bobick et al., 2009). The highly sulphated glyscosaminoglycan (GAG) chains of aggrecan are negatively charged, attracting osmotically active cations, which in turn draw large amounts of water into the extracellular matrix. Aggrecan monomers assemble within the extracellular matrix into large aggregates that are non-covalently bound to hyaluronan. Expression of *aggrecan* gene transcripts begins at the onset of condensation of prechondrogenic

mesenchymal cells. Moreover, *aggrecan* expression is almost exclusively limited to cartilage tissue (Sai et al., 1986).

Increased cell-cell contacts during condensation of prechondrogenic mesenchyme are mediated by a number of cell surface adhesion molecules, including neural cadherin (N-cadherin) and neural cell adhesion molecule (N-CAM) (DeLise et al., 2000). N-cadherin is a single-pass transmembrane glycoprotein, whereas N-CAM, belonging to the immunoglobulin superfamily of cell adhesion molecules, is a homophilic calcium-dependent binding protein. Both types of cell adhesion molecules are abundantly expressed at the surfaces of prechondrogenic mesenchymal cells (Oberlender and Tuan, 1994). Using a monoclonal antibody directed against N-cadherin, Oberlender et al. (1994) demonstrated that reduced N-cadherin activity inhibited chondrogenesis in chick limb bud mesenchyme micromass cultures (Oberlender and Tuan, 1994). This chondro-inhibitory effect, however, was time dependent, as the effect of the antibody treatment was only observed during condensation of prechondrogenic mesenchyme (Oberlender and Tuan, 1994). Similarly, Widelitz et al. (1993) demonstrated functional reduction of N-CAM activity inhibits chondrogenesis in chick limb bud mesenchyme micromass cultures (Widelitz et al., 1993). These studies suggest that N-cadherin and N-CAM both function as positive regulators of early stages of chondrogenic differentiation.

Fibronectin and syndecan-3, two additional extracellular matrix macromolecules, have also been implicated in the regulation of condensation of prechondrogenic mesenchyme cells (DeLise et al., 2000). Fibronectin, a large glycoprotein, is secreted into the extracellular space as a dimer composed of two subunits linked by a pair of disulfide bonds within their carboxyl termini. Upon secretion, additional disulfide bonds form between fibronectin dimers creating large stable polymers (DeLise et al., 2000). As chondrogenesis proceeds, *fibronectin* mRNA gene transcripts, like those of type II collagen, undergo alternative gene splicing events to yield numerous isoforms (DeLise et al., 2000). Within the pre-cartilage extracellular matrix, the fibronectin isoform containing the exon EIIIA is abundantly present, in addition to isoforms IIIB and V. Notably, expression of the EIIIA-containing fibronectin isoform ceases upon overt initiation of chondrogenic differentiation (DeLise et al., 2000). The switch in regulation of fibronectin mRNA alternative splicing occurs after the condensation of prechondrogenic mesenchyme, as

antibodies directed against the region encoding the EIIIA exon prevent cellular condensation of prechondrogenic mesenchymal cells *in vitro* (Gehris et al., 1997). This evidence strongly suggests the EIIIA fibronectin isoform is required for the condensation events associated with early stages of chondrogenesis.

Additional evidence suggests that syndecan-3, a transmembrane heparan sulphate proteoglycan is also involved in regulation of condensation events of prechondrogenic mesenchyme (Gould et al., 1995). *In situ* hybridization studies have revealed that condensations of chick limb prechondrogenic mesenchyme express high levels of syndecan-3 (Koyama et al., 1995). Syndecan-3 plays an important role in establishing the boundaries of condensations of prechondrogenic mesenchyme, thereby limiting the size of such condensations (Hall and Miyake, 2000).

Tenascin-C, a large extracellular matrix glycoprotein, is closely associated with syndecan-3 (Hall and Miyake, 2000). During condensation of chondrogenic mesenchymal precursor cells, expression levels of tenascin-C are high. Non-chondrogenic mesenchyme cells situated near such condensations, however, do not express *tenascin*-C (Mackie and Murphy, 1998). Although Tenascin-C is believed to function alongside syndecan-3 to set the boundaries of prechondrogenic mesenchyme condensations (Hall and Miyake, 2000), the exact nature of its involvement remains unclear, as *tenascin-C* knockout mice develop normally (Saga et al., 1992).

Hyaluronan, also called hyaluronic acid, is a large non-sulphated, non-branched glycosaminoglycan consisting of a repeating disaccharide of glucuronic acid and N-acetyl glucosamine (Bastow et al., 2008). In contrast to other glycosaminoglycans, hyaluronan is not covalently linked to a core protein (Laurent and Fraser, 1992). During embryonic development, hyaluronan is abundantly present within the extracellular matrices of migrating and proliferating cells (Knudson and Knudson, 1993). Within the precartilage matrix, Hyaluronan is thought to facilitate migration of prechondrogenic mesenchyme cells (Bastow et al., 2008), and to assist in regulation of condensation initiation by limiting mesenchymal cell-cell interactions through interactions with other matrix molecules and cell surface hyaluronan-binding proteins (Knudson and Knudson, 1993). Specifically, the expression of CD44, a well characterized hyaluronan-binding cell surface receptor, coincides with the condensation events associated with early stages of chondrogenic differentiation (Rousche and Knudson, 2002). As condensation proceeds, extracellular levels of

Hyaluronan decline. In addition, hyaluronidase activity, the enzyme responsible for hyaluronan degradation, increases throughout the condensation process (Kulyk and Kosher, 1987). Importantly, some hyaluronan continues to be produced by differentiating chondrocytes and serves as a scaffold upon which aggrecan monomers align, forming supramolecular complexes in the cartilage extracellular matrix (Laurent and Fraser, 1992).

1.2.2 Initiation of chondrocyte differentiation and cartilage matrix production

The close proximity and intimate cell-cell interactions within the cellular condensations permits the subsequent initiation of overt chondrogenesis (Bobick and Kulyk, 2008). Chondrogenic precursors undergo extensive phenotypic changes, exchanging their stellate, fibroblastic morphology for the more spherical morphology typical of mature chondrocytes (Hoffman et al., 2003). Differentiating chondrocytes within these cellular aggregates then begin to synthesize cartilage specific extracellular matrix molecules, such as collagen type II, IX, and XI (Bobick and Kulyk, 2008). Moreover, the expression patterns of many of the genes involved in the condensation events of early chondrogenesis are dramatically altered.

For example, while type I collagen is abundantly expressed within the extracellular matrices of condensed prechondrogenic mesenchymal cells, its expression ceases at the onset of overt chondrogenic differentiation (DeLise et al., 2000). Moreover, while the predominant collagen within the extracellular matrices of chondroprogenitor cells is collagen type IIA, the onset of overt chondrogenic differentiation is marked by a switch to expression of collagen type IIB (Bobick and Kulyk, 2008). Interestingly, while collagen type IIA is also expressed by certain other embryonic cell types, the expression of type IIB collagen is almost exclusively limited to differentiated chondrocytes (McAlinden et al., 2005). During overt chondrogenic differentiation there is a progressive increase in both type II collagen and aggrecan levels which parallels the progressive increase in extracellular matrix accumulation (Kosher et al., 1986b). The restricted expression of type II collagen and aggrecan in hyaline cartilage enables their routine use as molecular markers of differentiated chondrocytes *in vitro*.

N-cadherin and N-CAM cease to be expressed following overt differentiation of prechondrogenic mesenchyme cells into chondrocytes (Oberlender and Tuan, 1994). Similarly, syndecan-3 is absent from the extracellular matrix of fully

differentiated chondrocytes (Gould et al., 1995) and expression of both tenascin-c and fibronectin isoform EIIIA declines greatly (Mackie and Murphy, 1998). In contrast, low levels of fibronectin IIIB and V isoform expression persist (DeLise et al., 2000).

1.2.3 Chondrocyte maturation and hypertrophy

Within the adult vertebrate skeleton, hyaline cartilage persists only in restricted regions of the body (i.e., articular cartilage at diarthrodal joint surfaces; costal cartilage in the rib cage and nasal septum cartilage). In all other regions, the cartilaginous skeletal elements that were formed during embryogenesis are replaced by bone through the process of endochondral ossification.

This process is initiated within the center of the hyaline cartilage template where the chondrocytes cease proliferating and mature to a stage of terminal differentiation known as hypertrophy, which is characterized by a dramatic increase in chondrocyte diameter and volume (Stanton et al., 2003). Importantly, hypertrophic chondrocytes cease to express type II collagen and instead begin to produce type X collagen, a non-fibrillar collagen comprised of three identical $\alpha 1(X)$ polypeptide chains. Type X collagen is a secretory product unique to hypertrophic chondrocytes and a characteristic molecular marker of hypertrophic cartilage matrix (Poole, 2000). As chondrocytes undergo hypertrophy, their cytoplasmic alkaline phosphatase activity rises dramatically (Mackie et al., 2008) and their extracellular matrix becomes mineralized through hydroxyapatite deposition. Concurrently, the hypertrophic chondrocytes release vascular angiogenic growth factor (VEGF) which stimulates the invasion of blood vessels from surrounding perichondrial tissue. This enables both bone-forming osteoblasts and cartilage-degrading chondroclasts to infiltrate the calcified cartilage matrix. Most of the hypertrophic chondrocytes subsequently die, although some may transform into osteoblast-like cells. The specific mechanism by which hypertrophic chondrocytes die is currently the subject of much debate (Shapiro et al., 2005).

1.2.4 Endochondral Ossification

The process of endochondral ossification, in which the mineralized cartilage tissue is gradually replaced by bone, follows the preceding events. This begins in the primary ossification center located in the middle region of each embryonic cartilage

template. Therein, the chondroclasts that invaded the hypertrophic cartilage tissue proceed to erode much of the mineralized extracellular matrix (Mackie et al., 2008). However, some calcified cartilaginous extracellular matrix persists and serves as a scaffold for the deposition of osteoid by the infiltrating osteoblasts. The type I collagen-rich osteoid matrix is subsequently calcified. The resulting woven bone overlying the calcified cartilage extracellular matrix is subsequently resorbed by osteoclasts, and replaced by mature bone (Mackie et al., 2008; Mackie et al., 2011; Olsen et al., 2000). At later embryonic or early postnatal stages, the sequence of endochondral ossification events begins within secondary ossification centers located at the distal epiphyseal ends of each cartilage template. However, disc-shaped "growth plates" of metabolically active cartilage tissue remain situated between the primary and secondary ossification centers at both ends of the developing long bone. The processes of chondrocyte proliferation, hypertrophy, and endochondral ossification continue within these growth plates throughout childhood and adolescence, which drives longitudinal elongation of the growing bones (Ross and Pawlina, 2006).

1.3 Development and Cartilage Formation in Embryonic Facial Primordia

All vertebrates share a common craniofacial morphology in early stages of embryonic development (Liu et al., 2010). The primitive vertebrate face consists of distinct primordia, discrete buds of neural crest- and mesoderm-derived mesenchyme. These four distinct facial primordia (frontonasal, mandible, maxilla, and hyoid prominences) are arranged in a similar pattern encircling a primitive oral cavity (Francis-West et al., 1998). Differential growth and cartilage formation within the facial primordia are predominant factors in determining face shape. As such, disruption of the cellular signalling cascades involved in outgrowth of the facial primordia can result in numerous congenital malformations including Treacher-Collins and Alagilles syndromes, and more commonly orofacial clefts (Winter, 1996).

The formation of all four facial primordia involves migration of neural crest derived ectomesenchyme cells (Wedden et al., 1988). The frontonasal prominence is derived from migrating anterior cranial neural crest cells, while the more posterior cranial neural crest cells give rise to the pharyngeal arches (Santagati and Rijli, 2003).

The first pharyngeal arch gives rise to both the mandibular and maxillary facial prominences, while the hyoid prominence is derived from the second pharyngeal arch (Richman and Lee, 2003). Myogenic precursor cells derived from the paraxial mesoderm also migrate into the developing facial primordia. These cells will ultimately give rise to the skeletal muscles of the face. Following the migration of cranial neural crest cells into the embryonic facial primordia, the cells aggregate into compact cellular arrangements, and initiate differentiation into either chondrocytes or osteocytes (Richman and Lee, 2003).

Within the avian embryo, some facial structures form via endochondral ossification of cartilaginous templates, while other form through intramembranous ossification. Within the frontonasal and mandibular process, both chondrogenesis and intramembranous ossification occur. The frontonasal primordia of developing chick embryos will ultimately form skeletal elements such as pre-nasal cartilage and the pre-maxillary bone (i.e. portions of the upper beak), whereas the mandibular process gives rise to Meckel's cartilage and the membranous bones of the lower beak (angular, suprangular, splenary, and dentary bones). Within the maxillary process, only intramembranous ossification occurs forming maxillary, jugal, quadratojugal, palatine and pterygoid bones. Finally, endochondral ossification within the hyoid process gives rise to skeletal elements such as the columella, ceratobranchial, epibranchial, and basibranchial cartilages (Richman and Lee, 2003).

The vertebrate hindbrain is a key source of patterning information within the embryonic head. During early embryogenesis, the hindbrain is transiently divided into eight segments known as rhombomeres (r). The identity of each rhombomere is based upon a unique expression pattern of *hox* genes. Hox gene expression patterns are both highly ordered and partially overlapping. Moreover, Hox gene expression patterns are critical for ensuring proper spatial organization of the cranial neural crest cell migration pathways and development of the facial primordia (Cobourne, 2000). Migrating cranial neural crest cells from the anterior portion of the neural crest (up to the level of r2) do not express *hox* genes (Hox-negative), whereas those from more posterior positions (from r3 to r8) express *hox* genes (Hox-positive). In the avian embryo, the frontonasal primordia and the first pharyngeal arch, which gives rise to both the mandibular and maxillary primordia, are populated by Hox-negative cells. The second pharyngeal arch, which gives rise to the hyoid primordia, is populated by

Hox-positive cells. The overall pattern of the developing skeletal system is specified, in part, by distinct patterns of Hox gene expression, which provide positional information to cells of early mesenchymal lineages (Erlebacher et al., 1995). Additional skeletal patterning information is also provided via localized regulation of prechondrogenic mesenchyme condensation via secreted paracrine/autocrine factors.

Epithelial-mesenchymal interactions are critical factors involved in cellular differentiation and patterning within the developing embryo (Greene and Pisano, 2004). Much of our knowledge of the molecular events controlling morphogenesis and pattern formation during skeletal development has come from experimental studies of the factors involved in embryonic limb bud outgrowth (Wedden et al., 1988). Outgrowth of the embryonic limb bud is directed by the epithelium of the apical ectodermal ridge (AER) located at the distal tip of the limb bud. The AER is responsible for maintaining the underlying chondrogenic and myogenic mesenchyme in a proliferative, undifferentiated state (Summerbell, 1974). As proliferating limb mesenchyme cells emerge from the "subridge/progress" zone beneath the AER, they initiate overt histogenesis of cartilage and muscle tissues in a proximal to distal sequence. Ectodermal signalling has also been implicated in anterior-posterior limb axis patterning, as reversal of the ectoderm 180° about its anterior-posterior axis within the developing limb results in an inversion of limb skeletal elements (MacCabe et al., 1974). Evidence suggests outgrowth and skeletal patterning along the dorsal ventral axis is regulated by several factors secreted from the ectoderm, including Wnt-7a and Fibroblast growth factors (FGF2, -4, and-8) (Francis-West et al., 1998).

Establishment of the anterior-posterior axis appears to involve mesodermal cells located at the posterior edge of the developing limb, within the zone of polarizing activity (ZPA) (Wedden et al., 1988). Transplantation of cells from the ZPA to the anterior border of the developing limb resulted in mirror image duplication of skeletal structures (Maccabe et al., 1973). Sonic hedgehog (Shh), a secreted factor expressed within the dorsal ectoderm, is largely believed responsible for cellular specification along the anterior-posterior axis (Francis-West et al., 1998).

While considerably less is known about specific mechanisms governing the patterning of facial skeletal structures, it is clear this regulation also involves epithelial-mesenchymal interactions (Brugmann et al., 2006). For example, studies have shown that removal of the epithelium in the developing mandibular primordia

halts proximal-distal outgrowth of the underlying mesenchyme (Richman et al., 1997; Wedden et al., 1988). Moreover, the resulting mesenchyme begins premature differentiation into cartilage and bone, suggesting the mandibular epithelium has chondro-inhibitory effects on the underlying mesenchyme (Mina et al., 1994). In addition, experimental evidence suggests that signalling centers analogous to the AER and ZPA of the developing limb are also present within the embryonic face (Helms et al., 1997).

Prechondrogenic mesenchyme cells isolated from distinct embryonic facial regions exhibit differences in their levels and patterns of spontaneous chondrogenic differentiation *in vitro* (Hoffman and Kulyk, 1999). In high density micromass cultures, mesenchyme isolated from the frontonasal and mandibular processes undergo extensive spontaneous chondrogenesis, yet mesenchyme isolated from the maxillary or hyoid process exhibit minimal levels of spontaneous chondrogenesis (Hoffman and Kulyk, 1999). In addition, micromass cultures of frontonasal mesenchyme form irregular patches of cartilage tissue, where mandibular mesenchyme cultures form discrete spherical cartilage nodules (Hoffman and Kulyk, 1999). The different *in vitro* behaviours of these facial mesenchyme cell populations is a reflection of their distinct *in vivo* cellular fates, and transplantation studies demonstrate that facial mesenchyme cells are at least partially committed to form specific skeletal structures even prior to migration from their sites of origin within the neural crest (Noden, 1991). In addition, the relative proportions of mesoderm-derived myogenic cells and neural crest derived skeletogenic cells, which come to reside within the four distinct facial primordia, may affect their capacity for chondrogenesis *in vitro* (Hoffman and Kulyk, 1999; Kulyk and Reichert, 1992).

1.4 Transcription Factors Implicated in Chondrogenic Differentiation and Maturation

A large number of transcription factors are involved in the regulation of chondrogenic differentiation of mesenchymal cells within the developing facial primordia (Akiyama and Lefebvre, 2011; Hartmann, 2009).

Sox9, a transcription factor of the SRY-related HMG box family, is often considered to be the master regulator of chondrogenic differentiation. Sox9 is both required and sufficie(Ross et al., 2003)t for chondrocyte specification and

differentiation (Akiyama and Lefebvre, 2011). Heterozygous loss of function mutations in the human *sox9* gene cause campomelic dysplasia, a severe form of dwarfism, and affected infants die soon after birth (Wagner et al., 1994). Since homozygous *sox9* deficiency results in early embryonic lethality, Bi et al. (1999) investigated the role of Sox9 in chondrogenesis by injecting homozygous *sox9* null embryonic stem cells (*sox9*-/-) into wild-type (*sox9*+/+) mouse blastocysts to generate embryonic chimeras (Bi et al., 1999). The skeletal elements that developed in these chimeras lacked *sox9*-/- cells, and were comprised solely of wild type cells. In addition, cartilage specific marker genes, such as type II collagen and aggrecan, failed to be expressed in homozygous *sox9* null cells (Bi et al., 1999). Kulyk et al. (2000) demonstrated that the onset of Sox9 expression occurs prior to overt chondrogenesis *in vitro*, as neither type IIA collagen or aggrecan are detectable prior to Sox9 expression (Kulyk et al., 2000).

Both chondrogenic mesenchyme precursor cells and fully differentiated chondrocytes co-express two additional members of the sox family, L-Sox5 and Sox6 that act cooperatively with Sox9 (Lefebvre et al., 1998). Evidence suggests the nature of this cooperative activity is to enhance Sox9 binding on enhancers of chondrocyte specific genes, such as type II collagen, thereby increasing transcriptional activation of Sox9 responsive genes (Han and Lefebvre, 2008). L-Sox5 and Sox6 are markedly similar in structure, and are believed to be functionally redundant in regulation of chondrogenic differentiation. *L-sox5*:*sox6* double null mutant mice develop severe, generalized chondrodysplasias characterized by a dramatic reduction in overall cartilage formation. However, mice with a homozygous deletion of only one of the *L-sox5* or *sox6* genes display only mildly impaired skeletal phenotypes (Smits et al., 2001).

1.5 Growth Factors and Other Signalling Ligands that Control Cartilage Formation

Numerous extracellular signals, including both systemic and local soluble factors and components of the extracellular matrix, are involved in the regulation of embryonic cartilage differentiation. Of particular importance are peptide growth factors, as embryonic skeletal tissues are particularly receptive to their actions (Goldring and Goldring, 1990).

Members of the transforming growth factor-β (TGFβ) superfamily are among the earliest signalling molecules to stimulate condensation of prechondrogenic mesenchyme (Goldring et al., 2006). Specifically, both TGF-β1 and TGF-β2, promote chondrogenesis of embryonic chick mesenchyme *in vitro* (Kulyk et al., 1989). TGF-β regulates condensation of prechondrogenic mesenchyme, in part, by increasing expression of both fibronectin (Leonard et al., 1991) and N-CAM (Goldring et al., 2006). Components of the cartilage extracellular matrix interact with N-CAM to initiate intracellular signal transduction cascades involved in overt differentiation of prechondrogenic mesenchyme to mature chondrocytes (DeLise et al., 2000).

Other members of the TGFβ superfamily involved in regulation of chondrogenesis include bone morphogenetic proteins (BMPs) and activin. BMPs stimulate *in vitro* chondrogenic differentiation of chick mesenchyme (Bobick et al., 2009). In early stages of chondrogenesis, BMPs upregulate N-cadherin expression, which stimulates condensation of prechondrogenic mesenchyme. Further evidence suggests that BMPs also regulate chondrogenesis in mouse limb bud mesenchyme cultures by stimulating accumulation of *sox9* mRNA, a hallmark of overt chondrogenic differentiation (Nishimura et al., 2012; Zehentner et al., 1999).

Activin has also been implicated in the regulation of chondrogenesis. Jiang et al. (1993) demonstrated that exogenous activin stimulates chondrogenesis in chick mesenchyme cell cultures as evidenced by increased levels of Alcian blue staining for cartilage matrix proteoglycans (Jiang et al., 1993). Furthermore, the chondrogenic stimulatory effects of activin are also associated with increased expression of N-CAM and tenascin-C in prechondrogenic mesenchyme condensations (Jiang et al., 1993).

Insulin-like growth factor 1 (IGF-1) is also a positive regulator of chondrogenesis. Studies have shown that IGF-1, in combination with BMP-7 and Fibroblast growth factor 2 (FGF2), stimulates proteoglycan synthesis and chondrocyte proliferation *in vitro* (Patil et al., 2012). In contrast, epidermal growth factor (EGF) is known to negatively regulate chondrogenesis *in vitro,* as addition of exogenous EGF to embryonic mesenchyme micromass cultures inhibits both condensation and overt chondrogenic differentiation as demonstrated by a reduction in Alcian blue staining for cartilage matrix proteoglycans (Yoon et al., 2000).

Fibroblast growth factors (FGFs) are responsible for mediating many of the epithelial-mesenchymal interactions involved in cellular differentiation within the

developing embryo (Greene and Pisano, 2004). Moreover, FGF family members have been implicated as both negative and positive regulators of chondrogenic differentiation. The various roles of FGFs and their receptors will be discussed in greater detail in the subsequent section.

1.6 The Roles of FGFs and FGF Receptors in Chondrogenesis and Facial Development

1.6.1 General characteristics of fibroblast growth factors

Fibroblast growth factors (FGFs) are a large family of evolutionarily conserved, structurally related growth factors which share a high affinity for heparin and heparan sulphate proteoglycans (Itoh and Ornitz, 2011). In vertebrates, at least 22 FGFs have been identified (Itoh and Ornitz, 2004). FGF family members are further divided into at least 6 subfamilies on the basis of common biochemical and functional properties (Bottcher and Niehrs, 2005; Ornitz and Itoh, 2001; Ornitz and Marie, 2002). FGFs have been implicated in a diverse array of cellular processes including proliferation, chemotaxis, migration, and differentiation (Francis-West et al., 1998).

Most FGFs contain amino-terminal secretion signal peptides and, as such, are present within the extracellular space. The majority of FGFs are secreted from cells via the endoplasmic reticulum-golgi apparatus pathway (Itoh and Ornitz, 2011). Interestingly, FGF1 and FGF2 lack N-terminal secretion signal peptides, and yet are still present within the extracellular space (Ornitz and Itoh, 2001). These FGFs may be released from damaged cells or by an endoplasmic reticulum-golgi apparatus independent exocytotic pathway (Nickel, 2010). Interestingly, FGFs 11 through 14 are strictly located within intracellular compartments and function in a FGF receptor-independent manner (Itoh and Ornitz, 2011).

FGFs found within the extracellular space mediate their respective biological responses by binding and activating FGF receptors (FGFRs). FGFs exist as monomers and their association with heparan sulphate proteoglycans enhances their ability to act as ligands for their cognate receptors (Itoh and Ornitz, 2004). Ligand binding to FGFRs induces homo- or heterodimerization of the extracellular immunoglobulin-like domains, leading to trans-autophosphorylation within the intracellular tyrosine kinase domain (Wilkie et al., 2002). Phosphorylation of specific tyrosine residues within the activation loop of the intracellular domain stimulates intrinsic catalytic activity of the

FGFRs and recruits members of downstream signalling pathways (McIntosh et al., 2000).

Although there are least 22 members of the FGF family, only four distinct FGF receptors have been identified to date (Tsang and Dawid, 2004). All FGFRs are composed of three essential domains. The first domain, an extracellular ligand-binding domain, consists of three distinct immunoglobulin-like domains. FGFRs also contain a single spanning transmembrane domain, and an intracellular domain which possesses tyrosine kinase activity (Jaye et al., 1992). Importantly, alternative pre-mRNA processing of the immunoglobulin-like domain of *fgfr1*, *fgfr2*, and *fgfr3* gene transcripts produces two distinct isoforms characterized by specific patterns of ligand binding (Bottcher and Niehrs, 2005), and generates tissue-specific isoforms. For example, FGFrb isoforms are primarily expressed in the epithelia of a variety of embryonic tissues, whereas FGFRc isoforms predominate in mesenchyme adjacent to FGFRb expressing epithelia (Richman et al., 1997; Wilke et al., 1997). To date, alternative splicing of the immunoglobulin-like domains of *fgfr4* mRNA has not been characterized (Loo et al., 2000).

Both FGFs and their cognate receptors are expressed in specific spatial and temporal patterns that serve to regulate FGF-signalling activity (McIntosh et al., 2000). Moreover, the specific binding affinities of FGFs to their receptors mediates signal strength and determines which downstream signal transduction pathway is activated (Lunn et al., 2007). Association with heparan sulphate-containing proteoglycans located within the extracellular matrix also serves to regulate FGF signalling activity and specificity (Ornitz and Marie, 2002). This association is thought to mediate the action of FGFs through a number of different mechanisms. One proposed mechanism is that heparan sulphate proteoglycans bound to FGFs may restrict extracellular diffusion of FGFs, thereby localizing FGF signalling to restricted regions. Another proposed mechanism is that binding of heparan sulphate-containing proteoglycans to FGFs may promote formation of active FGF dimers or oligomers. In addition, association with heparan sulphate containing proteoglycans may stabilize the FGF-FGFR complex (Eswarakumar et al., 2005; Itoh and Ornitz, 2011).

The specific ligands responsible for FGFR activation during chondrogenesis *in vivo* have been difficult to identify, as signalling is dependent upon the temporal and spatial expression patterns of both ligand and receptors (Jiang et al., 1993; Miraoui

and Marie, 2010). Furthermore, Szebenyi et al. (1995) demonstrated changes in the expression patterns of FGFRs are intrinsic properties of differentiating chondrocytes (Szebenyi et al., 1995). For example, undifferentiated and proliferating mesenchyme cells predominately express FGFR1, whereas in condensations of prechondrogenic mesenchyme the predominant receptor is FGFR2. Fully differentiated chondrocytes primarily express FGFR3 (Szebenyi et al., 1995).

Within the developing embryo, FGFs and their receptors constitute a crucial signalling module, as loss of FGF-signalling results in embryonic lethality (Bottcher and Niehrs, 2005). FGFR activation can lead to activation of several distinct intracellular signal transduction cascades, such as the extracellular signal regulated kinase (ERK), signal transducer and activator of transcription 1 (STAT1), protein kinase C (PKC), and PLCγ-phosphatidylinositol 4,5-bisphosphate (PIP_2) pathways (Debiais et al., 2001; Havens et al., 2006; Sahni et al., 2001). The large number of distinct intracellular signalling cascades activated by this family of ligands suggests the presence of multiple negative and positive regulators of FGF signalling. Indeed, members of the Sprouty and Mitogen-activated protein phosphatase families have been implicated as negative modulators, whereas ETS transcription factor family members (including Pea3 and Erm) have been implicated as positive regulators (Tsang and Dawid, 2004).

1.6.2 FGF signalling in facial chondrogenesis

At least 6 FGFs (FGF1, -2, -4, -5, -8, and -12) are known to be expressed within the developing facial primordia along with all four types of FGFRs (FGFR1-4) (Francis-West et al., 1998). Utilizing *in situ* hybridization techniques with a probe antibody directed against FGF2, Richman et al. (1997) demonstrated that chick embryos of stages 15 through 24 ubiquitously express FGF2 throughout the mesenchyme and ectoderm of the frontonasal, mandibular, and maxillary facial primordia (Richman et al., 1997). At stages 24 and 28, the authors also demonstrated expression of FGF4 in the ectoderm at the medio-cranial surface of the mandibular arch and at the lateral portions of the ectoderm covering the nasal slits. Additionally, stage 20 chick embryos were found to express FGF8 throughout the ectoderm of the frontonasal primordia. This expression was downregulated at the center of the frontonasal primordia at stages 24 and 28, just prior the onset of chondrogenesis but

persisted in the lateral regions of the frontonasal primordia of stage 24 and stage 28 chick embryos (Richman et al., 1997).

1.7 MAPK Signal Transduction Pathways and their Roles in Chondrogenesis

Responsiveness of chondrogenic cells to both BMPs and FGFs requires activation of the highly conserved mitogen-activated protein kinase (MAPK) intracellular signalling cascades (Bobick and Kulyk, 2008). To date, four distinct MAPK families have been characterized: the extracellular signal regulated kinase (ERK1/2), p38-MAPK, c-Jun N-terminal kinase (JNK), and ERK5 (also known as big map kinase 1; BMK1) signal transduction pathways.

The common architecture of all MAPK signal transduction pathways is the presence of three or more sequentially acting protein-serine/threonine kinases. In its simplest form, the MAPK pathway involves the activation of a MAPK kinase kinase (MAPKK) via a dual phosphorylation event by a MAP kinase kinase kinase (MAPKKK). The phosphorylated MAPKK then phosphorylates a specific target MAPK (either ERK1/2, p38 MAPK, JNK, or ERK5). The activated MAPK then influences cell metabolism and gene expression via phosporylation induced activation or repression of a diverse array of various cytostolic and nuclear protein substrates (Widmann et al., 1999).

All MAPK signalling cascades are regulated to some extent by growth factors (Katz et al., 2007). MAPK signalling cascades have been shown to play diverse roles in the regulation of embryonic chondrogenesis (Bobick and Kulyk, 2004; Stanton et al., 2003). Stimulation of prechondrogenic mesenchyme cells by BMPs leads to p38-MAPK activation and a positive effect on embryonic cartilage differentiation. In contrast, ERK1/2 activation in response to FGFs can either enhance or inhibit chondrogenesis depending on the anatomical location of the prechondrogenic mesenchyme cells. The ERK1/2 pathway, of particular relevance to my research, will be discussed in greater detail in the subsequent section.

1.7.1 Extracellular signal regulated kinase (ERK) signalling

The extracellular signal-regulated kinase (ERK1/2) signalling pathway, also known as the MEK/ERK pathway, is a critical signal transduction pathway involved

in proliferation, differentiation, and survival of eukaryotic cells (Bobick and Kulyk, 2008). A large number of mitogens, including growth factors and cytokines, and their cognate receptors are capable of inducing activation of the ERK pathway (reviewed in (Johnson and Lapadat, 2002). The ERK pathway is a critical downstream signalling pathway responsible for relaying extracellular FGF signals to the cell nucleus (Corson et al., 2003). Moreover, during embryogenesis the sites of active dual phosphorylated ERK1/2 expression coincide closely with sites of FGF signalling. The association of FGF action with sites of ERK1/2 activity occurs in both chondrogenic (i.e. future skeletal elements) and non-chondrogenic regions (i.e. embryonic brain tissue) (Corson et al., 2003).

Consistent with the basic signalling architecture of all MAPK pathways, the ERK1/2 pathway includes three sequentially acting protein kinases. Located furthest upstream is Raf (a MAPKKK), followed by MEK (a MAPKK), and finally ERK1/2 (a MAPK). Although the molecular identities of the upstream stimuli may differ, the principal steps in the ERK1/2 signal transduction cascade remain the same. Upstream of the triple phospho-kinase relay system, the binding of a signalling ligand to its receptor induces phosphorylation of tyrosine residues located within the activation loop in the cytoplasmic tail of the receptor (Katz et al., 2007). Adaptor proteins, such as src-homology 2 domain containing transforming protein (SHC) and growth factor receptor-bound protein 2 (Grb2), link activated receptors to a guanine nucleotide exchange factor. These GTP/GDP exchange factors actively recruit small GTP binding proteins, such as Ras, to the receptor and phosphorylate them (Katz et al., 2007). Ras, in turn, recruits members of the Raf family of serine threonine kinases to the receptor. The Raf family (i.e. MAPKKKs) includes A-Raf, B-Raf, and c-Raf, which are activated by multiple phosphorylation and dephosphorylation events (Ramos, 2008). Activated Raf then dual phosphorylates specific serine residues within the activation loop of MEK1/2. Activated MEK1/2 in turn phosphorylates its specific downstream target, ERK1 and ERK2 (Ramos, 2008). Phosphorylation of ERK1/2 by MEK1/2 allows ERK to dissociate from the cytoplasmic anchored MEK/ERK complex (Adachi et al., 1999). Once dissociated, phosphorylated ERK1/2 can activate more than 100 targets at various cellular locations (Ramos, 2008). Notably, dimerized ERK1/2 can be translocated to the nucleus, where it assists in regulation of gene expression through modification/phosphorylation of its nuclear

targets, such as Ets-like transcription factor 1 (ELK1) and members of the ETS family of transcription factors (Tsang and Dawid, 2004).

1.7.2 ERK1/2 signalling in chondrogenesis

Much of what is known regarding the role of the ERK1/2 pathway in the regulation of cartilage differentiation has been elucidated through examinations of *in vitro* chondrogenesis of embryonic limb and facial mesenchyme. Current studies suggest that ligand bound FGF receptor kinases activate Ras, which in turn, activates the ERK signalling cascade (Dhillon and Kolch, 2002). Active phosphorylated ERK1/2 is abundant at sites of prospective chondrogenesis (Bobick and Kulyk, 2008; Corson et al., 2003). Moreover, ERK1/2 has been shown to function as either a negative or positive regulator of chondrogenesis depending on the embryonic origin of the prechondrogenic cells (e.g. limb bud vs. mandible) and their state of differentiation (Bobick, 2006b; Bobick et al., 2007; Bobick, 2006c).

A number of experimental observations suggest the ERK1/2 pathway functions as a negative regulator of cartilage differentiation in prechondrogenic mesenchyme within developing limb buds (Bobick et al., 2007). Endogenous levels of phosphorylated ERK (i.e. active ERK) progressively decline throughout the course of spontaneous chondrogenesis of chick limb bud mesenchyme *in vitro* (Chang et al., 1998). Inhibition of MEK, the specific upstream activator of ERK1/2, within limb mesenchyme cultures increases production of both type II collagen and cartilage matrix proteoglycans (Bobick and Kulyk, 2004; Chang et al., 1998; Oh et al., 2000), and elevated expression of *sox9*, *aggrecan*, and type II collagen mRNAs (Bobick and Kulyk, 2004). Conversely, when a constitutively active MEK transgene was expressed within prechondrogenic limb mesenchyme cells, the activity of a sox9-responsive collagen II enhancer-luciferase reporter gene was dramatically reduced (Bobick and Kulyk, 2004).

The MAPK/ERK signalling pathway may also be involved in the regulation of chondrogenesis of embryonic facial mesenchyme. An examination of spatial and temporal expression patterns of ERK signalling during mouse embryogenesis revealed prominent and sustained regions of ERK activation within the developing frontonasal process and pharyngeal arches (Corson et al., 2003). To define the roles of the MAPK/ERK pathway in facial chondrogenesis, Bobick and Kulyk (2006)

established micromass cultures of mesenchyme from embryonic chick facial primordia (Bobick, 2006b). In cultures of frontonasal mesenchyme isolated from stage 24/25 chick embryos, pharmacological inhibition of MEK increased chondrogenesis as evidenced by elevated levels of type II collagen, extracellular glycosaminoglycan accumulation, and expression of chondrogenic marker genes (*sox9*, *col2a1*, and *aggrecan*) (Bobick, 2006b). This suggests, that as in chick embryonic limb bud mesenchyme micromass cultures, the MEK/ERK pathway functions as a negative regulator of chondrogenesis in early stage frontonasal mesenchyme. Notably, however, in cultures of frontonasal mesenchyme isolated from stage 28/29 chick embryos, MEK inhibition decreased chondrogenesis, suggesting a stage-related shift in the chondrogenic regulation. Pharmacological inhibition of MEK in cultures of mandibular mesenchyme isolated from stage 24/25 chick embryos decreased chondrogenesis, as evidenced by a reduction in levels of type II collagen, extracellular matrix glycosaminoglycan accumulation, and expression of chondrogenic marker genes (Bobick, 2006b). This suggested that the ERK1/2 signalling functions as a positive regulator of chondrocyte differentiation in mandibular mesenchyme cells. It was concluded that the ERK1/2 pathway plays both chondro-stimulatory and chondro-inhibitory roles in facial chondrogenesis, depending on the anatomical site from which the prechondrogenic mesenchyme cells originate as well as their specific stage of development.

Studies in which stage 24/25 chick frontonasal mesenchyme micromass cultures were treated with FGF2, -4, or -8 at concentrations of 10, 20, and 40 ng/ml found decreased cartilage matrix production and reduced expression of three cartilage specific genes: collagen type IIA, *aggrecan*, and *sox9*. Conversely, similar FGF treatment of chick stage 24/25 mandibular mesenchyme increased cartilage differentiation (Bobick et al., 2007). This study demonstrated a relationship between FGF signalling and the ERK1/2 pathway in facial chondrogenesis, since suppression of ERK activity by treatment with a pharmacological MEK inhibitor was able to block both the inhibitory effects of FGFs on frontonasal chondrogenesis and the stimulatory effects of FGFs on mandibular mesenchymal cells (Bobick et al., 2007). This indicates that FGF signalling can function in diverse or even opposite manners within distinct facial populations. Moreover, the response of facial mesenchyme cells to FGF was reported to be both stage and region specific (Bobick et al., 2007).

Some members of the ETS superfamily of transcription factors have been implicated as downstream effectors of FGF and/or MAPK signalling (Wasylyk et al., 1998). Thus, the various effects of FGFs on facial chondrogenesis are likely to be mediated, at least in part, through these ETS transcription factors.

1.8 ETS Transcription Factors

1.8.1 General characteristics of ETS transcription factors

The superfamily of ETS (E-twenty six) transcription factors consists of approximately 30 members (Wasylyk et al., 1998). They are evolutionarily conserved nuclear phosphoproteins involved in the regulation of cellular proliferation, differentiation and oncogenic transformation (Seth et al., 1992; Wasylyk et al., 1998). The characteristic feature of ETS transcription factors is the presence of a conserved 85-amino acid DNA binding motif (ETS-DBM) that mediates binding to purine rich DNA sequences with a central GGAA/T core consensus and additional flanking sequences (Graves and Petersen, 1998). Structural composition and slight variations within the ETS-DBM allow further classification of ETS transcription factors into several subfamilies. Moreover, alteration of a single amino acid within the ETS domain can alter its DNA binding specificity (Oikawa and Yamada, 2003).

Several ETS family proteins are preferentially expressed in specific cell lineages, whereas others display ubiquitous expression (Oikawa and Yamada, 2003). For example, ternary complex factor ETS subfamily members, which includes Ets-like transcription factor-1 (ELK-1), are expressed throughout a wide variety of tissues (Oikawa and Yamada, 2003), whereas E-74-like factor (ELF1) expression is restricted to hematopoietic cells and developing epithelial tissues, and epithelial specific ETS-1 (ESE1) is exclusively expressed in epithelial cells (Oettgen et al., 1997).

ETS transcription factors influence gene expression by binding ETS-binding sites in the enhancers or promoters of target genes (Sharrocks, 2001). Specificity of target gene activation is mediated, in part, through interactions with other transcription factors and co-factors, which promotes or represses DNA binding (Oikawa and Yamada, 2003). For example, some ETS transcription factors associate with members of the Jun family of proteins. Members of these two families act cooperatively to bind DNA sequences, known as Ras-responsive elements, thereby enhancing transcriptional activation of target genes. Ras-responsive elements are

found within a variety of genes which are responsive to MAPK signalling (Oikawa and Yamada, 2003).

Evidence suggests ETS members are critical downstream effectors of MAPK signalling cascades (Wasylyk et al., 1998). Post-translational modification of ETS proteins, such as phosphorylation, regulates their downstream activity by altering DNA binding activity, affecting interactions with other co-regulators, and enhancing or repressing transcriptional activation capacities (Sharrocks, 2001). Phosphorylation of ETS proteins has also been shown to affect subcellular localization and/or protein stability (reviewed in (Oikawa and Yamada, 2003).

Importantly, transcription factors from at least 6 ETS subfamilies, including the Pea3 subfamily, have been directly implicated as downstream nuclear phosphorylation targets of the ERK signal transduction cascade (Wasylyk et al., 1998).

1.8.2 Pea3 subfamily of transcription factors

The polyoma enhancer activator-3 (Pea3) subfamily of ETS transcription factors is composed of three members: *pea3*, also known as ets-variant 4 (etv4); *erm*, also known as ets-variant 5 (etv5); and *er81*, also known as ets-variant 1 (etv1) (Sharrocks et al., 1997). Current evidence suggests that Pea3, Erm, and Er81 function primarily as transcriptional activators, and are capable of acting synergistically (de Launoit et al., 1997). *In situ* hybridization studies in mice and chick embryos have shown differential, although partial overlapping, patterns of *pea3*, *erm*, and *er81* mRNA expression in a number of developing organs (Chotteau-Lelievre et al., 1997; Lin et al., 1998). Furthermore, the sites of Pea3, Erm, and Er81 expression usually coincide with sites of endogenous FGF signalling (Raible and Brand, 2001; Roehl and Nusslein-Volhard, 2001).

Previous studies have also demonstrated FGF signalling is both necessary and sufficient for expression of *pea3*, *erm*, and *er81* (Firnberg and Neubuser, 2002; Raible and Brand, 2001; Roehl and Nusslein-Volhard, 2001). Cellular levels of mRNA transcripts for *pea3*, *erm*, and *er81* transcription factors are often upregulated in response to FGF signalling (Lunn et al., 2007; Roehl and Nusslein-Volhard, 2001). Moreover, Znosko et al. (2010) demonstrated that simultaneous knockdown of *pea3*, *erm*, and *er81* expression in zebrafish embryos results in phenotypes reminiscent of

embryos deficient in FGF signalling (Znosko et al., 2010). Taken together, these findings suggest that Pea3 family of transcription factors are essential components of the FGF signalling pathway.

1.9 Micromass Culture Model for Analysis of Mechanisms Regulating Chondrogenesis

Embryonic cartilage formation involves complex and intricate epithelial-mesenchymal, cell-cell and cell-matrix interactions between multiple cell populations of different embryological origins. To clarify the mechanisms involved in embryonic cartilage differentiation, a simplified *in vitro* model, the "micromass" cell culture system, was developed in 1977 in the laboratory of Dr. Michael Solursh (Ahrens et al., 1977). The micromass system was initially employed for the experimental analysis of embryonic limb chondrogenesis (Ahrens et al., 1977).

To establish micromass cultures, a high-density cell suspension (typically 2 x 10^7 cells/ml) is prepared from a prechondrogenic mesenchyme cell population. The prechondrogenic mesenchyme cells are usually isolated from limb buds dissected from stage 23 to stage 25 chick embryos, or from similarly staged rat and mice embryos. Micromass cultures can also be established from mesenchyme of the developing facial primordia (frontonasal, mandibular, maxillary, and hyoid). The dissociated cells are spotted at superconfluent density in 10 µl drops (2 x 10^5 cells per drop) onto tissue culture dishes. After a short period of time to allow for cellular attachment to the surface of the tissue culture dish, the cultures are flooded with serum-containing culture medium and are then incubated at 37°C in 5% CO_2 for a period of 3 to 4 days (Daniels et al., 1996).

During this short incubation period, the mesenchyme cells spontaneously progress through the various stages of chondrogenic differentiation. The three-dimensional, high density seeding of the prechondrogenic mesenchyme cells recapitulates the condensation/aggregation and differentiation events that occur during the initial stages of chondrogenesis *in vivo* (DeLise et al., 2000). Importantly, *in vitro* gene expression patterns throughout the chondrogenic differentiation process closely resemble those occurring *in vivo* (Kulyk et al., 2000). Specifically, mesenchyme cells within these aggregates begin to express high levels of type II collagen and aggrecan, and progressively accumulate Alcian-blue stainable cartilage

extracellular matrix. As such, the extent of chondrogenic differentiation can be measured by qualitative and quantitative assessment of levels of type II collagen, aggrecan, and Alcian blue stainable extracellular matrix.

Variations of the micromass culture system have been adopted in numerous laboratories for the analysis of cartilage differentiation. Several features make it an especially effective *in vitro* model for investigations of embryonic chondrogenesis. The progression of chondrogenic differentiation in micromass culture is rapid and closely parallels the principal phases of chondrogenic differentiation *in vivo*. Plating of cells in small 10 μl drops allows for the establishment of a large number of replicate high-density cell cultures from a relatively sparse amount of embryonic starting tissue. Micromass cultures are readily amenable to experimental manipulations, such as the addition of pharmacological inhibitors, growth factors, or siRNA constructs to the culture medium, and targeted gene transfections. Much of our current understanding of molecular events regulating *in vivo* cartilage differentiation were elucidated through *in vitro* studies of chondrogenesis in embryonic limb bud mesenchyme micromass cultures (Daniels et al., 1996).

In addition to its original application for studying embryonic limb chondrogenesis, the micromass method has been applied to the culture of embryonic facial mesenchyme cells, to the study of cartilage differentiation by multipotent mesenchymal stem cells derived from bone marrow or other adult tissues, for investigations into the regulation of chondrocyte hypertrophy and endochondral ossification, and for teratogenic drug screening. In addition, micromass culture strategies are being adapted for cartilage tissue engineering applications (Bobick et al., 2009).

1.10 Gene Expression Analysis using RT-qPCR

Since its invention nearly 30 years ago, the polymerase chain reaction (PCR) has made significant contributions to modern biology, biotechnology, medicine and agriculture (VanGuilder et al., 2008). Remarkably simple, yet extremely sensitive, PCR technology relies upon repeated heating and cooling cycles of a mixture of DNA, specific oligonucleotides, deoxynucleotriphosphates (dNTPs), and DNA polymerase, for exponential amplification of a specific target sequence (Chandler and Colitz, 2006).

Real-Time quantitative PCR (RT-qPCR) has rapidly become the method of choice for analysis of relative gene expression (Nolan et al., 2006). Simultaneous amplification and quantification of specific nucleic acid sequences throughout the duration of the reaction are made possible with the inclusion of a single fluorescent reagent (DNA intercalating dye or dye-labelled probe) to the polymerase chain reaction. RT-qPCR has been reported to be more sensitive than RNase protection assays and RNA dot blot hybridizations, and has even been reported to be capable of detection of extremely low gene transcript expression (i.e. 5 gene transcripts). Moreover, RT-qPCR assays are capable of distinguishing even small differences (as low as 23%) in gene expression between samples (Wong and Medrano, 2005). Since RT-qPCR requires much less RNA template than other methodologies, it is also particularly useful in embryonic studies which are frequently limited by the nucleic acid content of the experimental samples (Wong and Medrano, 2005)

The conceptual and practical simplicity of RT-qPCR methodologies, lead to a dramatic increase in both the number of researchers using the technique and the number of papers citing the methodology (Pfaffl, 2010). However, critics argue that the increased use of RT-qPCR, combined with the nature of scientific journal publication itself, which traditionally only permits inclusion of minimal technical information, has resulted in a large number of unreliable and conflicting reports (Bustin, 2010). To improve upon the accuracy, reliability, and repeatability of RT-qPCR experiments, the Minimum Information for Publication of Quantitative Real-Time PCR (MIQE) guidelines were established (Bustin et al., 2009). The MIQE guidelines attempt to standardize RT-qPCR experiments by addressing three key areas: (i) sample preparation, storage and quality, (ii) primer selection and design for both the reverse transcription and qPCR reaction, and finally (iii) statistical analysis and interpretation RT-qPCR data (Bustin et al., 2009).

According to the MIQE guidelines, sample acquisition and handling is the first source of potential experimental error, particularly in experiments designed to examine RNA expression profiles (Bustin et al., 2009). As such, the MIQE guidelines stipulate that all details pertaining to sample acquisition (i.e. type of starting tissue, time of storage before processing) must be reported along with detailed information regarding nucleic acid extraction methodology. Moreover, since comparisons across samples should involve the same amount of input RNA, it is crucial to accurately

quantify RNA. While a variety of different techniques are conventionally employed for total RNA quantification, the absolute measured values (in micrograms) frequently differ between methods (Bustin, 2005). As such, it is essential the same method of RNA quantification be used for all experimental samples and that the instrument used to perform the measurements is specified (Bustin et al., 2009).

The MIQE guidelines also requires performing quality control assessments of isolated nucleic acid sample integrity, as both the reverse transcription reaction and PCR amplification efficiencies can be dramatically affected by nucleic acid degradation (Bustin et al., 2009). Furthermore, partially degraded samples may reduce assay sensitivity such that expression ratios of low level transcripts (e.g. the mRNA of many transcription factors) do not accurately reflect their *in vivo* expression levels (Bustin et al., 2009). The MIQE guidelines state that simple measurement of a RNA sample's A_{260}/A_{280} ratio is insufficient for proper quality control, as the presence of contaminating genomic DNA or residual phenols can alter the ratio. As such, the authors of the MIQE guidelines recommend the use of either the Agilent Technologies BioAnalyzer instrument or BioRad's Experion™ microfluidic electrophoresis system for assessment of nucleic acid sample integrity (Bustin et al., 2009).

The second major source of variation in RT-qPCR experiments is the reverse transcription step (Bustin et al., 2009; Stahlberg et al., 2004). The MIQE guidelines require that all experimental conditions relating to cDNA synthesis be reported, and that such conditions are consistent across all compared samples (Bustin et al., 2009). In addition, all primer information (i.e. sequence, NCBI accession number, evidence of primer optimization) must be reported, as RT-qPCR amplification efficiencies are highly dependent upon primer design. The authors also strongly encourage all validated RT-qPCR primer information be submitted to open-access databases, such as RTprimerDB (http://medgen.ugent.be/rtprimerdb/), to improve standardization of RT-qPCR experiments across different laboratories (Bustin et al., 2009).

To date, while much effort has been directed at addressing the first two objectives of the MIQE guidelines (i.e. aspects related to experimental design), the methods employed for statistical analysis and interpretation of the data generated by RT-qPCR experiments remain highly variable (Pfaffl, 2010). Determination of relative gene expression levels in RT-qPCR experiments is based on the expression

ratio of a target gene versus an appropriate reference gene, that is assumed to be constitutively expressed. While this allows greater ease in analysis of gene expression trends, it is highly influenced by the choice of the reference gene and the normalization strategy (Pfaffl et al., 2002). There is also a need to determine amplification efficiency for each target and reference gene examined, as amplification efficiencies vary with the specific primer combination used (Bustin et al., 2009).

The Livak method (2-ΔΔC(T)) is the most commonly used mathematical model to calculate relative gene expression (Livak and Schmittgen, 2001; Pfaffl, 2010). While this method allows for efficiency correction, it does not permit normalization of the data to multiple reference genes. Since reporting of RT-qPCR data involves relative expression ratios, which often have high variances, application of traditional parametric statistical methods has been suggested to be inappropriate as normal distribution of the data would not be expected (Pfaffl et al., 2002). To address the issues of uncertainty in measurement of expression ratios, the Relative Expression Software Tool (REST©) was developed (Pfaffl, 2001).

Utilizing randomization and bootstrapping techniques, REST© determines relative gene expression using the Pfaffl method: (Pfaffl et al., 2002)

$$R = (E_{target})^{\Delta CQ(control-sample)} / (E_{reference})^{\Delta CQreference(control-sample)}$$

where R is the relative expression ratio, E_{target} and $E_{reference}$ are the PCR amplification efficiencies of the target and reference gene respectively, and ΔCQ_{target}(control-sample) and $\Delta CQ_{reference}$(control-sample) are the differences in quantification cycles between a control versus reference genes, respectively. A major advantage of the mathematical model used within REST© is that it makes no assumptions about the data distribution (i.e. does not assume a normal distribution). REST© graphically displays the data as box and whisker plots which provide a visual representation of variation for each gene.

2 RESEARCH OBJECTIVES AND HYPOTHESIS

2.1 Experimental Rationale

Previous studies in our laboratory had shown that FGF treatment increased levels of dual phosphorylated (active) ERK in both frontonasal and mandibular mesenchyme cells, while inhibition of ERK signalling blocked the effects of FGFs in both cell populations (Bobick et al., 2007). Paradoxically, FGF had opposite effects on chondrogenic differentiation in the frontonasal and mandibular mesenchyme cell populations. Specifically, whereas FGF treatment inhibited cartilage differentiation in micromass cultures of frontonasal mesenchyme cells, it increased chondrogenesis in mandibular cultures (Bobick et al., 2007). This suggests that the mechanism responsible for the differential response of frontonasal and mandibular mesenchyme cells to FGF treatment lies at a point downstream of ERK activation. The transcription factors of the Pea 3 subfamily (Pea3, Erm, and Er81) are potential targets of ERK phosphorylation (O'Hagan et al., 1996), and have been shown to be crucial components of the downstream effector pathway through which FGFs influence gene expression (Raible and Brand, 2001). Moreover, embryonic tissues often differ in the specific combination of Pea3, Erm, and Er81 transcription factors that they express (Lunn et al., 2007), which might result in differential responses to upstream signals. The purpose of my M.Sc. project was to examine whether differential expression of Pea3, Erm, and Er81 transcription factors could underlie the opposing responses of embryonic frontonasal and mandibular mesenchyme cells to FGF treatment.

2.2 Hypothesis

Mesenchyme cells from the frontonasal and mandibular regions of the developing chick embryo face express the Pea3, Erm, and Er81 genes in distinct manners, which might account for their different responses to FGF signalling and ERK1/2 activation.

2.3 Specific Objectives

2.3.1 To test this hypothesis, the specific objectives of this study were:

1. To determine whether frontonasal and mandibular mesenchyme cells of the chick embryo exhibit distinct profiles of endogenous Pea3, Erm, and/or Er81 gene transcript expression.

2. To determine whether there are differences in the extents to which treatment with exogenous FGF alters Pea3, Erm, and Er81 gene transcript levels in cultures of prechondrogenic mesenchyme cells isolated from the frontonasal and mandibular processes of the stage 24/25 and stage 28/29 chick embryo.

3. To examine whether Pea3, Erm, and Er81 protein levels differ in embryonic frontonasal and mandibular mesenchyme cells.

4. To compare the effects of FGF treatment on cartilage differentiation in cultures of facial mesenchyme cells isolated from the frontonasal and mandibular regions of the chick embryo.

3 MATERIALS AND METHODS

3.1 Isolation of Frontonasal and Mandibular Mesenchyme and Preparation of Cultures

3.1.1 Establishment of micromass and explant cultures

Fertilized Giant Cornish Cross chicken eggs were purchased from a commercial hatchery (Anstey Hatchery, Saskatoon, SK). Embryos were staged according to previously established methods (Hamburger and Hamilton, 1951). Frontonasal and mandibular facial processes of stage 24/25 and stage 28/29 chick embryos were excised and used for establishment of high density micromass as previously described (Kulyk et al., 1991; Kulyk and Reichert, 1992). Excised facial processes from similarly staged chick embryos were also used for establishment of explant cultures.

3.1.2 Micromass cultures

To establish micromass cultures, excised facial processes were treated with 0.8 U/ml dispase for 1 h, and all surface epithelial tissues (ectoderm and endoderm) were carefully removed. Isolated mesenchyme from each distinct facial process of approximately 3-5 dozen chick embryos were pooled, incubated for 20 min in 0.25% (v/v) trypsin, and dissociated into a suspension of 2 x 10^7 cells/ml in DMEM:F12/10% FBS medium (a 1:1 mixture of Dulbecco's modified Eagle's medium and Ham's F12 medium supplemented with 10% [v/v] fetal bovine serum, 2mM glutamine, and antibiotics [100µg/ml kanamycin, 100 U/ml penicillin G, 100 µg/ml streptomycin, and 0.25 µg/ml amphotericin B]). High density micromass cultures were established by spotting 10 µl drops of cell suspension (2 x 10^5 cells per spot) onto 35 mm or 4-well NUNC tissue culture dishes. For the 4-well NUNC tissue culture dishes, a single 10 µl drop of cell suspension was dispensed into each 13 mm diameter well. For the 35 mm tissue culture dishes, approximately 5-10 cell suspension spots were plated onto each plate, unless otherwise indicated. Following a 90 min incubation at 37°C/5% CO_2 to permit cellular attachment, cultures were flooded with fresh media DMEM:F12/10% FBS medium and incubated for up to 3 days.

3.1.3 Explant cultures

For analysis of frontonasal and mandibular mesenchyme 'explant' cultures, stage 24/25 facial processes were excised and the adherent epithelia were removed as described above. Eight to ten intact facial processes, which retained their native cell-cell contacts, were cultured in 35 mm NUNC culture dishes in DMEM: F12/10% FBS medium at 37°C/5% CO_2. Micromass and explant cultures were subsequently harvested for RNA analysis (RNA dot-blots, Northern blots and/or Real Time Quantitative PCR (RT-qPCR), Alcian blue histochemical staining, type II collagen immunohistochemistry, measurement of sulphated proteoglycan accumulation (DMMB assay), and/or Western blotting, following methods detailed below.

3.1.4 FGF administration

To examine the effects of FGF on the RNA expression profiles of the Pea3 group of transcription factors (*pea3*, *erm*, and *er81*), frontonasal and mandibular mesenchyme cultures were treated with exogenous FGF2 at a final concentration of 20 ng/ml or 40 ng/ml (approximately 1.20 nM and 2.40 nM respectively), as previously reported (Bobick et al., 2007). FGF2 was omitted from parallel control cultures. Recombinant human FGF2 (basic FGF) was purchased from R & D Systems (Minneapolis, MN, USA; catalogue no. 233-FB-02533) or from Peprotech Canada (Dollard des Ormeaux, Quebec; catalogue no. 100-18B).

To minimize the negative effects of FGFs on cell viability, FGF2 was added to micromass cultures 12-13 h after the initial medium feed (see Figure 1). Micromass cultures were collected for RNA analysis 2 h after the administration of FGF2 unless otherwise indicated.

For explant cultures, the mesenchyme tissues isolated from stage 24/25 chick frontonasal and mandibular explant cultures were treated with recombinant human FGF2 (20 ng/ml) immediately after removal of all surface epithelia. Since the mesenchyme tissues in frontonasal and mandibular explants were not dissociated as with micromass cultures, a 12 h recovery period before administration of FGF2 was not considered necessary. Explant cultures were collected for RNA analysis 6 h after addition of FGF2 unless otherwise indicated. The FGF administration regimens for facial mesenchyme micromass cultures and explant cultures are summarized in Figure 1.

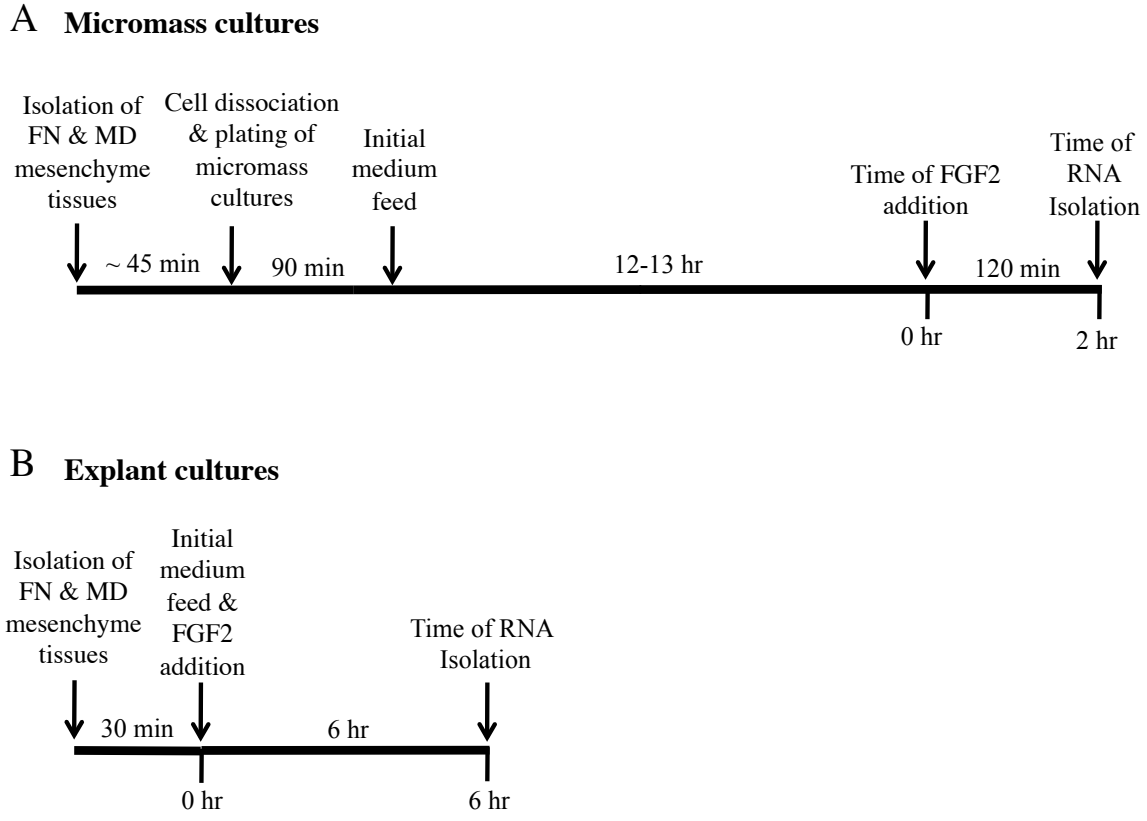

Figure 1 Administration of Growth Factors Experimental Timeline. A timeline detailing the establishment of frontonasal (FN) and mandibular (MD) mesenchyme cultures, administration of FGF, and isolation of total cellular RNA. (A) For micromass cultures, the facial mesenchyme cells were allowed to recover for a period of 12-13 h after tissue dissociation, cell plating and the initial medium feed prior to addition of exogenous FGF2. (B) For explant cultures, the intact facial mesenchyme tissues were treated with FGF2 immediately after excision and removal of adherent epithelia. For both micromass cultures and facial explants, control cultures were established in parallel except that FGF2 was omitted from the culture medium. (Note: timelines are not drawn to scale.)

3.2 RNA isolation & RNA integrity analysis

Stage 24/25 and stage 28/29 chick frontonasal and mandibular micromass and explant cultures were established in triplicate in 35 mm NUNC culture dishes as described above (for micromass cultures: ten to twelve 10 µl spots per plate; for explants: eight to ten intact facial processes per plate). Total RNA was isolated using an E.Z.N.A Total RNA kit (Omega, BioTek, Norcross, GA, USA) according to the manufacturer's protocol. All RNA isolations included a 30 min on-column DNAse I digestion (Omega, BioTek, Norcross, GA, USA) as per the manufacturer's directions. The concentration and purity of the isolated RNA were determined by measuring of total sample absorbance at A_{260} and the A_{260}/A_{280} ratio using a Biorad SmartSpec UV/Vis spectrophotometer (Biorad, Hercules, CA, USA).

Representative samples of total RNA isolated from frontonasal and mandibular micromass and explant cultures were selected randomly and used for verification of RNA integrity prior to further downstream analysis. Overall integrity was assessed using a standard sensitivity RNA microfluidic chip (catalogue no. 700-7110) on an Experion™ Automated Electrophoresis Station (Biorad, Hercules, CA, USA) according to the manufacturer's protocol.

3.3 RNA Dot-Blot and Northern Blot Methodology

3.3.1 RNA dot blot analysis

For RNA dot blot analysis of *pea3*, *er81*, and *erm* gene transcript levels, total RNA was isolated from FGF2 treated and untreated stage 24/25 chick frontonasal and mandibular micromass cultures, and RNA concentration was determined by optical density measurements performed on a NanoVue spectrophotometer (GE Life Science, Fairfield, CT, USA). RNA dot-blot analysis was performed as described previously (Kosher et al., 1986a; Kosher et al., 1986b.; Kulyk et al., 2000).

Briefly, equivalent amounts of each RNA sample were spotted onto 0.45 µm MagnaGraph nylon transfer membrane (GE Water & Process Technologies, Trevose, PA, USA) using a BioDot apparatus (BioRad, Hercules, CA, USA). Nylon blots were subsequently baked in a vacuum oven at 80°C for 90 min, and pre-hybridized for 2-4 h at 42°C in ULTRAHyb™ solution (Ambion, Life Technologies, Carlsbad, CA, USA). The nylon blots were then hybridized overnight in ULTRAHyb™ solution

containing [^{32}P]-labelled single-stranded antisense cDNA probes specific for chicken *pea3*, *erm*, *er81* and glyceraldhyde-3-phosphate dehydrogenase (*gapdh*) mRNAs. For detection of *erm* mRNA transcripts, hybridization was performed at 47°C. For all other genes of interest, the hybridization was performed at a higher stringency temperature of 50°C. The [^{32}P]-labelled single-stranded antisense cDNA probes were synthesized following a modification of the method of Konat (Konat, 1996) as detailed in Section 3.3.3 of Material & Methods below.

After overnight hybridization, the blots were washed in 2X SSC/0.1% (w/v) SDS (4 x 5 min/wash), followed by three 10 min washes in 0.1X SSC/0.1% SDS. All washes were performed at high stringency temperature (55°C) (Kosher et al., 1986a; Kosher et al., 1986b.; Kulyk et al., 2000). Blots were exposed to either Kodak BioMax AR (VWR, Radnor, PA, USA) or HyBlot CL™ AR film (Denville Scientific, Metuchen, NJ, USA) with an intensifier screen at -80°C. When signal strength permitted, densiometric measurements at a wavelength of 540 nm on a Tecan SLT Spectra II spectrophotometric plate reader were used to quantify hybridization signals of exposed autoradiograph. The hybridization signals for *pea3, erm*, and *er81* mRNA were normalized against signals for constitutively expressed *gapdh* transcripts.

3.3.2 Northern blotting

Northern blots were used to verify the specifities of the [^{32}P]-labelled cDNA probes employed in our RNA dot-blot analyses. For Northern blots, total RNA was isolated from whole heads of stage 24/25 chick embryos, then separated by electrophoresis on 1% (w/v) agarose gels containing 6% (w/v) formaldehyde in 1X 3(n-morpholino)propane sulfonic acid (MOPS) buffer at 5 V/cm gel following the methods of Ausebel et al. (Ausubel, 1987). Following electrophoresis, the RNA was transferred by upward capillary action to MagnaGraph nylon membranes (GE Water & Process Technologies, Trevose, PA, USA). The membranes were baked at 80°C for 90 min, prehybridized in ULTRAHyb™ solution, and hybridized to [^{32}P]-labelled single-stranded cDNA probes in ULTRAhyb™ solution. Prehybridization (at 42°C), hybridization (47°-50°C) and subsequent washes (55°C) were performed under the same high stringency conditions described above for RNA dot blots (Materials & Methods Section 3.3.1).

3.3.3 Design and synthesis of [^{32}P]-labelled single-stranded antisense cDNA probes for RNA dot blot & Northern blot assays

In order to generate the [^{32}P]-labelled single-stranded antisense cDNA probes used in Northern blot and RNA dot blot analyses, we followed a modification of the LPCR (linear PCR) strategy of Konat (Konat, 1996). The LPCR method is essentially a modified PCR strategy in which a gene-specific DNA template is used in combination with a single reverse PCR primer and [^{32}P]-dATP to generate labelled single-stranded antisense DNA probes complementary to a gene transcript of interest. Unlike conventional PCR in which the amplicons are double-stranded DNA fragments, the LPCR method generates only antisense amplicons that are complementary to the target mRNA sequence. This greatly increases the sensitivity of the resulting probe for detecting gene transcripts in Northern and RNA dot-blot applications (Konat, 1996). In our lab, we have refined the procedure further by employing strategically designed, custom synthesized single-stranded DNA templates in the LPCR reactions, as summarized below.

First, we used the NCBI nucleotide sequence database and NCBI/Primer-Blast software to identify partial cDNA sequences of 93 - 152 nucleotide length specific for the chicken *pea3*, *erm*, and *er81* mRNA transcripts. Next, a single-stranded synthetic DNA corresponding to each sequence was custom synthesized (Integrated DNA Technologies, Coralville, IA, USA) to serve as a sense-strand template in subsequent LPCR reactions. In addition, a reverse LPCR primer (20-23 nucleotide length) complementary to the 3'-end of each synthetic DNA template was synthesized. (Detailed sequence information for all LPCR templates and primers that were used is provided in Table 1).

The [^{32}P]-dATP labelled single-stranded antisense cDNA probes used in our Northern blot and RNA dot blot analyses were generated using a Strip-EZ® PCR labelling kit (Ambion, Austin, TX, USA) following the manufacturer's linear amplification protocol. The reaction mixtures were subjected to 30 cycles at the following parameters: 94°C for 2 min; 55°C for 2 min, and 72°C for 5 min in an MJ Research Thermocycler (MJ Research, Waltham, MA, USA). The reaction products were passed through a Sephadex G-50 spin column packed in a Costar® spin-X 0.2 µm micropore filtration unit (Sigma, St Louis, MO, USA) to remove unincorporated label, and then used as probes in Northern and RNA dot blot procedures.

Table 1 Primer & Template Sequences Used to Generate Gene-Specific Probes for Northern and RNA dot blot analyses.

Gene	LPCR Primer Sequence (5'-3') (antisense)	Primer T_m°C	Sense Template Sequence (5'-3')	NCBI Accession Number	Corresponding Nucleotides
pea3	TGCTGGGAAGCCA CAGCTGC	63.4	TGGGTGCTGGTGGTGCCAACCCCATATCTGGAGGATG GGACCACTCCTCAGTGTGAAGTCATCACCTGAGCAG GGCAGCTGTGGCTCCCAGCA	AF075708	1195-1291
erm A	TCCATCGTGGCTG CTGGGGA	60.0	AGCAGGAGCCGGGACTACTGCATCGACTCAGAAGTG CCTAACTGCCAGTCCTCATATGTGAGAGGGGGCCTCT TCCCCAGCAGCCACGATGGAC	AF075706	57-153
erm B	CTATAGGGAGGAC GTGTCATC	53.9	GCTTCTACGACCAGCAGGTCCCCTTCATGGGCCCTG GGAAATCCTGTGCCGAGGAGGGCCGAGGCCGGTTG GGCTCCGAGAGGAAAAGGAAGTTTTTGGAGACCGA CCTGGCCCACGACTCGGCCTCCCTATAGTGAGTCGTA TTAGAGCTC	AF075706	91-194
er81	AAGCAAACCCACC CTTTTCCTCCTG	61.6	TCCTATGGTCTGCCATGGACAGCGCACTTTATTTGAA AGGGGAGGGTTGGAAACTAAACATTATTGTGTGTAA CAGGAGGAAAAGGGTGGGTTTGCTT	AF075707	1755-1851
gapdh	CACTCCTTGGATG CCATGTGG	58.4	CACTGTCCATGCCATCACAGCCACACAGAAGACGGT GGATGGCCCCTCTGGGAAGCTGTGGAGAGATGACAG AGGTGCTGCCCAGAACATCATCCCAGCGTCCACTGG GGCTGCTAAGGCTGTGGGGAAAGTCATCCCTGAGCT GAATGGGAAGCTTACTGGAATGGCTTTCCGTGTGCC AACCCCCAATGTCTCTGTTGTTGACCTGACCTGCCGT CTGGAGAAACCAGCCAAGTATGATGATATCAAGAGG GTAGTGAAGGCTGCTGCTGATGGGCCCCTGAAGGGC ATCCTAGGATACACAGAGGACCAGGTTGTCTCCTGTG ACTTCAATGGTGACAGCCATTCTTCCACCTTTGATGC GGGTGCTGGCATTGCACTGAATGACCATTTCGTCAAG CTTGTTTCCTGGTATGACA	K01458	578-1057

Note: The *pea3*, *erm* and *er81* templates were custom synthesized single-stranded DNA sequences. For *gapdh*, the template used was a previously cloned double-stranded partial cDNA. Two different template/primer sets were used for *erm* transcript detection. The *erm* A template/primer combination was used in preliminary RNA dot-blot experiments (see legend for Figure 4). Due to problems with probe labelling, however, a new template/primer combination (*erm* B) was employed for all subsequent RNA dot blot and Northern blot experiments.

3.4 RT-qPCR Analysis Methodology

3.4.1 RT-qPCR primer design

For RT-qPCR analyses of *pea3*, *er81*, *erm*, *gapdh* and *RNA polymerase II b* (*RNA pol II b*) mRNA levels, gene-specific primer pairs were designed using sequence information from the NCBI nucleotide sequence database and the Gene Ensembl database (European Molecular Biology Laboratory; European Bioinformatics Institute), with the assistance of IDT Oligo-analyzer, NCBI Primer Blast and NCBI Blast software programs. All qPCR primers were designed in accordance with published guidelines (Bustin et al., 2009). Wherever possible, the forward qPCR primer and/or reverse qPCR primer were designed so as to span putative exon/intron junctions, in order to minimize the possibility of amplifying genomic DNA sequences in RT-qPCR reactions. Sequence information for all qPCR primers employed is provided in Table 2.

3.4.2 Reverse transcription (cDNA synthesis)

First strand cDNA synthesis from total RNA isolated from chick frontonasal and mandibular mesenchyme cultures was performed using the QuantiTect™ Reverse Transcription Kit (Qiagen, Valencia, CA, USA) which includes a DNAse I digestion step, following the manufacturer's protocol. For each reverse transcription reaction, 1 μg of total RNA was used.

3.4.3 qPCR reactions

The effects of FGF treatment on *pea3*, *erm*, and *er81* gene transcript levels were determined in micromass and explant cultures of stage 24/25 frontonasal and mandibular mesenchyme by RT-qPCR analysis, as detailed below. Gene expression was quantified using chicken-specific qPCR primers and the Maxima® SYBR Green (Fermentas, ThermoScientific, Waltham, MA, USA) reagent system according to manufacturer's protocols. Amplification reactions were performed on an MJ Mini™ Thermal Cycler equipped with a MiniOpticon™ Real-Time PCR detection system (BioRad, Hercules, CA, USA). Gene expression of two reference genes, *gapdh* and *RNA pol II b*, was also analyzed to enable normalization of the *pea3*, *erm*, and *er81* qPCR data in accordance with the MIQE guidelines (Bustin et al., 2009). To prevent

Table 2 Primers used for RT-qPCR analysis.

Gene	NCBI Accession Number	Forward Primer (5'-3')	Reverse Primer (5'-3')	T_m°C	PCR Product Size (nt)
pea3	AF075708	GTGACATCAAGCAGGAGGTC	ACAGCCTGGCTACCTCCTCTG	55.5/58.8	183
erm	AF075706	CAGCCACGATGGATTCTCGTATG	GCTTCACCTTACCCTCCAGTCTC	57.6/58.9	146
er81	AF075707	CCTTCAGGCTGATTGGAGTCC	GGATTATTGGTGACCATGTAAGG	57.6/53.4	91
gapdh	K01458	AGCTGAATGGGAAGCTTACTGG	ACTTGGCTGGTTTCTCCAGACG	57.1/59.4	96
RNA pol II b	NM_001006448	CAAGATCAGGGTACGGTCTG	GAAGGGCATATCCTCTTGCCTG	54.7/57.7	112

contamination of qPCR reactions, all reactions were prepared in a biological safety cabinet decontaminated with a 10% (v/v) bleach solution followed by a 30 min UV irradiation cycle. In addition, 1 µl of uracil-DNA glycosylase (UDG; ThermoScientific, Waltham, MA, USA) was included in each reaction to prevent carry-over contamination (Longo et al., 1990).

Thermocycling parameters were as follows: 50°C for 2 min (UDG pre-treatment), 95°C for 10 min (initial denaturation), and 40 cycles of 95°C for 15 s (denaturation), 55°C (*pea3*)/61°C(*erm*)/58°C (*er81*)/60°C (*gapdh* and *RNA pol II b*) for 30 s (optimal annealing temperatures), and 72°C for 30 s (extension). Melt curve analysis was performed immediately upon the completion of each qPCR reaction to ensure amplification of a single gene product.

For each experiment, RNA was isolated from three replicate cultures for each different treatment group (i.e. 3 biological replicates per treatment, (n = 3); see Figure 2). Each RT-qPCR experiment was repeated a total of three or four times (i.e. 3-4 independent experimental repeats x 3 biological replicates per treatment per experiment; therefore n = 9 or 12).

The mean Cq value for each biological replicate was used for relative gene expression analysis using the Relative Expression Software Tool (REST©) (Qiagen, Valencia, CA, USA) (Pfaffl et al., 2002). For all RT-qPCR experiments involving micromass cultures, two additional independent qPCR experiments were performed, and the resulting data from all experiments pooled for final REST analysis (n = 9). For RT-qPCR gene expression analysis of stage 24/25 frontonasal and mandibular explants, three additional independent qPCR experiments were performed (n = 12).

3.4.4 qPCR primer validation

To determine the optimal annealing temperature for each gene specific primer pair, cDNA generated from the RNA of stage 24/25 chick embryo heads was used in 12-step temperature gradient reactions (covering a temperature range of 52°C-64°C) using the Maxima® SYBR Green RT-qPCR reagent system (Fermentas, ThermoScientific, Waltham, MA, USA) according to the manufacturer's protocol on a MJ Mini Thermal Cycler/MiniOpticon™ instrument (Biorad, Hercules, CA, USA). The annealing temperature that resulted in the earliest quantification cycle (i.e. lowest Cq value) and highest melt peak for each gene specific primer pair was used for all

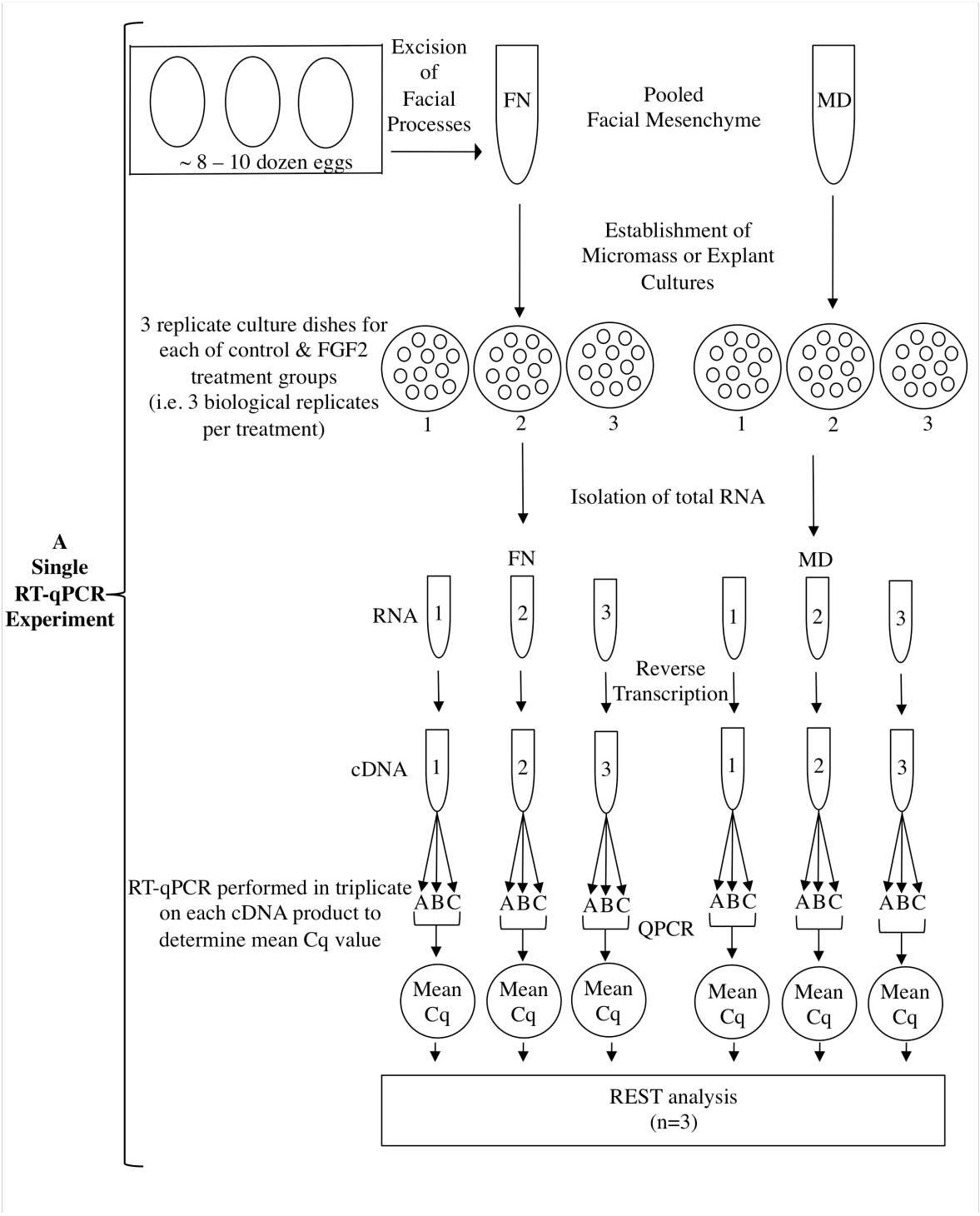

Figure 2 Schematic diagram representing the experimental design for Real-Time Quantitative Polymerase Chain Reaction Experiments. This schematic represents the experimental design of a single RT-qPCR experiment. Each individual RT-qPCR experiment resulted in an n=3 per treatment group. Pooled data from 3 or 4 independent experiments increased the n number for final REST analysis to n=9 for micromass cultures, and n=12 for explant cultures. FN = frontonasal processes (pooled); MD = mandibular processes (pooled); Cq = quantification cycle as determined by RT-qPCR.

subsequent qPCR reactions. To ensure each primer pair amplified only its specific target gene sequence, qPCR temperature gradient products were separated by electrophoresis on a 15% (w/v) polyacrylamide gel using standard protocols. In addition, a melt-curve analysis was performed immediately upon completion of the RT-qPCR reaction to ensure amplification of a single gene product. Reactions containing no cDNA (i.e. no template controls; NTCs) were run alongside samples to verify the absence of primer-dimer formation or contamination of the reagents. Additionally, to ensure adequate removal of genomic DNA (gDNA), six randomly selected samples were used as no reverse transcription controls (NRTs).

3.4.5 Determination of qPCR amplification efficiencies

Amplification efficiencies between gene specific primer pairs commonly differ as a result of variations in primer annealing, G-C content and length of sequence amplified. Therefore, standard curves for each target gene (*pea3*, *erm*, and *er81*) and reference genes (*gapdh* and *RNA pol II b*) were prepared in triplicate. Standard curves for *gapdh* and *RNA pol II b* were created by a 10-fold serial dilution (10x, 1x, 1/10x, 1/100x, 1/1000x, 1/10000x, 1/100000x) of cDNA generated from isolated RNA from heads of stage 24/25 chick embryos. Standard curves for *pea3*, *erm*, and *er81* were prepared by a 5-fold serial dilution of cDNA generated from isolated RNA from heads of stage 24/25 chick embryos (5x, 1x, 1/5x, 1/25x, 1/125x).

3.4.6 Statistical analysis of qPCR data

Relative gene expression of each target gene (*pea3*, *erm*, and *er81*) was normalized to both *gapdh* and *RNA pol II b* in compliance with MIQE guidelines (Bustin et al., 2009). All comparisons were performed using the Relative Expression Software Tool (REST©; Qiagen, Valencia, CA, USA), which employs the Pfaffl method for determination of relative gene expression (Pfaffl, 2001; Pfaffl et al., 2002). The data resulting from all REST™ comparisons are displayed graphically as box-and-whisker plots. For final REST™ analysis, data from three independent micromass culture experiments were pooled (n= 9). Data from four independent explant culture experiments were pooled for final REST™ analysis (n=12).

3.5 Determination of Chondrogenic Differentiation

3.5.1 Alcian blue histochemical detection of sulfated proteogylycans

Alcian blue histochemical staining was used to examine sulfated cartilage matrix proteoglycan accumulation in stage 24/25 and stage 28/29 micromass cultures. Micromass cultures were established and treated with FGF2 as described in Materials & Methods Sections 3.1.2 and 3.2.4. FGF treated and untreated (control) frontonasal and mandibular micromass cultures were collected after 2 or 3 days, respectively, of incubation at 37°C/5% CO_2. Cultures were then stained overnight with 0.2% (w/v) Alcian blue 8 GX (Fluka, Sigma, St Louis, MO, USA), pH 1.0 (Chang et al., 1998; Hassell and Horigan, 1982). After staining, cultures were rinsed once with distilled water to remove unbound dye. Representative Alcian blue stained cultures were air dried and photographed.

For other cultures, the bound Alcian blue stain was eluted and quantified spectrophotmetrically as previously described (Chang et al., 1998; Hassell and Horigan, 1982). Briefly, 4 M guanidine hydrochloride was added to each stained culture, the plates were sealed with parafilm, then incubated overnight at room temperature. Equal volumes of the eluted dye solution were transferred to a 96-well microtiter plate and absorbance of each sample was measured using a Tecan SLT Spectra II plate reader at a wavelength of 600 nm. For some experiments, absorbance readings were then normalized against the average DNA content of replicate parallel cultures. A fluorescence assay (Labarca and Paigen, 1980) was used to determine total DNA of micromass cultures, as detailed below.

3.5.2 Hoechst 33258 DNA fluorescence assay

The total DNA content of frontonasal and mandibular facial mesenchyme micromass cultures was quantified using a Hoechst 33258 (Sigma, St Louis, MO, USA) fluorescence assay (Labarca and Paigen, 1980). Each micromass culture was sonicated in 350 µl Hank's buffered saline solution (HBS). Then a 100 µl volume of each sonicate was combined with 100 µl of 4 µg/ml Hoechst dye, and 200 µl assay buffer (0.1 M $NaPO_4$, 4 M NaCl, pH 7.4). Aliquots (200 µl) of each sample were transferred to individual wells of a black 96-well microtiter plate, and read on a fluorometer (Fluorolite 1000, Dynex, Richfield, MN, USA) at an excitation wavelength of 365 nm and an emission wavelength of 458 nm. A series of chicken

DNA (Pharmacia, Piscataway, NJ, USA) standards (0.25, 0.50, 1, 2, and 4 μg total DNA) was prepared in a similar manner and run alongside cell culture sonicate samples. The DNA content of each sample was determined from a standard curve and quantified by linear regression analysis using InStat 2.01 (GraphPad) software. The resulting DNA values were used to normalize densitometric data of eluted Alcian blue eluted from frontonasal and mandibular mesenchyme micromass cultures.

3.5.3 Quantification of sulfated glycosaminoglycan accumulation

A 1,9-dimethylmethylene blue (DMMB) assay, based on the methods of (Barbosa et al., 2003), was used for quantification of total sulphated GAGs in the cell layer and medium fractions of stage 24/25 and stage 28/29 frontonasal and mandibular micromass cultures. To prepare the DMMB stock solution, 16 mg of 1,9-dimethylmethylene blue dye was dissolved in 25 ml ethanol and filtered through standard filter paper. The DMMB working solution was prepared in several steps to prevent the DDMB dye from precipitating out of solution. First, 35 ml of distilled water, 8.3 ml of 6 M guanidine hydrochloride, 0.5 g sodium formate, and 0.5 ml of 98% (v/v) formic acid was mixed, and brought to a final volume of 50 ml in distilled water (solution A). Solution B was prepared by adding 25 ml of solution A to 6.25 ml absolute ethanol. The solution was then brought to a final volume of 125 ml in distilled water. To prepare solution C, 25 ml of solution B was added to 6.25 ml DMMB stock solution, mixed quickly and brought to a final volume of 125 ml in distilled water. To prepare the final DMMB working solution, equal volumes of solutions B and C were combined and stored in the dark at room temperature. DMMB Wash Solution was prepared by the addition of 35 ml of distilled water, 8.33 ml of 6 M guanidine hydrochloride, 0.5 mg sodium formate, and 0.5 ml 98% (v/v) formic acid in a final volume of 50 ml in distilled water. To this solution, 12.5 ml of 95% (v/v) ethanol and 187 ml of distilled water was added. DMMB Decomplexing Solution was prepared by combining, 134 ml 6 M guanidine hydrochloride, 40 ml 0.25 M sodium acetate solution [pH 6.8], 20 ml 1-propanol, and 6 ml of distilled water.

To perform the DMMB assay, the medium was removed from each facial mesenchyme micromass culture and transferred to a microcentrifuge tube. The micromass cell layer was detached from the culture dish, collected in 350 μl Hank's buffered saline solution (HBSS), and transferred to separate microcentrifuge tubes. A

1µl volume of 5 mg/ml Proteinase K (Invitrogen Life Technologies, Carlsbad, CA, USA) solution (20 mg proteinase K in 4 ml of 10mM Tris HCl [pH 7.5], 20mM $CaCl_2$ (Sigma, St Louis, MO, USA), and 50% glycerol) was added to both the medium and cell layer fractions. Following overnight incubation at 50°C, all samples were heated for 10 min at 90°C. Cell layer fractions were homogenized by repeated pipetting and a 100 µl aliquot was withdrawn for determination of total DNA content by the Hoechst 33258 fluorescence assay as described in Materials & Methods Section 3.5.2. The remainder of the cell layer homogenate was passed through a Millipore Ultrafree spin-filter (Millipore, Billerica, MA, USA) to remove DNA and cellular debris. A series of chondroitin sulphate standards (0 µg/100 µl to 8 µg/100 µl) was prepared alongside the cellular and medium fraction samples. To 100 µl of each cell layer, medium, or chondroitin sulphate standard, 1 ml of DMMB working solution was added. The samples were vortexed vigorously for 30 min, then centrifuged at 16,000g for 15 min at 4 °C. Following careful aspiration of the supernatant, 1 ml of DMMB Wash Solution was added to each sample. The samples were re-centrifuged (16,000g, 15 min, 4°C), and the supernatant removed by aspiration. To each pelleted insoluble GAG/DMMB complex, 1 ml of Decomplexing Solution was added. Samples were vortexed vigorously for 20 min, and 200 µl aliquots of each sample were transferred to individual wells of a 96-well transparent microtiter plate. A Tecan SLT Spectra II spectrophotometric plate reader was used to measure absorbance at a wavelength of 650 nm. The concentration of total sulfated GAGs in each cell layer and medium sample was then determined from the linear regression equation of the chondroitin sulphate standard curve using InStat 2.01 software.

3.5.4 Type II collagen immunostaining

Accumulation of type II collagen in stage 24/25 and stage 28/29 frontonasal and mandibular micromass cultures was detected by immunocytochemical staining with a monoclonal antibody against chicken type II collagen as previously described (Bobick and Kulyk, 2004). Briefly, frontonasal and mandibular micromass cultures were harvested after 2 or 3 days of incubation, washed twice in phosphate buffered saline (PBS) Tween-20 (PBST) (1 x 1 min; 1 x 5 min), and fixed for 30 min in 95% (v/v) ethanol containing 2% (v/v) acetic acid. After fixation, the cultures were rinsed in 70% (v/v) ethanol 3 times (1 x 1 min; 2 x 5 min/wash), and stored in 70% (v/v) ethanol for up to 2 weeks. Micromass cultures were rehydrated by rinsing for 5 min

each in decreasing ethanol concentrations (70%, 50%, 25%, 0% (v/v) ethanol in distilled water) and post-fixed for 1 h in 4% (v/v) formalin/PBST. Following post-fixation, cultures were washed (3 x 5 min) in PBST, and blocked for 90 min in 5% sheep serum (v/v) (Sigma, St Louis, MO, USA)/PBST. Micromass cultures were incubated for 1 h in a 1:50 dilution of chicken collagen II monoclonal antibody II-II6B3 hybridoma supernatant (Developmental Studies Hybridoma Bank, University of Iowa) in 5% (v/v) sheep serum/PBST. Following primary antibody incubation, micromass cultures were washed (4 x 5 min/wash) in PBST and incubated for 1 h in a 1:250 dilution of alkaline phosphatase-conjugated goat anti-mouse IgG antibody (Sigma, St Louis, MO, USA) in 5% (v/v) sheep serum/PBST. Cultures were subsequently washed (3 x 10 min/wash) in PBST containing 0.05% levamisole and then washed (2 x 15 min/wash) in NTMT (100 mM Tris HCl, pH 9.5, 50 mM MgCl2, 100 mM NaCl, 0.1% (v/v) Triton X-100, 0.05% (w/v) levamisole). Micromass cultures were incubated for 30-60 min in nitroblue tetrazolium chloride (0.34 mg/ml) and 5-bromo-4-chloro-2-indolylphosphate (0.175 mg/ml) dissolved in NTMT to permit colour development. Following development, cultures were rinsed 3 times in PBST, then stored in CMFET solution (0.137 M NaCl, 0.003 M KCl, 0.008 Na_2HPO_4, 0.0015 M KH_2PO_4, 0.7 mM EDTA, 0.1% [v/v] Tween-20) at 4°C prior to photographing.

3.6 Western Blot Protein Analyses

3.6.1 Protein quantification

The method of Minamide and Bamburg were used to determine cellular protein content (Minamide and Bamburg, 1990) of samples used for Western blot analysis. This filter paper based adaptation of the Bradford protein-dye binding assay (Bradford, 1976), has several advantages over the original Bradford method, including increased sensitivity and a resistance to interference by reagents used in cell lysis buffers, such as sodium dodecyl sulphate (SDS) and bromophenol blue.

In brief, sonicated cell/tissue homogenates (see below) were spotted in aliquot volumes ranging between 0.625 µl and 25 µl onto individual squares of a 1.5 cm x 1.5 cm grid drawn on Whatman No.1 filter paper. A series of protein standards (a 1:3 mixture of BSA and ϒ-globulin; 0 to 20 µg total protein per square) were spotted alongside samples of unknown protein concentration. All samples were spotted in

triplicate. Spotted filter paper was air-dried, rinsed in absolute methanol for approximately 1 min to remove non-proteinaceous materials, and re-dried. The filter paper was washed in 0.5% (w/v) Coomasie brilliant blue G in 7% (v/v) acetic acid for 30 min at room temperature with gentle agitation, then washed in 7% acetic acid (v/v) to reduce background staining. After air-drying, individual filter paper squares were cut out and placed in microcentrifuge tubes containing 1 ml of extraction buffer (66% (v/v) methanol, 1% (v/v) ammonium hydroxide, and 33% (v/v) distilled water). A 300 µl aliquot of each sample was transferred to a 96-well microtiter plate and the absorbance of each sample at 600 nm wavelength was read on a Tecan SLT Spectra II plate reader. A standard curve was generated by plotting the absorbance values of the protein standards against their known protein content. The linear regression equation of the standard curve was then used to determine cellular protein content for each experimental sample.

3.6.2 Western blot analysis

For Western blot protein analysis, stage 24/25 chick frontonasal and mandibular micromass cultures were spotted on 35 mm NUNC tissue culture plates (10 - 12 spots per dish) and treated with FGF2 as described previously. Micromass cultures were harvested at representative time points (2, 6, 12, 24, and 48 h following FGF2 treatment), and cells from each individual culture plate were homogenized in 250 µl lysis buffer (Puck's saline containing protease inhibitors (4 mM phenylmethylsulfonyl fluoride; PMSF) and Sigma protease inhibitor cocktail P8340 (used at 2X final concentration; Sigma, St Louis, MO, USA). A 50 µl volume of 1 M dithioreitol (DTT) and 50 µl of 6X Laemmli SDS-sample reducing buffer (BioPLUS Fine Research Chemicals, distributed by Cedarlane, Burlington, ON, CA) were added to each lysate. The samples were sonicated, subjected to denaturing gel electrophoresis and protein transfer to NitroPure supported nitrocellulose (GE Water & Process Technologies, Trevose, PA, USA) using the Biorad Protean II Minigel apparatus (Biorad, Hercules, CA, USA) according to standard protocols. Proteins were separated on 12.5% (w/v) polyacrylamide gels containing 0.1% (w/v) SDS. Following overnight wet transfer at 4°C onto nitrocellulose membranes, blots were air dried and blocked in 10% (w/v) blotting-grade non-fat dry milk (BioRad, Hercules, CA, USA)/PBST for 3 h. Primary and secondary antibodies were diluted in 2% (w/v) blotting-grade non-fat dry milk in PBST. Total Pea3 was detected using a 1:5000

dilution of polyclonal antibody against mouse Pea3 protein (Abcam, Cambridge, MA, USA; catalogue no. ab101455). Total Er81 was detected using a 1:2500 dilution of monoclonal hybridoma supernatant 72.5B10 against chicken Er81 (Developmental Studies Hybridoma Bank, University of Iowa). GAPDH was detected using a 1:10000 dilution of anti-GAPDH antibody (Calbiochem, Millipore, Billerica, MA, USA; catalogue no. CB1001). Attempts to detect total Erm using a rabbit polyclonal antibody (Aviva Systems Biology, San Diego, CA, USA; catalogue no. ARP38468_P050) were unsuccessful as developed blots exhibited non-specific multiple banding patterns. All primary antibody incubations were carried out overnight at 4°C. Following primary antibody incubation, nitrocellulose blots were washed (3 x 1 min; 2 x 5 min) in PBST, and incubated at room temperature for 90 min in the appropriate anti-mouse or anti-rabbit horseradish peroxidase-conjugated secondary antibodies (Calbiochem, Millipore, Billerica, MA, USA) at the following concentrations: 1:10000 (for Pea3 detection); 1:5000 (for Er81); and 1:100,000 (for GAPDH). Blots were subsequently washed in PBST (1 x 1 min; 3 x 5 min). Signal detection was performed using the SuperSignal West Femto Chemiluminescent Substrate (ThermoScientific, Waltham, MA, USA) as per the manufacturer's instructions. The chemiluminescence signals were captured using the Versadoc™ (Biorad, Hercules, CA, USA) imaging system.

3.7 Statistical analysis

Statistical analysis of data pertaining to Alcian blue staining, cellular DNA measurements, and sulfated GAG accumulation was performed by a one-way analysis of variance (ANOVA) with the Bonferroni multiple comparison post-hoc test using InStat 2.01 software, and graphed with Microsoft® Excel® 2008. All RT-qPCR gene expression comparisons were performed using REST© software as described in Material & Methods Section 3.4.6. P-values less than 0.05 were considered statistically significant.

4 RESULTS

4.1 Initial Investigation of *pea3*, *erm*, and *er81* mRNA expression

4.1.1 Confirmation of cDNA probe specifities by Northern blot analysis

In initial experiments, conventional methods of Northern blot hybridization and RNA dot blot hybridization were used to examine expression of the *pea3*, *erm*, and *er81* gene transcripts in chick embryo facial mesenchyme tissues. Antisense cDNA probes for each gene were generated from custom synthesized synthetic DNA templates as described in Material & Methods Section 3.3.3.

Northern blot analysis was performed to determine the specificity of the cDNA probes for their mRNA respective targets (*pea3*, *er81*, and *erm*). Since the mRNA of Pea3 transcription factors is expressed in relatively high levels within the developing brains of chick embryos (Lunn et al., 2007), total RNA was isolated from freshly excised whole heads of stage 24/25 chick embryos. Equivalent amounts (5 μg) of total RNA were separated by agarose gel electrophoresis and blotted by upward capillary transfer onto nylon membrane. The membranes were hybridized to ^{32}P-labelled antisense cDNA probes and washed under high stringency conditions following standard protocols.

The *pea3* cDNA probe specifically recognized a single transcript of approximately 3.9 kb (Figure 3A). A solitary transcript of approximately 3.45 kb was recognized by the *erm* cDNA probe (Figure 3 B). The *er81* cDNA probe specifically recognized two transcripts of approximately 3.7 kb and 3.2 kb (Figure 3C), which is consistent with a previous report that there are two alternatively spliced *er81* mRNA isoforms in the mouse and human (Coutte et al., 1999). Consistent with previously published results, the *gapdh* cDNA probe specifically recognized a single transcript of approximately 1.5 kb (Figure 3D) (Bobick et al., 2007; Milner et al., 1983).

4.1.2 Preliminary RNA dot blot analysis

RNA dot-blot analysis was used to examine the effects of FGFs on *pea3*, *erm*, and *er81* mRNA expression profiles during chondrogenesis. Micromass cultures of stage 24/25 frontonasal mesenchyme and stage 24/25 mandibular mesenchyme cells were cultured for 2, 5, 12, or 20 h in control DMEM:F12/10% FBS medium or in

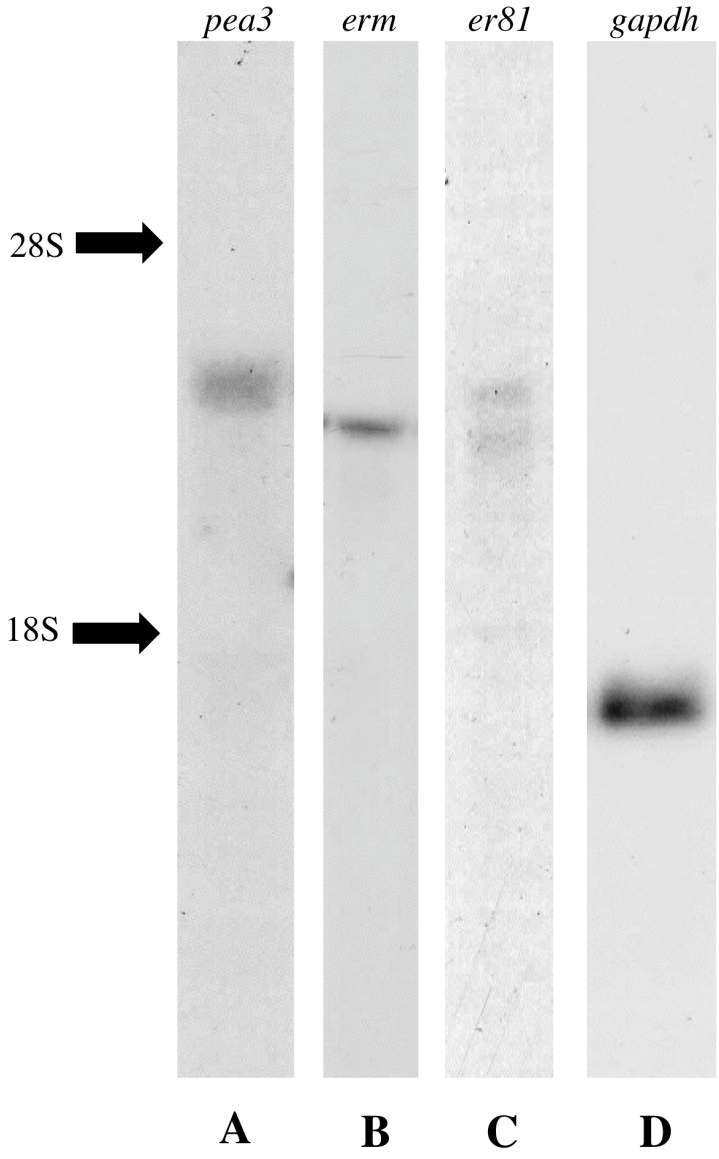

Figure 3 Northern blot analysis of *pea3*, *erm*, *er81*, and *gapdh* gene cDNA probe specifities. Total RNA was isolated from the whole heads of stage 24/25 chick embryos and processed for Northern blot analysis. The *pea3* (A) and *erm* (B) cDNA probes each recognized a single mRNA transcript of approximately 3.9 kb and 3.45 kb length, respectively. The probe for *er81* (C) recognized two gene transcripts of approximately 3.2 kb and 3.7 kb. The cDNA probe for *gapdh* (D) specifically recognized a probe of approximately 1.5 kb.

FGF supplemented (20ng/ml) DMEM:F12/10% FBS medium.

In both stage 24/25 frontonasal and mandibular mesenchyme micromass cultures, FGF2 treatment elevated expression of *pea3* mRNA in comparison to untreated controls at all examined time points (2, 5, 12, and 20 h) (Figure 4 A). Similarly, FGF2 also elevated expression of *er81* mRNA transcripts at all time points in stage 24/25 frontonasal and mandibular mesenchyme micromass cultures relative to untreated controls (Figure 4B). This suggests FGF2 upregulates *pea3* and *er81* in both frontonasal and mandibular mesenchyme micromass cultures. In control cultures, the signals for *pea3* and *er81* were barely detectable above background levels. Since it was not possible to perform accurate densitometric measurements on the very faint hybridization signals from control cultures on these RNA dot blots, it was not possible to determine the quantitative extents to which the *pea3* and *er81* transcript levels were upregulated following FGF treatment.

Despite detection of a single *erm* mRNA transcript on a Northern blot of stage 24/25 chick embryo head RNA, *erm* transcripts were not detected in RNA dot blots of stage 24/25 frontonasal and mandibular mesenchyme micromass cultures (data not shown). The number of *erm* mRNA transcripts may have been below the detection limit of the RNA dot blot assay. In addition, since densitometric quantification of *pea3* and *er81* mRNAs was not feasible in untreated control cultures of facial mesenchyme, more sensitive detection methods were required. Real-Time Quantitative PCR (RT-qPCR) is reported to be capable of detecting less than five copies of a target sequence (VanGuilder et al., 2008), and was therefore utilized for further expression analysis of *pea3*, *erm*, and *er81* mRNA gene transcripts.

4.2 Validation of RNA Isolation Methodology & RT-qPCR Optimization

4.2.1 Isolation of high quality RNA

RT-qPCR consists of multiple rounds of enzymatic reactions, and is thus more sensitive to impurities which can interfere with fluorescence detection such as proteins, phenol/chloroform and other chemical solvents, than single-step enzymatic reactions (Bustin, 2005). Additionally, RT-qPCR requires RNA preparations to be free of contaminating genomic DNA (gDNA) as even low levels of gDNA contamination are capable of dramatically shifting quantification cycle (Cq) values. This is of particular importance for genes with a low copy number

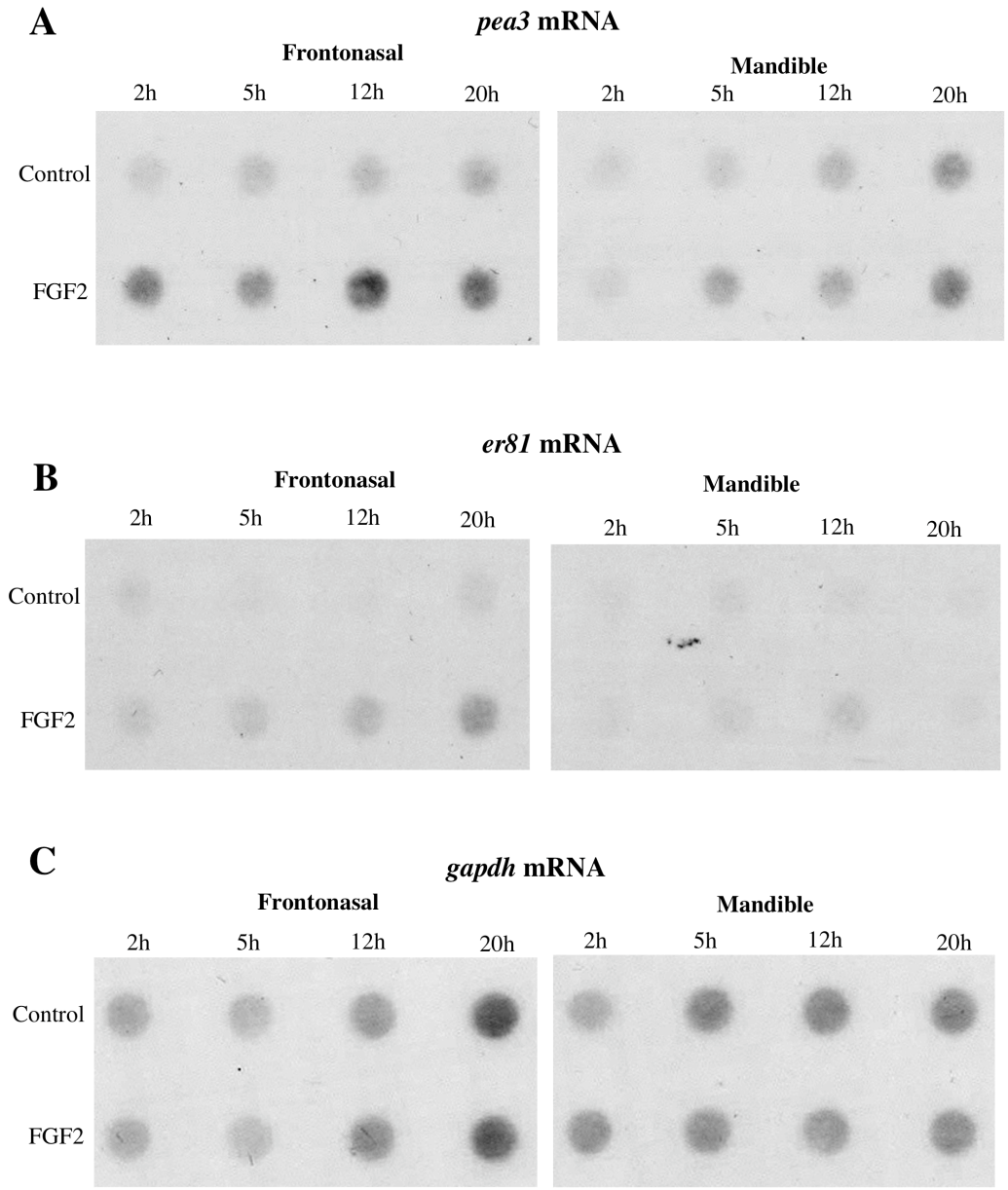

Figure 4 RNA dot blot analysis demonstrating the effects of FGF2 treatment on *pea3* and *er81* mRNA levels in chicken stage 24/25 frontonasal and mandibular mesenchyme micromass cultures. Cultures were incubated for 2, 5, 12, or 20 h in medium supplemented with 20 ng/ml FGF2 or unsupplemented medium alone (control). (A) In stage 24/25 frontonasal and mandibular mesenchyme micromass cultures, FGF2 increased accumulation of *pea3* gene transcripts at all time points. (B) *er81* mRNA transcripts also increased at all time points in both frontonasal and mandibular mesenchyme micromass cultures treated with FGF2. (C) mRNA transcript levels of the constitutively expressed *gapdh* were similar in control and FGF2 treatment samples at most time points.

(Fleige and Pfaffl, 2006). Accordingly, it was important to validate the quality of the RNA isolation protocol and the integrity of the resulting product.

Representative samples of total RNA prepared from stage 24/25 and 28/29 chick frontonasal and mandibular micromass and explant cultures were selected at random for quality and purity analysis using a standard sensitivity RNA microfluidic chip on an Experion™ Automated Electrophoresis Station (Biorad, Hercules, CA, USA). The Experion™ system generates a RNA quality indicator (RQI) score of 1-10 as a quantitative assessment of RNA integrity. The RQI scores are determined on the ratio of the 28S to 18S rRNA concentration of a sample as well as the sharpness of the two rRNA peaks. A score of 10 represents highest RNA integrity, while samples with RQI values below 7 are not recommended for downstream applications.

A representative electrophoretogram (Figure 5A) and virtual gel (Figure 5B) generated on the Experion™ system of for a sample of total RNA isolated from FGF2 treated stage 24/25 mandibular mesenchyme are shown in Figure 5. A random group of isolated RNA samples consistently yielded RQI scores ranging between 9 and 10, and 28S:18S ratios ranging between 1.48-2.20 (Figure 5C). Therefore, the RNA is of sufficiently high quality to perform RT-qPCR analysis.

4.2.2 RT-qPCR profiles

Following validation of the RNA isolation methods, the optimal annealing temperature (T_a) for each gene specific qPCR primer pair was determined by performing a 12-step temperature gradient PCR at temperatures ranging from 52°C-64°C. Amplified products from temperature gradient reactions were analyzed on 15% polyacrylamide gels. This verified that a single amplicon of the predicted size was generated for each gene specific primer set (Figure 6A-E).

The currently recommended practice is that qPCR amplification efficiency for each specific target gene and reference gene must be determined separately through the use of standard curves to enable accurate computations of relative gene expression levels (Ruijter et al., 2009). This is accomplished by performing qPCR on serially diluted cDNA samples (Nolan et al., 2006; Pfaffl, 2001). As shown in Figure 7A-E, the standard curves that were generated for the *pea3*, *erm*, and *er81* target genes, as well as for the *gapdh* and *RNA pol II b* reference genes, yielded reaction efficiencies ranging from 86% - 105.2%. In accordance with the MIQE guidelines, NTC

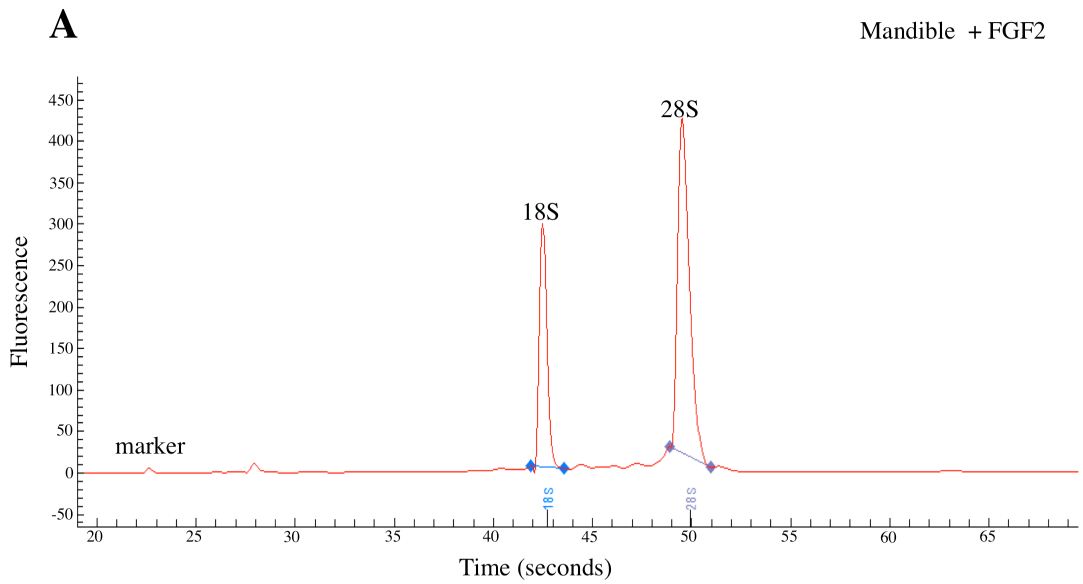

B

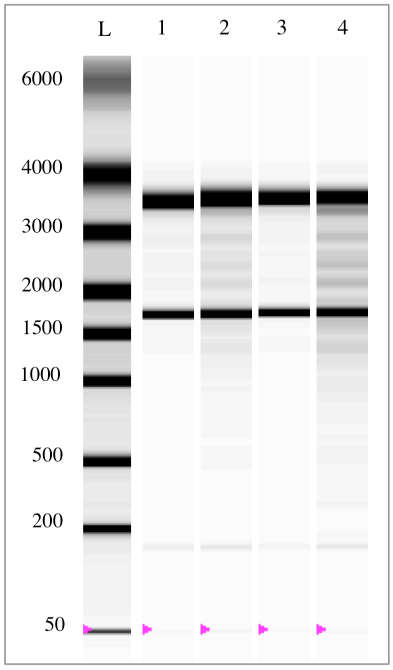

C

Lane	Sample	Ratio (28S/18S)	RQI
1	Frontonasal Control	2.20	10.0
2	Frontonasal + FGF2	2.12	9.9
3	Mandible Control	2.02	10.0
4	Mandible + FGF2	1.73	9.6

Figure 5 RNA integrity analysis. (A) An electrophoretogram and corresponding virtual gel (B) for a representative total RNA sample isolated from a FGF2 treated stage 24/25 mandibular mesenchyme micromass culture as generated by the Biorad Experion™ Automated Electrophoresis Station. The electrophoretogram shown in panel A corresponds to the RNA sample in lane 4 of panel B. Relative positions of the lower alignment marker, 18S rRNA, and 28S rRNA, are indicated. (B) In the virtual gel shown in panel B, the left column (L) of the virtual gel represents the relative positions of the RNA standards, which ranged from 50 - 6000 base length. The prominent 18S and 28S rRNA bands of the different facial RNA samples are seen in lanes 1 to 4. The 28S/18S ratios and corresponding RQI values for these same representative samples are shown in (C).

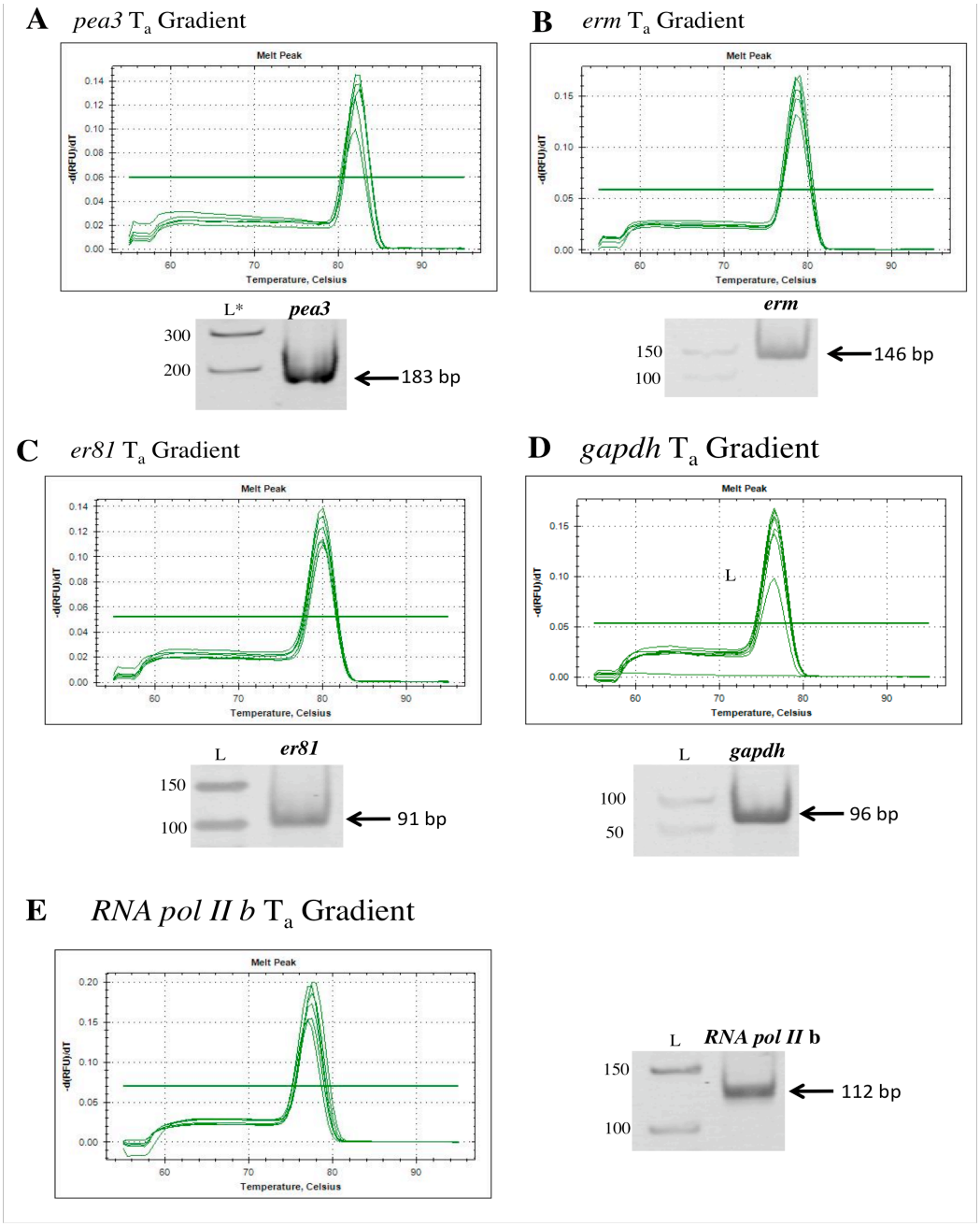

Figure 6 RT-qPCR primer annealing temperature optimization. Each gene specific primer pair was tested in a 12-step temperature gradient PCR using cDNA prepared from stage 24/25 chick embryo head RNA in order to determine optimal primer annealing temperature (T_a). Optimal annealing temperatures were: *pea3*/55°C, *erm*/61°C, *er81*/58°C, gapdh and *RNA pol II* b/60°C. Melt curve analysis was performed immediately upon completion of the RT-qPCR reaction. Amplified products were separated by electrophoresis on 15% polyacrylamide gels to ensure amplification of a single gene product. (A) Primers for *pea3* specifically amplified a single transcript of approximately 183 bp. Single products of approximately 146 bp and 91 bp were amplified by specific primers for *erm* (B) and *er81* (C), respectively. (D) Primers for *gapdh* amplified a single transcript of approximately 96 bp. (E) A single transcript of approximately 112 bp for *RNA pol II b* was amplified. L*= Gene Ruler, 100 bp DNA ladder; L=Gene Ruler 50 bp DNA ladder (Thermo Scientific).

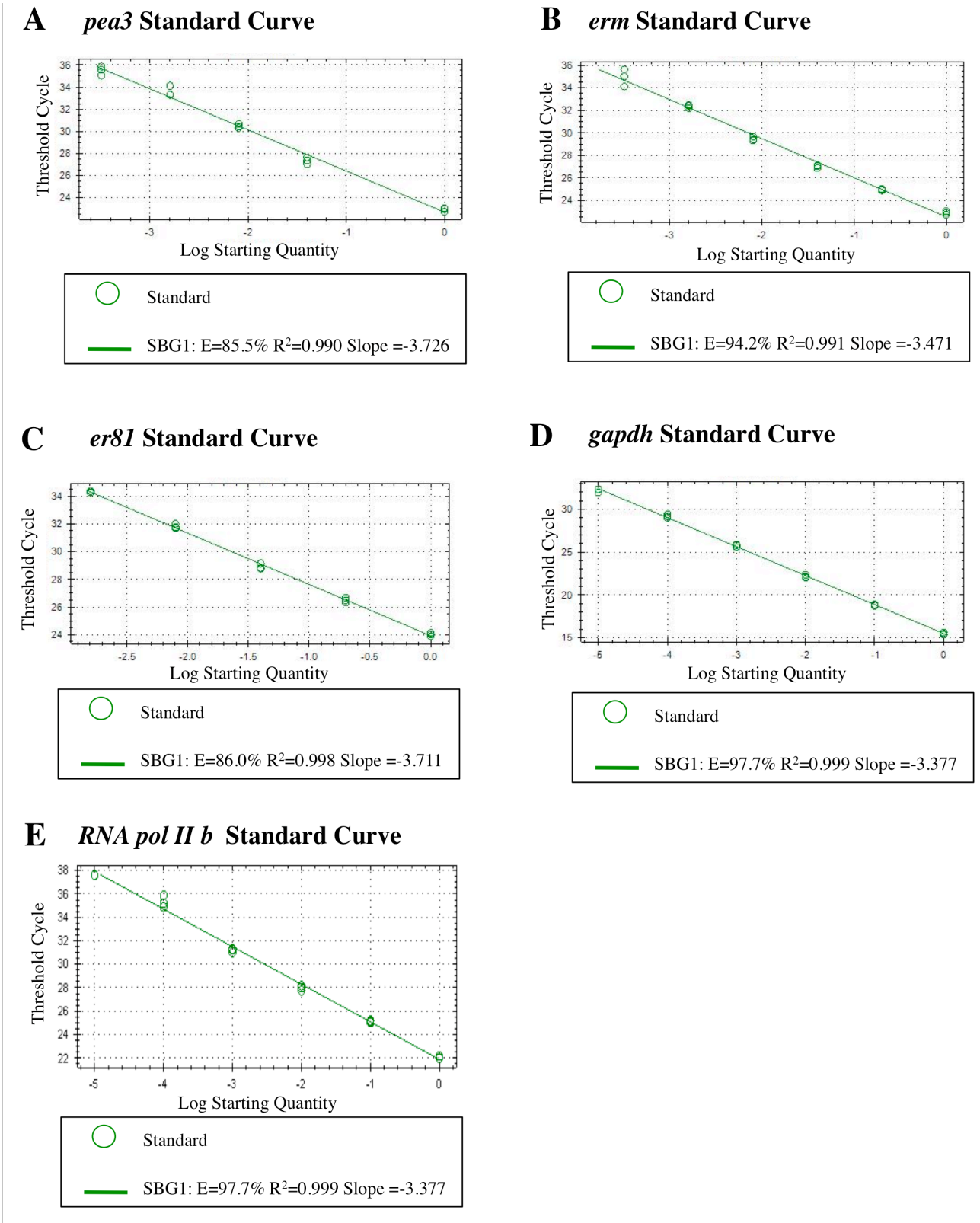

Figure 7 Determination of RT-qPCR amplification efficiencies for *pea3*, *erm*, *er81*, *gapdh* and *RNA pol II b*. Standard curves for (A) *pea3*, (B) *erm*, (C) *er81*, (D) *gapdh*, and (E) *RNA polymerase II b* were created by 5 fold (*pea3*, *erm*, *er81*) or 10 fold (*gapdh*, *RNA pol II b*) serial dilutions of cDNA generated from RNA of stage 24/25 chick embryo heads. All efficiencies and correlation coefficients fall within the acceptable range as recommended by BioRad and closely adhere to MIQE guidelines.

reactions, used to verify the absence of primer-dimer formation and reagent contamination, had Cq values at least 5 cycles greater than the least expressed transcript in experimental reactions (Bustin et al., 2009).

4.3 RT-qPCR RNA Analyses of Pea3, Erm and Er81 Expression in Frontonasal and Mandibular Mesenchyme Cultures

4.3.1 RT-qPCR analysis of FGF effects on micromass cultures

Micromass cultures of stage 24/25 chick embryo frontonasal and mandibular mesenchyme cells were incubated in the presence or absence of 20 ng/ml FGF2 for 2 h, and collected for isolation of total RNA. cDNA was synthesized by reverse transcription, and used for RT-qPCR to determine the effects of FGF2 treatment on *pea3*, *erm* and *er81* mRNA levels. The resulting qPCR data were statistically analyzed using the Relative Expression Software Tool (REST™).

As shown in Figure 8A, stage 24/25 frontonasal mesenchyme micromass cultures treated with FGF2 exhibited significantly increased levels of *pea3* gene transcripts relative to untreated control cultures by approximately 2.8-fold ($p = 0.003$). In addition, *er81* gene transcripts were significantly elevated in response to FGF2 by approximately1.6-fold relative to untreated controls ($p = 0.022$). However, *erm* gene transcript levels in stage 24/25 chick frontonasal mesenchyme were not significantly different in control versus FGF2 treated micromass cultures.

Similar to the frontonasal cultures, micromass cultures of stage 24/25 mandibular mesenchyme micromass cultures treated with FGF2 exhibited elevated levels of *pea3* gene expression by approximately 2.5-fold ($p = 0.001$) relative to untreated mandibular cultures (Figure 8B). Unlike the frontonasal micromass cultures, *erm* mRNA transcripts were increased approximately 1.6 fold in stage 24/25 mandibular mesenchyme micromass cultures treated with FGF2 relative to untreated controls ($p = 0.014$). In addition, whereas FGF2 treatment elevated *er81* expression in stage 24/25 frontonasal micromass cultures, FGF2 treatment had no significant effect on *er81* transcript levels in treated mandibular micromass cultures (Figure 8B).

4.3.2 RT-qPCR analysis of explant cultures

Establishment of micromass cultures requires the dissociation of the facial mesenchyme tissue, resulting in loss of the original cell-cell contacts. Since the nature of cell-cell interactions might influence the response of prechondrogenic mesenchyme

Figure 8 Effects of FGF2 on *pea3*, *erm*, and e*r*81 mRNA transcript levels in stage 24/25 chick frontonasal and mandibular mesenchyme micromass cultures. Relative gene expression ratios generated using the REST™ qPCR data analysis software are represented as "box and whisker" graph. The graph for each gene of interest (i.e. *pea3*, *er81*, *erm*) indicates the level of mRNA expression in FGF2 treated cultures as a ratio of level in untreated control cultures. Therefore, the position of "1" on the "y" axis represents the median control value, while the position of the dotted line within the "box" for each gene of interest represents the median value for FGF2-treated cultures. The top and bottom of each "box" represent the 75^{th} and 25^{th} percentile limits, whereas bars at the upper and lower ends of the "whiskers" represent the highest and lowest individual sample values. Asterisks (*) indicate FGF2 treatment effects that were statistically significant at $p < 0.05$.
(Note: All RT-qPCR data shown in Figures 8 through 11 are represented in the same manner. In all cases, the relative expression values for the *pea3*, *er81* and *erm* gene transcripts were normalized against the expression levels of the *gapdh* and *RNA pol II b* reference genes, as described in Materials and Methods). (A) REST analysis revealed that *pea3* transcript levels were upregulated by a factor of 2.8-fold in FGF2 treated stage 24/25 frontonasal mesenchyme micromass cultures relative to untreated controls ($p = 0.003$). In the same cultures, *er81* transcript levels were elevated 1.6-fold in response to FGF2 exposure ($p = 0.022$). In contrast, FGF2 treatment had no significant effect on erm transcript levels. (B) *pea3* expression was upregulated 2.5-fold in stage 24/25 mandibular micromass cultures treated with FGF2 ($p = 0.001$), and *erm* was upregulated 1.6-fold ($p = 0.014$). *er81* mRNA levels were not significantly different in control and by FGF2 treated cultures.

A

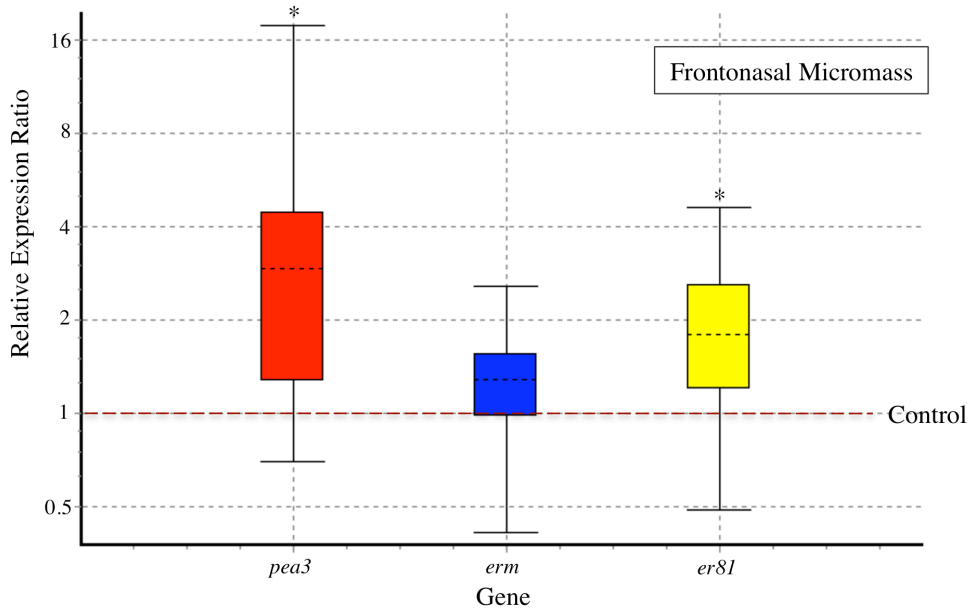
Frontonasal Micromass
Relative Expression Ratio
16
8
4
2
1
0.5
Control
*
*
pea3
erm
er81
Gene

B

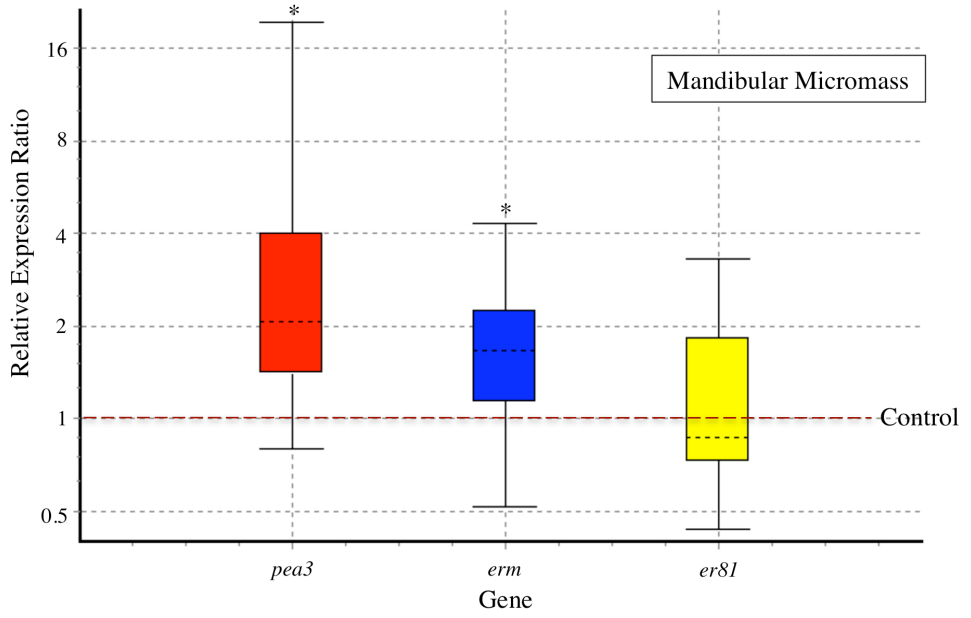
Mandibular Micromass
Relative Expression Ratio
16
8
4
2
1
0.5
Control
*
*
pea3
erm
er81
Gene

cells to growth factors, we also examined the effects of FGF2 on *pea3*, *erm* and *er81* expression in facial mesenchyme explants, which preserved native intercellular contacts. Isolated stage 24/25 frontonasal and mandibular mesenchyme tissue explants were cultured in the presence or absence of 20 ng/ml FGF2 for 6 h, and harvested for total RNA isolation and cDNA synthesis, then *pea3*, *erm*, and *er81gene* expression was examined by RT-qPCR as described previously.

As shown in Figure 9A, in stage 24/25 frontonasal explants, FGF2 treatment upregulated *pea3* expression approximately 2.9-fold relative to untreated control explants ($p = 0.036$). However, FGF2 treatment had no significant effect on either *er81* or *erm* mRNA levels in stage 24/25 frontonasal explants.

Interestingly, in mandibular mesenchyme explant cultures, FGF2 exposure had no significant effects on either *pea3* or *er81* expression (Figure 9B). There appeared to be a trend towards elevated *erm* mRNA expression in response to FGF2 treatment in mandibular explant cultures, although the difference fell short of statistical significance ($p = 0.055$). This contrasts with the situation for frontonasal explants, where FGF2 elevated pea3 expression by 2.9-fold. It also differs from the situation observed for micromass cultures of both frontonasal and mandibular mesenchyme cells.

4.3.3 Expression of *pea3*, *erm*, and *er81* expression in facial mesenchyme micromass cultures of stage 28/29 relative to stage 24/25

Bobick and Kulyk (2007) reported the effects of FGFs on chondrogenesis in both frontonasal and mandibular mesenchyme micromass cultures are mediated by the MEK-ERK mitogen activated protein kinase (MAPK) pathway at stage 24/25 of chick embryo development (Bobick and Kulyk, 2004). In contrast, by stage 28/29 of development, pharmacological inhibition of the MEK/ERK pathway was no longer able to block the inhibitory effects of FGF on chondrogenesis in frontonasal mesenchyme cultures. This suggested that maturation of the frontonasal process is accompanied by a stage-related shift from an ERK-dependent to ERK-independent pathway of FGF signal transduction (Bobick et al., 2007).

Since the Pea3 group of transcription factors are putative targets of ERK phosphorylation, we questioned whether this stage-dependent shift in FGF signalling pathways might be correlated with stage-associated changes in levels of endogenous

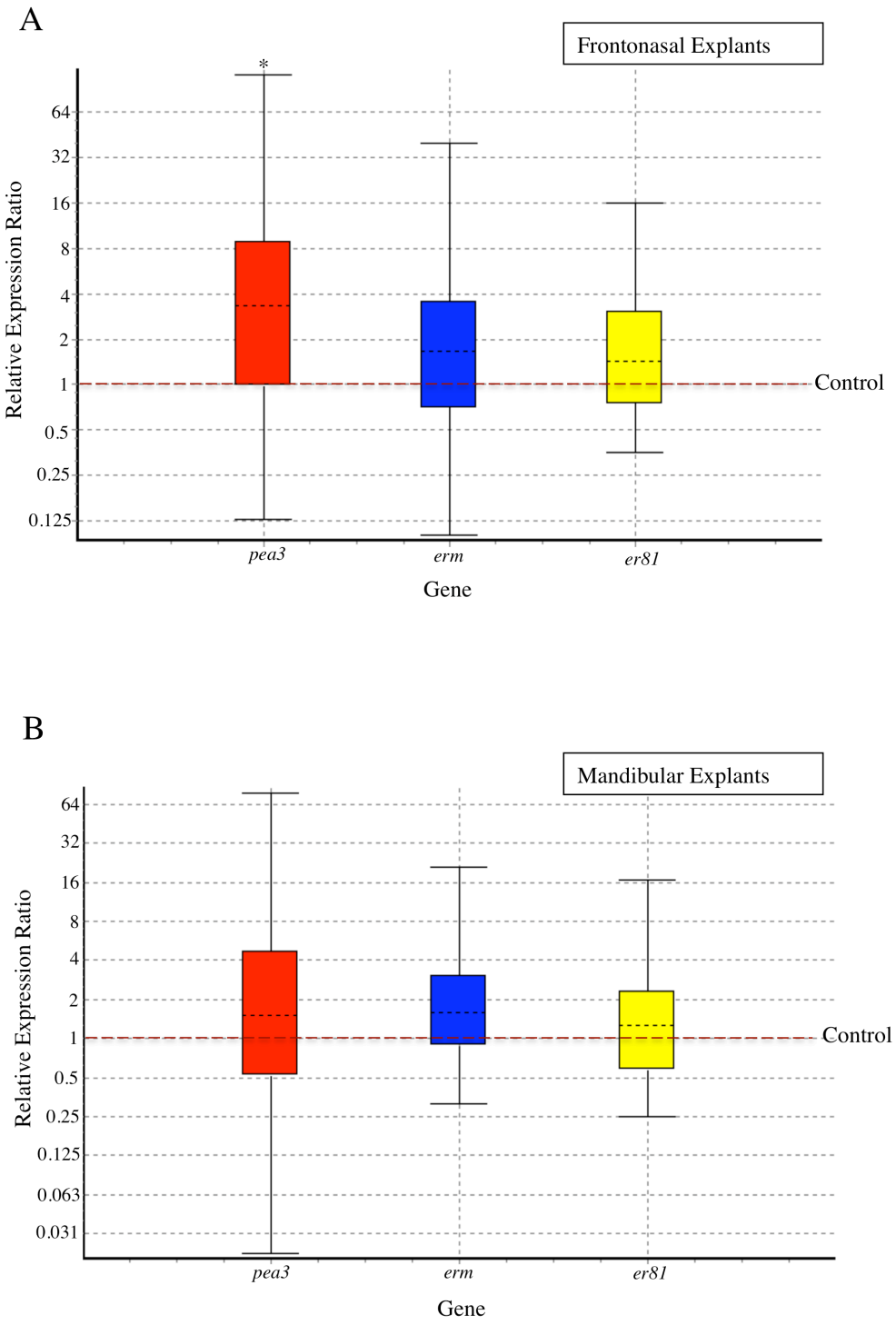

Figure 9 Effects of FGF2 on *pea3*, *erm*, and *er81* mRNA transcript levels in stage 24/25 chick frontonasal and mandibular mesenchyme explant cultures. Box and whisker graphs representing relative gene expression levels as determined using REST™ qPCR data analysis software. (A) *pea3* expression is upregulated approximately 2.9-fold in frontonasal explant cultures treated for 6 hours with FGF2 relative to untreated controls ($p = 0.036$). Expression levels of *erm* and *er81* were not significantly affected by FGF2. (B) Stage 24/25 mandibular mesenchyme explant cultures exhibited no significant changes in expression of *pea3*, *erm*, or *er81* in response to FGF2 treatment.

pea3, *er81*, or *erm* expression in the facial mesenchyme. To address this possibility, expression levels of the Pea3 group of transcription factors were compared in micromass cultures of stage 24/25 versus stage 28/29 frontonasal and mandibular mesenchyme cells undergoing spontaneous chondrogenic differentiation *in vitro*. RNA for qPCR analysis was harvested after 2 days of culture in frontonasal micromass cultures. RNA was isolated from mandibular cells after 3 days, due to their slower rate of chondrogenic differentiation in micromass culture.

Comparisons of stage 28/29 relative to stage 24/25 frontonasal mesenchyme micromass cultures revealed no significant differences in levels of endogenous *pea3*, *erm*, or *er81* gene expression (Figure 10A). However, surprisingly, stage 28/29 mandibular mesenchyme micromass cultures exhibited significantly lower levels of *pea3* mRNA transcripts relative to stage 24/25 mandibular cultures ($p = 0.023$) (Figure 10B). There were no significant differences in either *erm* or *er81* transcript levels in stage stage 28/29 relative to stage 24/25 mandibular mesenchyme micromass cultures.

4.3.4 Comparisons of endogenous *pea3*, *erm*, and *er81* expression between mesenchyme of stage 24/25 frontonasal and mandibular facial primodia

Bobick and Kulyk previously reported that micromass cultures of stage 24/25 frontonasal and mandibular mesenchyme have opposite responses to exogenous FGF (Bobick et al., 2007). Since the Pea3 transcription factors are thought to be critical downstream effectors of FGF signalling, we questioned whether the frontonasal and mandibular cell populations might exhibit qualitative or quantitative differences in endogenous *pea3*, *erm* and/or *er81* gene transcript levels. However, REST™ analysis revealed no significant differences between levels of *pea3*, *erm*, or *er81* mRNAs in stage 24/25 mandibular micromass cultures relative to stage 24/25 frontonasal micromass cultures (Figure 11).

We also investigated if stage 24/25 frontonasal and mandibular explants, which retain their native cell contacts, exhibited qualitative differences in endogenous levels of Pea3 transcription factor expression. REST™ analysis revealed no significant differences between levels of *pea3*, *erm*, and/or *er81* in stage 24/25 mandibular explants relative to stage 24/25 frontonasal mesenchyme (data not shown).

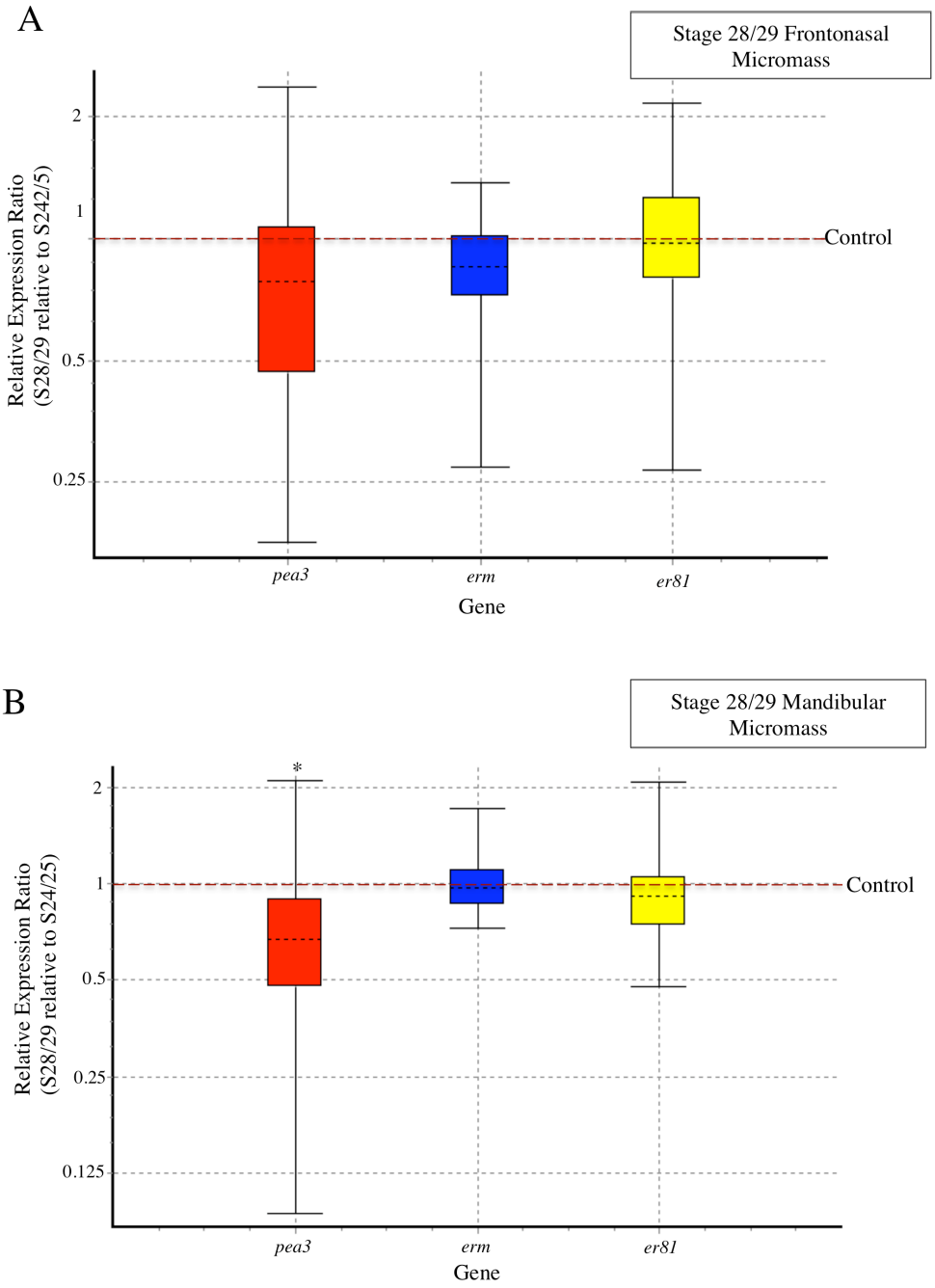

Figure 10 Endogenous *pea3*, *erm*, and *er81* mRNA expression in stage 28/29 chick frontonasal and mandibular mesenchyme micromass cultures relative to stage 24/25. (A) Analysis of RT-qPCR data using REST™ software revealed no significant differences in *pea3*, *erm*, or *er81* transcript levels between stage 24/25 and stage 28/29 frontonasal mesenchyme micromass cultures. (B) Stage 28/29 mandibular mesenchyme micromass cultures exhibited significantly lower levels of *pea3* mRNA transcripts relative to stage 24/25 mandibular mesenchyme micromass cultures ($p = 0.023$). No significant differences were observed in levels of *erm* or *er81* mRNA transcripts between stage 28/29 and stage 24/25 mandibular mesenchyme micromass cultures.

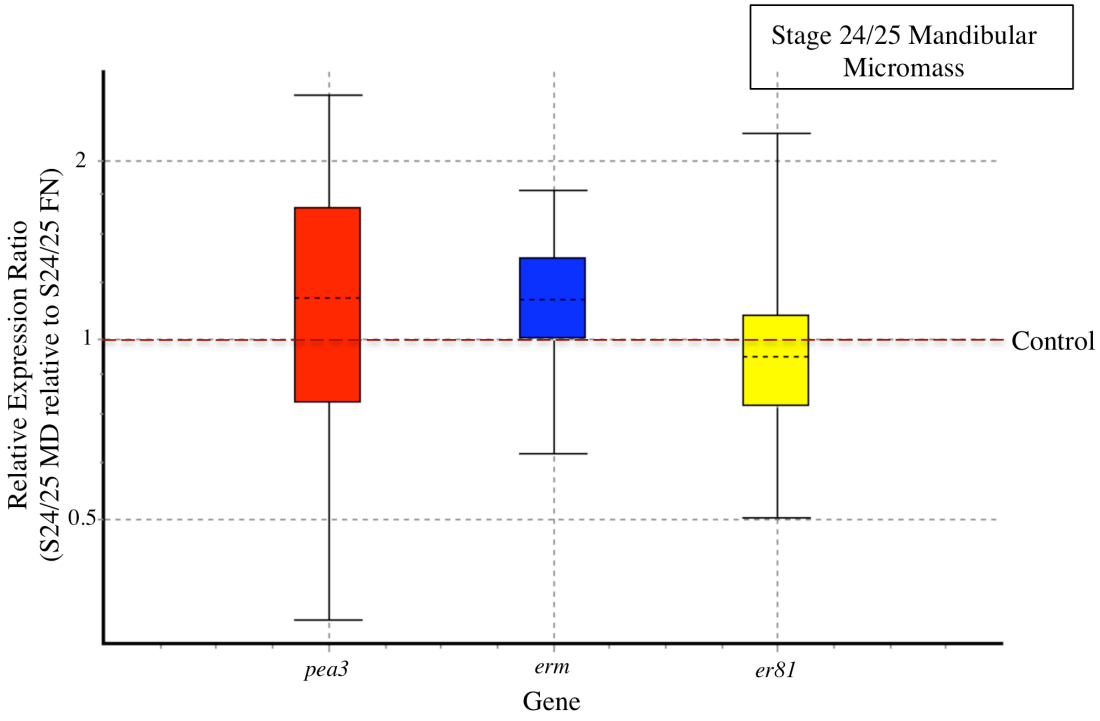

Figure 11 Endogenous *pea3*, *erm*, and *er81* mRNA expression in stage 24/25 chick mandibular mesenchyme relative to stage 24/25 frontonasal mesenchyme micromass cultures. A box and whisker graph representation of relative gene expression levels obtained using the REST™ software tool. No significant differences were observed in *pea3*, *erm*, or *er81* gene transcripts between stage 24/25 mandibular and stage 24/25 frontonasal mesenchyme micromass cultures.

4.4 RNA Dot Blot Validation of RT-qPCR Results

4.4.1 RNA dot blot validation of micromass RT-qPCR results

RNA dot blot analysis was used to independently validate the measurements of *pea3*, *erm*, and *er81* transcript levels as determined by RT-qPCR experiments. Aliquots of the total RNA remaining from a single micromass culture RT-qPCR experiment and a single facial mesenchyme explant experiment were used to determine the effects of FGF2 on *pea3*, *erm*, and *er81* expression. To ensure there were sufficient amounts of RNA for dot blot analysis, the RNA from all three biological replicates of each experiment was pooled, then equivalent amounts were spotted onto nylon membranes, and probed with [^{32}P]-labelled cDNA probes for *pea3*, *erm*, and *er81* as described in Materials & Methods Section 3.3.3. The hybridization signal for each gene of interest was normalized against the signal for constitutively expressed *gapdh* transcript to correct for any differences in sample loading.

In one set of stage 24/25 frontonasal mesenchyme cultures (3 biological replicates per treatment group), RT-qPCR analysis had indicated that 2 h FGF2 treatment significantly increased both *pea3* and *er81* mRNA transcripts by factors of approximately 3.8- and 2-fold, respectively (data not shown). Subsequent dot blot analysis performed on pooled RNA from the same cultures confirmed these trends, as *pea3* signal intensity was elevated approximately 4.7-fold and the *er81* signal was approximately 5.6-fold higher in FGF2 treated cultures relative to controls (Figure 12). In regard to *erm* expression, RT-qPCR analysis had revealed no significant difference between control and FGF2 treated stage 24/25 frontonasal micromass cultures. This was consistent with the RNA dot blots that indicated FGF affected *erm* transcript levels to a much lesser degree in comparison to its effects on *pea3* and *er81* expression.

In the same RT-qPCR experiment, FGF2 treated stage 24/25 mandibular mesenchyme micromass cultures had significantly higher levels of both *pea3* and *erm* mRNA transcripts by factors of approximately 2-fold (data not shown). Subsequent RNA dot blot analysis confirmed these trends, as *pea3* and *erm* signal intensities were elevated approximately 1.5- and 2.7-fold respectively in FGF2 treated cultures

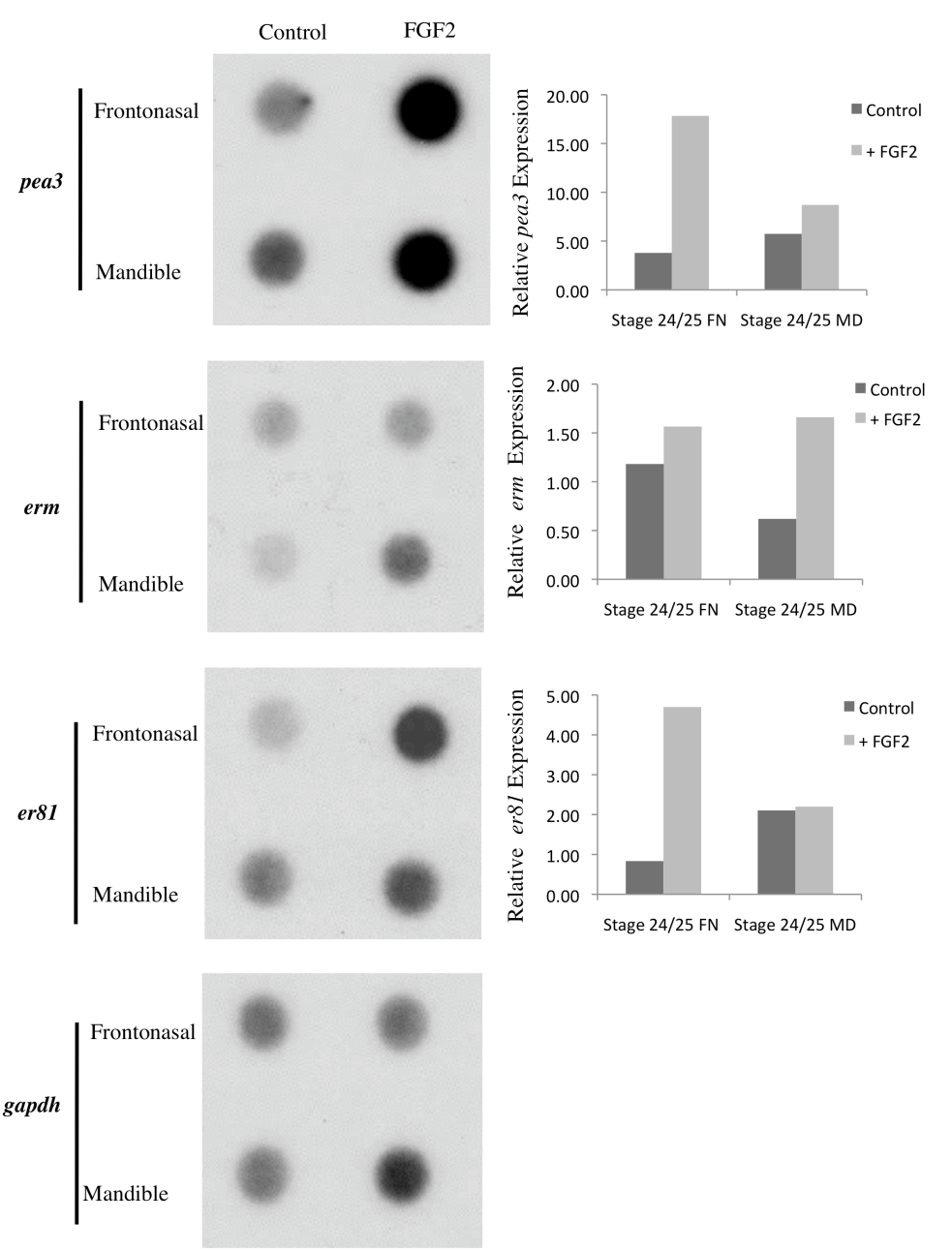

Figure 12 RNA dot blot analysis of FGF2 effects on *pea3*, *er81*, and *erm* expression in stage 24/25 frontonasal and mandibular mesenchyme micromass cultures. Micromass cultures were treated for 6 h in the presence or absence of 20 ng/ml FGF2. For each treatment group, total RNA from three replicate cultures in a single experiment was pooled and used for dot blot analysis. The cultures were from an individual experiment in which the RT-qPCR data for that specific experimental run most closely matched the general trends revealed by REST™ analysis of pooled RT-qPCR data from all independent experimental runs. The panels on the left are autoradiographs of RNA dot blots hybridized with ^{32}P-labelled cDNA probes for *pea3*, *er81*, *erm* and *gapdh*. The histograms represent the relative expression levels of *pea3*, *erm*, and *er81* mRNAs as determined by densitometric measurements. To compensate for any differences in sample loading, the hybridization signals for each gene were normalized against the signal for the constitutively expressed *gapdh* transcript. (n = 1 for each treatment group)

relative to controls (Figure 12). In regard to *er81* expression, RT-qPCR analysis had revealed no significant difference between control and FGF2 treated stage 24/25 mandibular micromass cultures. This was consistent with the RNA dot blots that indicated FGF2 had minimal affect on *er81* expression in comparison to its effects on *pea3* and *er81* expression.

4.4.2 RNA dot blot validation of explant RT-qPCR results

In one set of three replicate stage 24/25 frontonasal explant RNA samples (3 biological replicates per treatment group), the earlier RT-qPCR analysis had indicated that a 6 h FGF2 treatment significantly upregulated *pea3* transcripts by 7.5-fold, *erm* mRNA transcripts by 3.4-fold, and *er81* mRNA by 1.8-fold relative to parallel control cultures (data not shown).

Dot blot analysis performed on pooled RNA samples from the same set of cultures indicated that *pea3* expression was upregulated 11-fold following FGF2 treatment, while *erm* mRNA transcripts were elevated 7.8-fold relative to controls (Figure 13). Additionally, *er81* mRNA transcripts in FGF2 treated frontonasal explant cultures were elevated 3-fold relative to controls as detected by RNA dot blot analysis. Thus, the RNA dot blot results confirmed the trends of FGF treatment on stage 24/25 frontonasal explant cultures that were previously determined by RT-qPCR analysis.

In stage 24/25 mandibular explant cultures from the same experiment, RT-qPCR analysis demonstrated a 5.8-fold increase in *pea3* mRNA transcripts in response to 6 h FGF2 treatment relative to untreated controls ($p = 0.053$) (data not shown). RT-qPCR found *erm* transcript levels were also upregulated in response to FGF2 treatment by 2.6-fold ($p = 0.045$), while the *er81* mRNA level was not significantly different than untreated controls (data not shown). Densitometric measurements performed on dot blots of pooled RNA samples from the same set of cultures indicated that *pea3* expression was approximately 9-fold higher in FGF treated cultures and *erm* transcripts were upregulated approximately 3-fold relative to controls (Figure 13). In regard to *er81* expression, RT-qPCR analysis revealed no significant difference between control and FGF2 treated stage 24/25 mandibular explant cultures. This is consistent with results obtained from RNA dot blots analysis demonstrating FGF treatment had the least affect on *er81* expression (~ 1.9 fold) in comparison to its affects on *pea3* and *erm* expression. As such, the RNA dot blot data

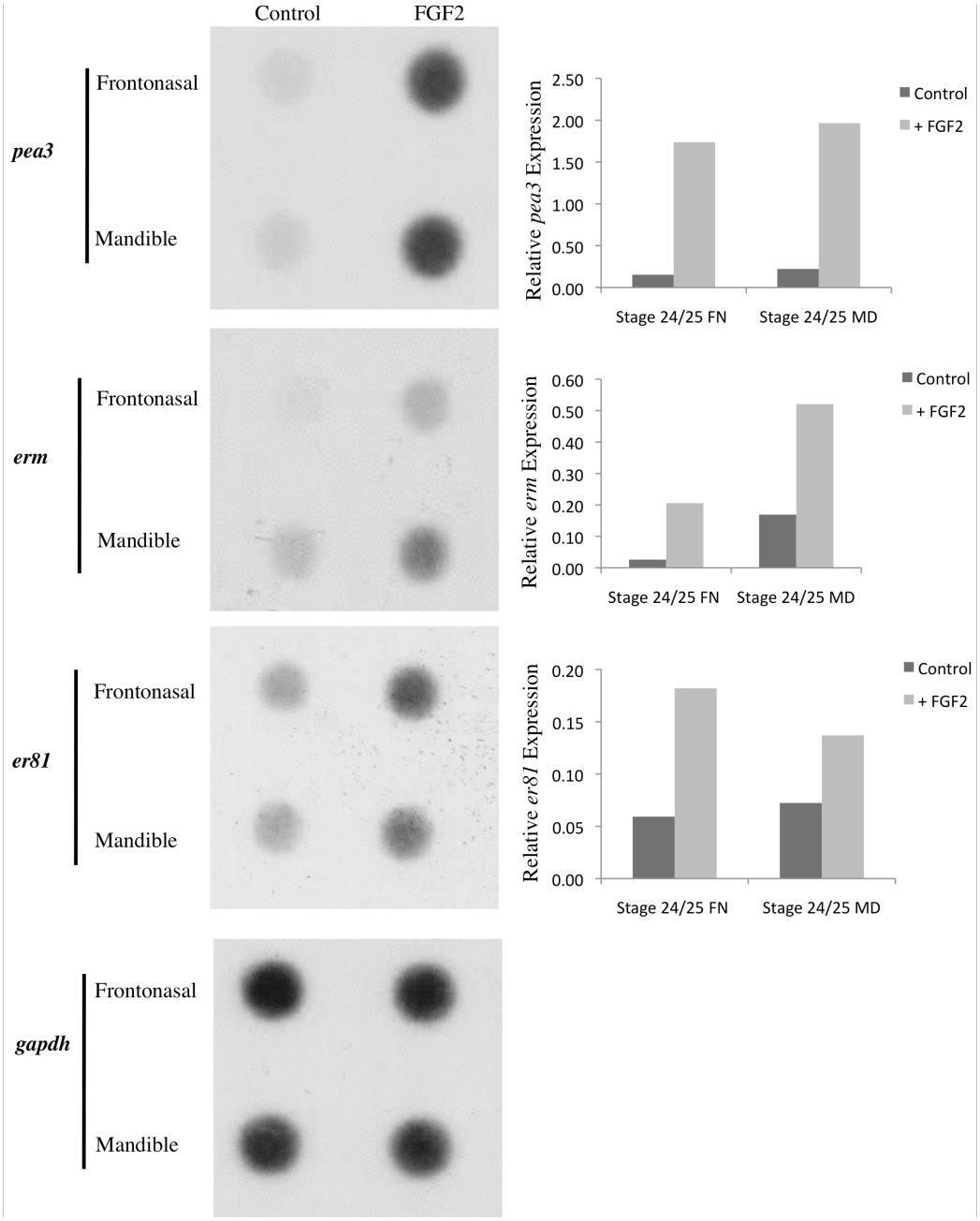

Figure 13 RNA dot blot analysis of FGF2 effects on *pea3*, *er81*, and *erm* expression in stage 24/25 frontonasal and mandibular explant cultures. The facial mesenchyme explants were treated for 6 h in the presence or absence of 20 ng/ml FGF2. For each treatment group, total RNA from three replicate cultures in a single explant experiment was pooled and used for dot blot analysis. The cultures were from an individual experiment in which the RT-qPCR data for that specific experimental run most closely matched the general trends revealed by REST™ analysis of pooled RT-qPCR data from all independent experimental runs. The panels on the left are autoradiographs of RNA dot blots hybridized with ^{32}P-labelled *pea3*, *er81*, erm and *gapdh* cDNA probes. The corresponding histograms were obtained by densitometric quantification of the dot blot signals for the *pea3*, *erm*, *er81* mRNAs. These values were normalized against the signal for the constitutively expressed *gapdh* transcript to compensate for any differences in sample loading.

demonstrating the effects of FGF treatment on stage 24/25 mandibular explant cultures is consistent with the prior RT-qPCR analysis.

4.5 Assessment of Chondrogenic Differentiation in Micromass Cultures of Frontonasal and Mandibular Mesenchyme

4.5.1 Alcian blue histochemical detection of sulphated proteoglycans

The magnitude of the differences in *pea3*, *erm*, and *er81* mRNA expression profiles in frontonasal versus mandibular mesenchyme cells were more modest than anticipated, in light of previous studies which reported that frontonasal and mandibular micromass cultures exhibit qualitatively opposite responses to exogenous FGFs or ERK pathway activation (Bobick and Kulyk, 2006; Bobick et al., 2007). Therefore, experiments were performed to determine whether these previous findings could be confirmed under the specific experimental conditions used in the present study. Micromass cultures of stage 24/25 and stage 28/29 frontonasal and mandibular mesenchyme cells were cultured in the absence or presence of 40 ng/ml FGF2, and collected after 2 or 3 days of incubation for histochemical staining with Alcian blue dye to determine cartilage matrix proteoglycan production. These experiments were also repeated in the presence or absence of 20ng/ml FGF2 (data not shown). In addition, total DNA accumulation in the presence or absence of FGF2 was determined in parallel replicate cultures as described in Section 3.5.2 of Materials and Methods.

For frontonasal mesenchyme micromass cultures, there was a significant reduction in the levels of Alcian blue stainable cartilage matrix proteoglycan accumulation in both stage 24/25 (Figure 14A) and stage 28/29 (Figure 14B) in response to FGF2 treatment ($p < 0.001$). This trend was consistent with the findings of Bobick et al. (2007), although the inhibitory effects of FGF2 on the frontonasal mesenchyme at both stages appeared to be of lesser magnitude than previously reported. Consistent with the previous study, stage 28/29 mandibular mesenchyme micromass cultures exhibited a much lower level of spontaneous chondrogenesis than stage 24/25 mandibular mesenchyme, as evidenced by only faintly detectable levels of Alcian blue staining (Figure 14B).

Bobick et al. (2007) reported that FGF2 treatment stimulates cartilage matrix accumulation in stage 24/25 mandibular micromass cultures (Bobick et al., 2007). In contrast, my own experiments showed no visible difference in Alcian blue staining in

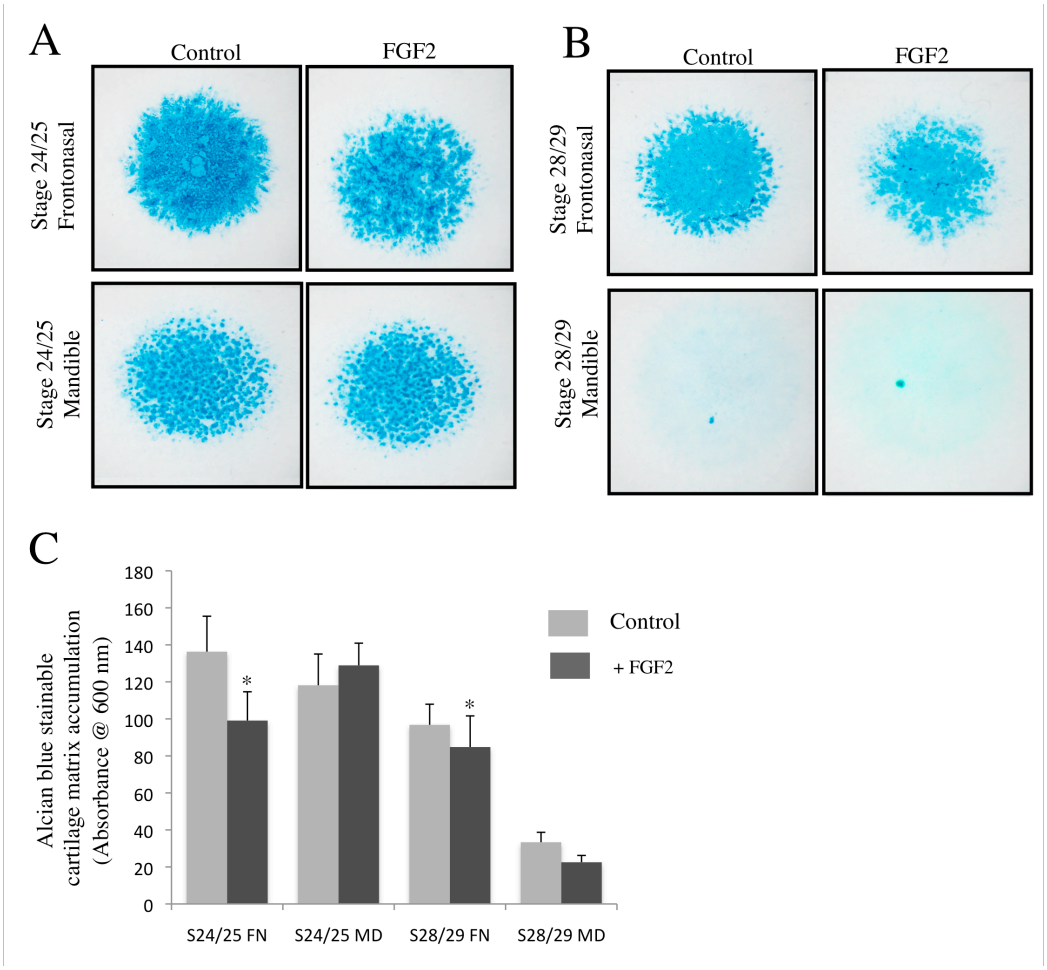

Figure 14 Effects of FGF2 on accumulation of Alcian-blue stainable cartilage matrix accumulation in micromass cultures prepared from stage 24/25 and 28/29 frontonasal and mandibular mesenchyme. Cultures were stained with Alcian blue histochemical dye after 2 or 3 days of incubation in the presence or absence of 40 ng/ml FGF2. (A, B) Photographs of Alcian blue-stained micromass cultures of stage 24/25 frontonasal and mandibular mesenchyme cells (A), and stage 28/29 frontonasal and mandibular mesenchyme cells (B) cultured with or without exogenous FGF2. (C) Histograms indicating relative levels of sulphated cartilage matrix glycosaminoglycan accumulation in control and FGF treated micromass cultures as determined by spectrophotometric quantification of eluted Alcian blue dye. Error bars represent the mean +/- standard deviation of measurements from six replicate cultures. Asterisks (*) denote values that are significantly different from the corresponding control at $p < 0.01$. The data demonstrate that FGF treatment caused a significant decrease in Alcian blue stainable cartilage matrix accumulation in both stage 24/25 and stage 28/29 frontonasal mesenchyme micromass cultures. In contrast, FGF2 treatment had no significant effect on Alcian blue stainable matrix production in either stage 24/25 or stage 28/29 mandibular mesenchyme cultures.

FGF2 treated mandibular mesenchyme cultures relative to untreated control cultures (Figure 14A). Elution of the Alcian blue dye and spectrophotometric quantitation confirmed that there was no significant effect of FGF treatment on sulphated GAG accumulation in the mandibular mesenchyme cultures (Figure 14C). As such, the opposing effects of FGF2 on stage 24/25 frontonasal and mandibular mesenchyme micromass cultures that were previously reported were not observed within the current study.

4.5.2 Effects of FGF2 on DNA accumulation in frontonasal and mandibular mesenchyme micromass cultures

The Hoechst 33258 DNA fluorescence assay was used to investigate whether 20 ng/ml FGF2 treatment differentially affected frontonasal and mandibular cell survival and/or proliferation, as monitored by measuring total DNA accumulation over the 2-3 day culture period. As demonstrated in Figure 15, FGF2 treatment had no significant effect on the overall DNA content of stage 24/25 frontonasal or mandibular micromass cultures. Similarly, FGF2 treatment showed no significant effect on the DNA content of stage 28/29 frontonasal mesenchyme micromass cultures (Figure 15B). In contrast, FGF2 treatment caused a significant increase in the DNA content of stage 28/29 mandibular mesenchyme relative to controls ($p < 0.01$).

4.5.3 Effects of FGF2 treatment on sulphated GAG accumulation in frontonasal and mandibular mesenchyme micromass cultures

To ensure the unexpected results from the previous experiments were not due to a limitation of the Alcian blue staining method, an alternate method for detection of sulphated GAG was used. Stage 24/25 and stage 28/29 frontonasal and mandibular mesenchyme micromass cultures were cultured in the presence or absence of 40 ng/ml FGF2. Relative amounts of sulphated GAG production were determined by measuring the ability of sulphated GAGs to bind the cationic dye 1,9 DMMB (Farndale et al., 1982; Whitley et al., 1989). Isolation and subsequent dissociation of the GAG-dye complex permits spectrophotometric quantification of sulphated GAG accumulation (Barbosa et al., 2003). An advantage of the DMMB method is that, unlike Alcian blue staining, it allows for quantification of sulphated GAGs secreted into the culture medium as well as sulphated GAGs deposited in the micromass cell layer.

A

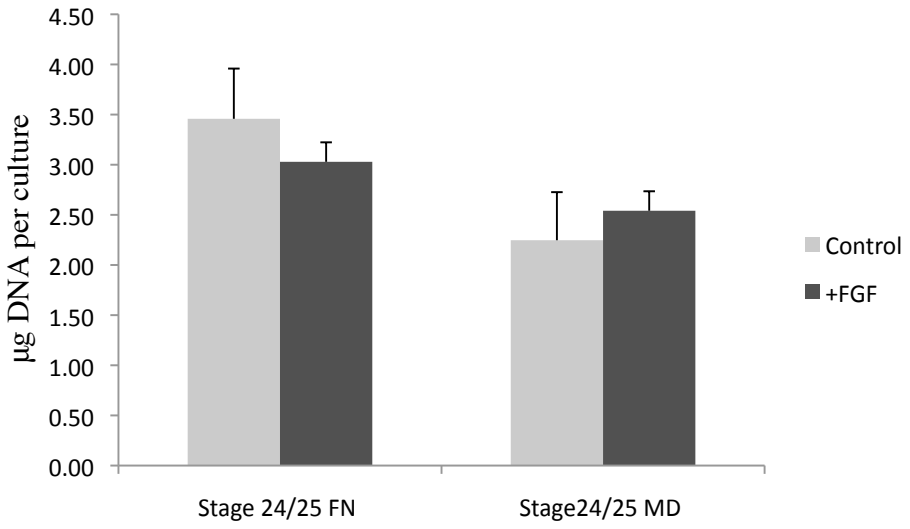

B

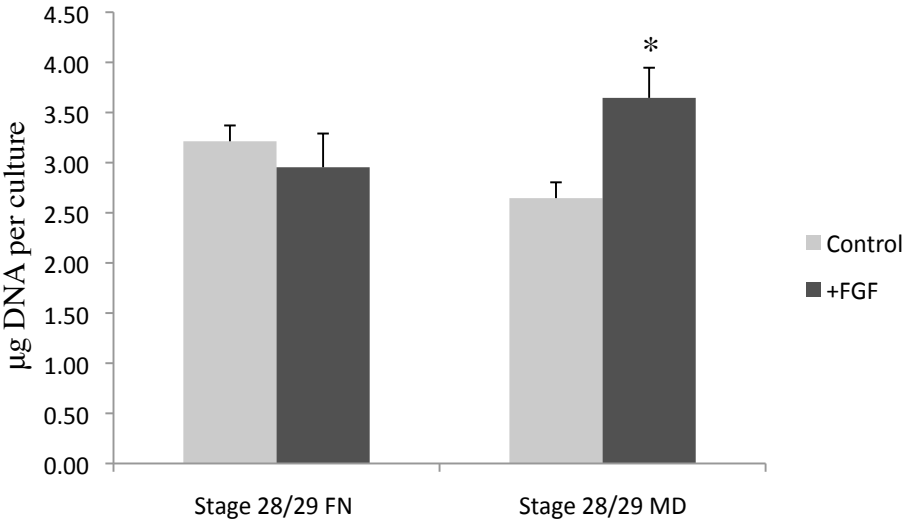

Figure 15 Effects of FGF2 treatment on levels of total cellular DNA in stage 24/25 and 28/29 chick frontonasal and mandibular micromass cultures. Micromass cultures were treated with 40 ng/ml FGF2 and collected after 2 or 3 days for analysis of cellular DNA content using the Hoescht 33258 fluorescence assay. (A) FGF2 treated stage 24/25 frontonasal and mandibular micromass cultures showed no differences in total DNA content relative to untreated controls. (B) The total DNA content of stage 28/29 frontonasal mesenchyme micromass cultures was not affected by FGF2 treatment, however stage 28/29 mandibular micromass cultures showed elevated levels of total DNA relative to untreated controls ($p < 0.01$). Error bars represent the mean +/- standard deviation of measurements from six replicate cultures.

Results of the DMMB assay indicated significantly less sulphated GAG was accumulated in the cell layer of stage 24/25 frontonasal mesenchyme micromasscultures treated with FGF2 than in controls ($p < 0.001$) (Figure 16A). This decrease was consistent with the results of the Alcian blue histochemical staining assay (Figure 14). There were no significant differences in the amount of GAG accumulation within the medium fraction of FGF2 treated stage 24/25 frontonasal micromass cultures relative to untreated to controls. Importantly, FGF2 treatment had no significant effect on sulphated GAG accumulation in either the cell layer or the medium fraction of stage 24/25 mandibular mesenchyme micromass cultures (Figure 16B). This was consistent with the Alcian blue histochemical data (Figure 14), but contrary to a previous report that demonstrated FGF treatment of mandibular mesenchyme micromass cultures increased sulphated GAG accumulation (Bobick et al., 2007).

In stage 28/29 frontonasal mesenchyme micromass cultures, there was significantly decreased GAG accumulation in both the cell layer and medium fractions of FGF treated cultures relative to controls ($p < 0.001$), as shown in Figure 17A. In control cultures of stage 28/29 mandibular mesenchyme, nearly all the sulphated GAG was deposited into the culture medium rather than the cell layer. FGF2 treatment had no significant effect on sulphated GAG accumulation in either compartment (Figure 17B). Sulphated GAGs were barely detectable in control and FGF2 treated cellular fractions of stage 28/29 mandibular mesenchyme micromass cultures. These results were consistent with those obtained by Alcian blue histochemical staining: while FGF2 treatment inhibited chondrogenesis in both stage 24/25 and stage 28/29 frontonasal mesenchyme micromass cultures, FGF2 treatment had no stimulatory or inhibitory effect on stage 24/25 or stage 28/29 mandibular mesenchyme micromass cultures. This strongly suggests the lack of chondro-stimulatory effect observed in mandibular mesenchyme micromass cultures in response to FGF is not related to the specific methodology (i.e. either Alcian blue or 1,9-DMMB) used to assess the extent of chondrogenic differentiation, but is rather due to changes in the cellular behaviour of mandibular mesenchyme.

4.5.4 Immunostaining for Type II Collagen

Immunohistochemical staining was used to determine how FGF2 affected the expression of type II collagen, the other principal cartilage matrix component, in

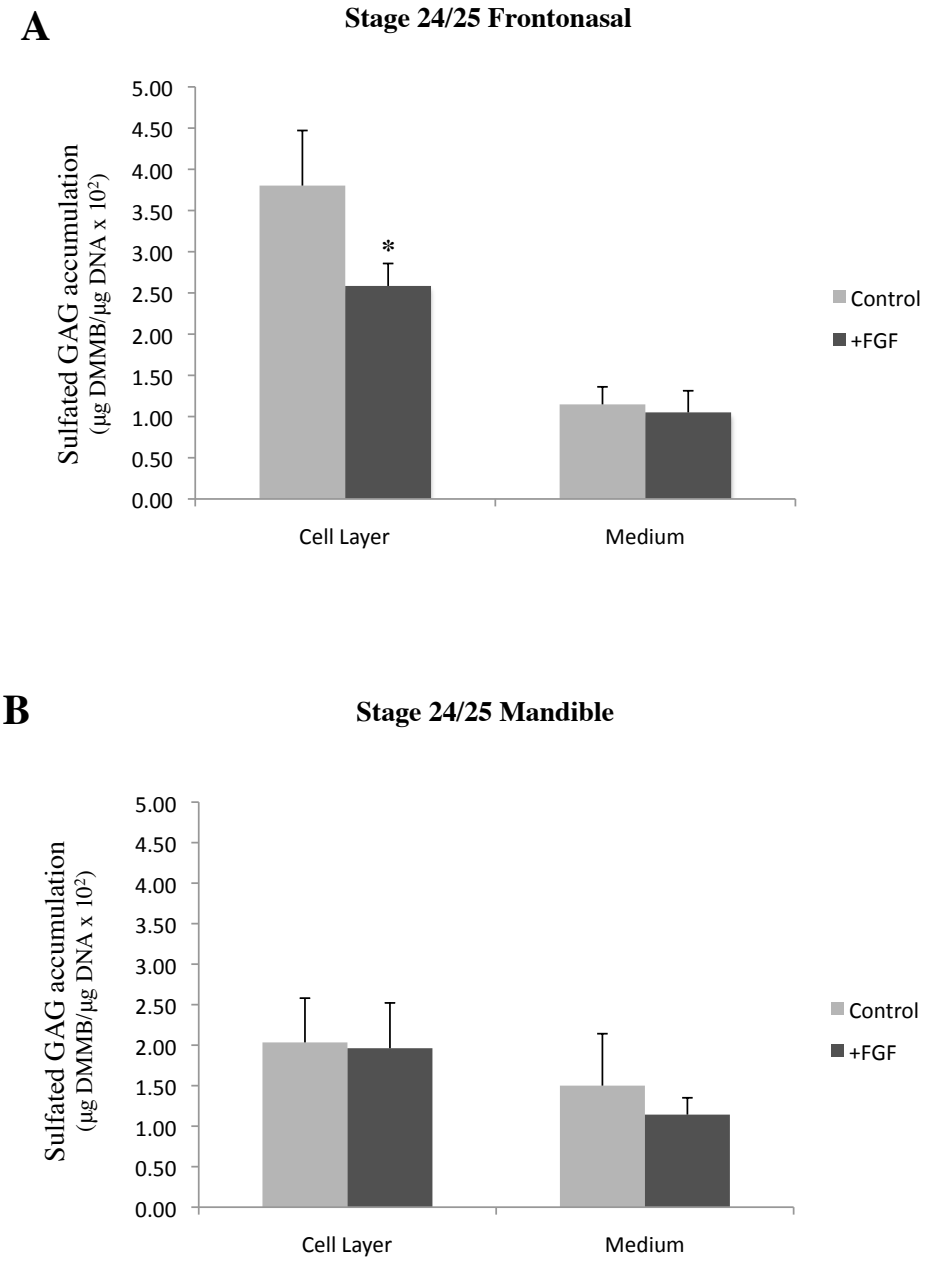

Figure 16 Effects of FGF2 treatment on sulphated GAG accumulation in the cellular layer and medium fractions of stage 24/25 chick frontonasal and mandibular mesenchyme micromass cultures. Micromass cultures were treated with 40 ng/ml FGF2 and collected after 2 or 3 days for analysis of sulphated GAG accumulation in both the cell layer and culture medium using the DMMB assay. GAG accumulation measurements were normalized against total cellular DNA content to correct for any differences in cell number between control and FGF treated cultures. (A) In stage 24/25 frontonasal mesenchyme, FGF2 treatment significantly decreased sulphated GAG deposition into cell layer-associated cartilage matrix ($p < 0.001$), but had no effect on accumulation of sulphated GAGs within the surrounding culture medium. (B) In stage 24/25 mandibular mesenchyme, FGF2 treatment did not affect sulphated GAG accumulation in either the cellular layer or medium fractions. Error bars represent the mean +/- standard deviation of measurements from six replicate cultures.

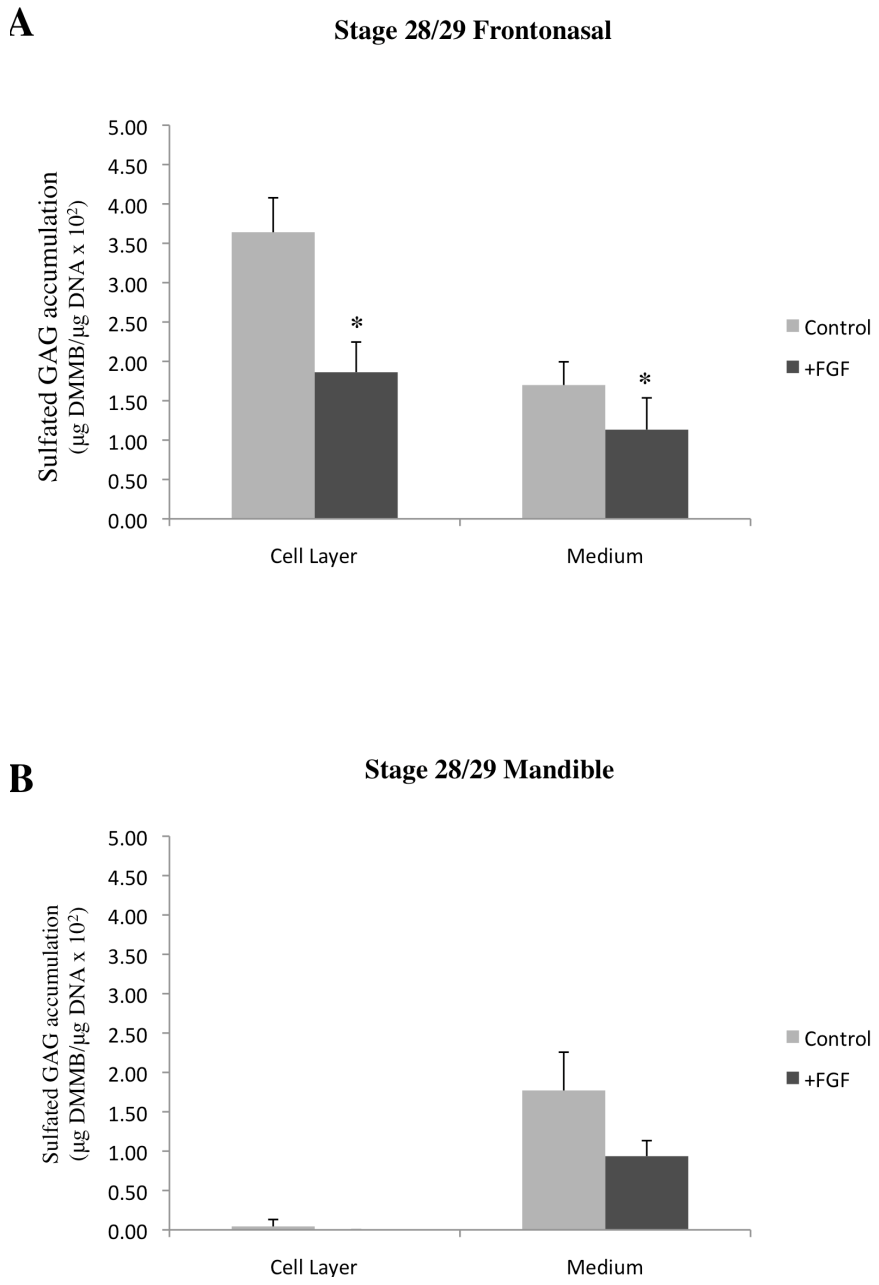

Figure 17 Effects of FGF2 treatment on sulphated GAG accumulation in the cellular layer and medium fractions of stage 28/29 chick frontonasal and mandibular mesenchyme micromass cultures. Micromass cultures were treated with 40 ng/ml FGF2 and collected after 2 or 3 days for analysis of sulphated GAG accumulation using the DMMB assay. GAG accumulation values are normalized against μg of total cellular DNA. (A) In stage 28/29 frontonasal mesenchyme, FGF2 treatment significantly decreased sulphated GAG deposition into the micromass cell layer, as well as GAG secretion into the surrounding culture medium ($p < 0.001$). (B) In stage 28/29 mandibular mesenchyme, FGF2 treatment had no effects on sulphated glycosaminoglycan accumulation in either the cell layer or medium fractions. Error bars represent the mean +/- standard deviation of measurements from six replicate cultures.

micromass cultures of stage 24/25 and stage 28/29 frontonasal and mandibular mesenchyme. Stage 24/25 (Figure 18A) and stage 28/29 (Figure 18B) frontonasal mesenchyme micromass cultures exhibited decreased type II collagen accumulation following treatment with 20 ng/ml FGF2 relative to untreated cultures. These results paralleled the effects of FGF2 on cartilage matrix proteoglycan production as determined by both the Alcian blue staining and the DMMB assay. FGF2 treatment had no observable effect on type II collagen synthesis in stage 24/25 mandibular micromass cultures relative to controls (Figure 18A). Interestingly, FGF2 treatment visibly increased type II collagen accumulation in stage 28/29 mandibular micromass cultures relative to controls (Figure 18B), although no similar stimulatory effect was observed on cartilage matrix GAG deposition.

4.6 Pea3, Erm, and Er81 Protein Expression Analysis

4.6.1 Western blotting of micromass cultures

Western blotting was used to examine if observed changes in levels of *pea3*, *erm*, and *er81* mRNA transcripts in micromass cultures were accompanied by similar changes in levels of the corresponding proteins. Stage 24/25 frontonasal and mandibular mesenchyme micromass cultures were established and treated with 20 ng/ml FGF2 for periods of 2 to 48 hours. Following removal of the culture media, cell lysates were prepared. Cell lysates containing equal amounts of total cellular protein were separated on SDS-polyacrylamide gels, transferred to nitrocellulose membranes, and probed with antibodies against Pea3, Erm, and Er81. Parallel Western blots were probed for detection of constitutively expressed Gapdh, and used to normalize relative signal intensities for Pea3 and Er81 proteins.

The Pea3 and Er81 antibodies successfully detected proteins of the appropriate size on Western blots (Figure 19A and D). Since antibodies specifically directed against chicken Erm are not currently commercially available, a polyclonal antibody against rabbit Erm was tested for its suitability. This particular Erm antibody proved to be unable to specifically detect chicken Erm within facial mesenchyme cell lysates as indicated by the presence of a large number of protein bands of various sizes on Western blots (data not shown). As such, only Pea3 and Er81 protein expression were examined in subsequent experiments.

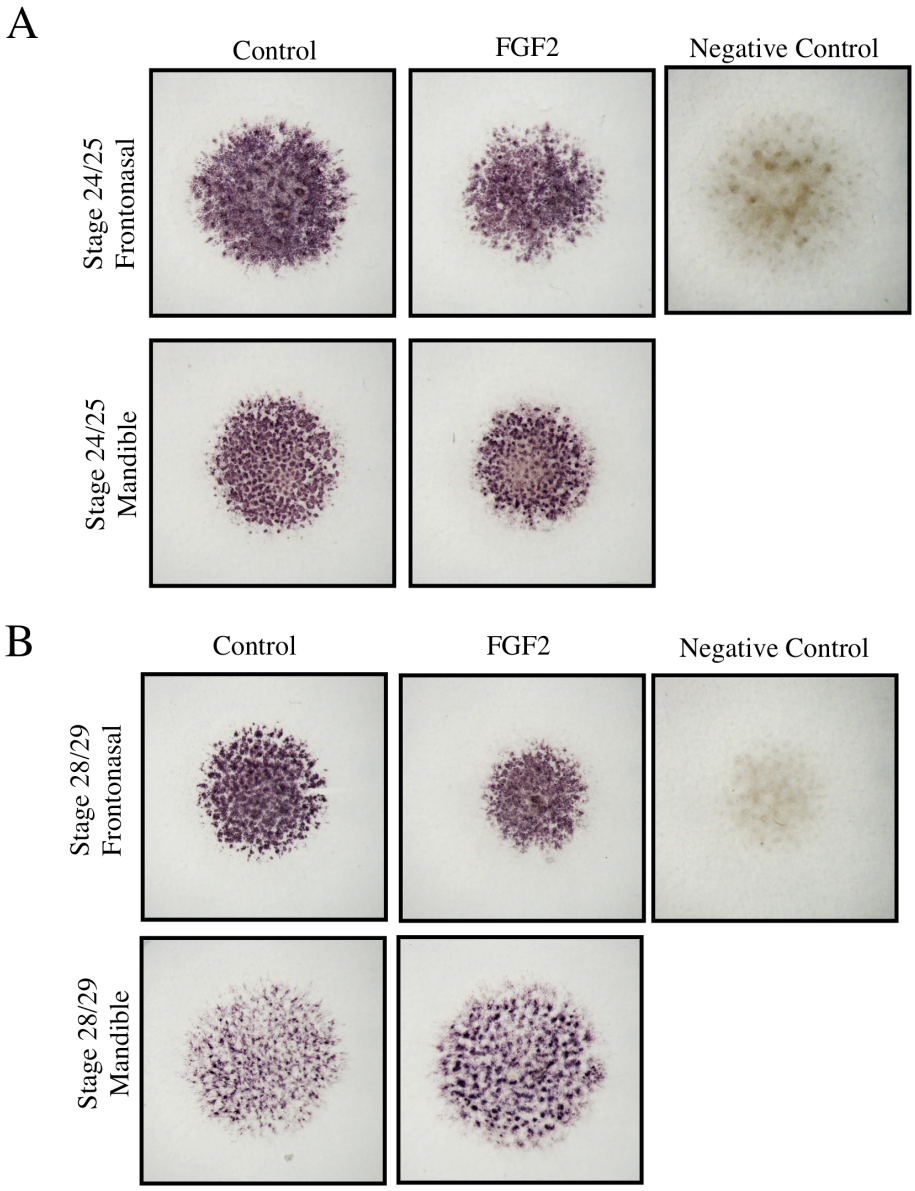

Figure 18 Effects of FGF2 treatment on accumulation of type II collagen in stage 24/25 and stage 28/29 frontonasal and mandibular mesenchyme micromass cultures. Cultures were incubated in either the presence or absence of 20 ng/ml FGF2 and the accumulation of type II collagen in the cell layer was visualized by immunocytochemical staining with a monoclonal antibody against chicken type II collagen. (A) In stage 24/25 frontonasal mesenchyme micromass cultures, FGF2 decreased accumulation of type II collagen relative to untreated control cultures. Levels of type II collagen in stage 24/25 mandibular mesenchyme micromass cultures were not affected by FGF2 treatment. (B) FGF2 treatment of stage 28/29 frontonasal mesenchyme micromass cultures reduced levels of type II collagen relative to untreated controls, but increased type II collagen accumulation in stage 28/29 mandibular mesenchyme micromass cultures. (The "Negative Controls" indicate the amount of background staining obtained when type II collagen primary antibody was omitted from the immunohistochemical procedure.)

Figure 19 Western blot analysis of the effects of FGF2 treatment on Pea3 and Er81 protein levels in micromass cultures prepared from stage 24/25 chick frontonasal and mandibular mesenchyme. The micromass cultures were cultured for 2, 6, 12, 24, or 48 hours in the presence or absence of 20 ng/ml FGF2. Relative levels of Pea3 and Er81 protein were determined by Western blot analysis using specific antibodies. Equivalent amounts of total protein were loaded in each lane. Values shown on graphs were obtained by NIH image analysis of relative band intensities on the Western blots, and were normalized to levels of constitutively expressed Gapdh. (A) Western blot of protein samples from frontonasal micromass cultures, together with histograms depicting relative levels of (B) Pea3 and (C) Er81 proteins. (D) Western blot of protein samples from mandibular micromass cultures, with corresponding histograms depicting relative levels of (E) Pea3 and (F) Er81 proteins.

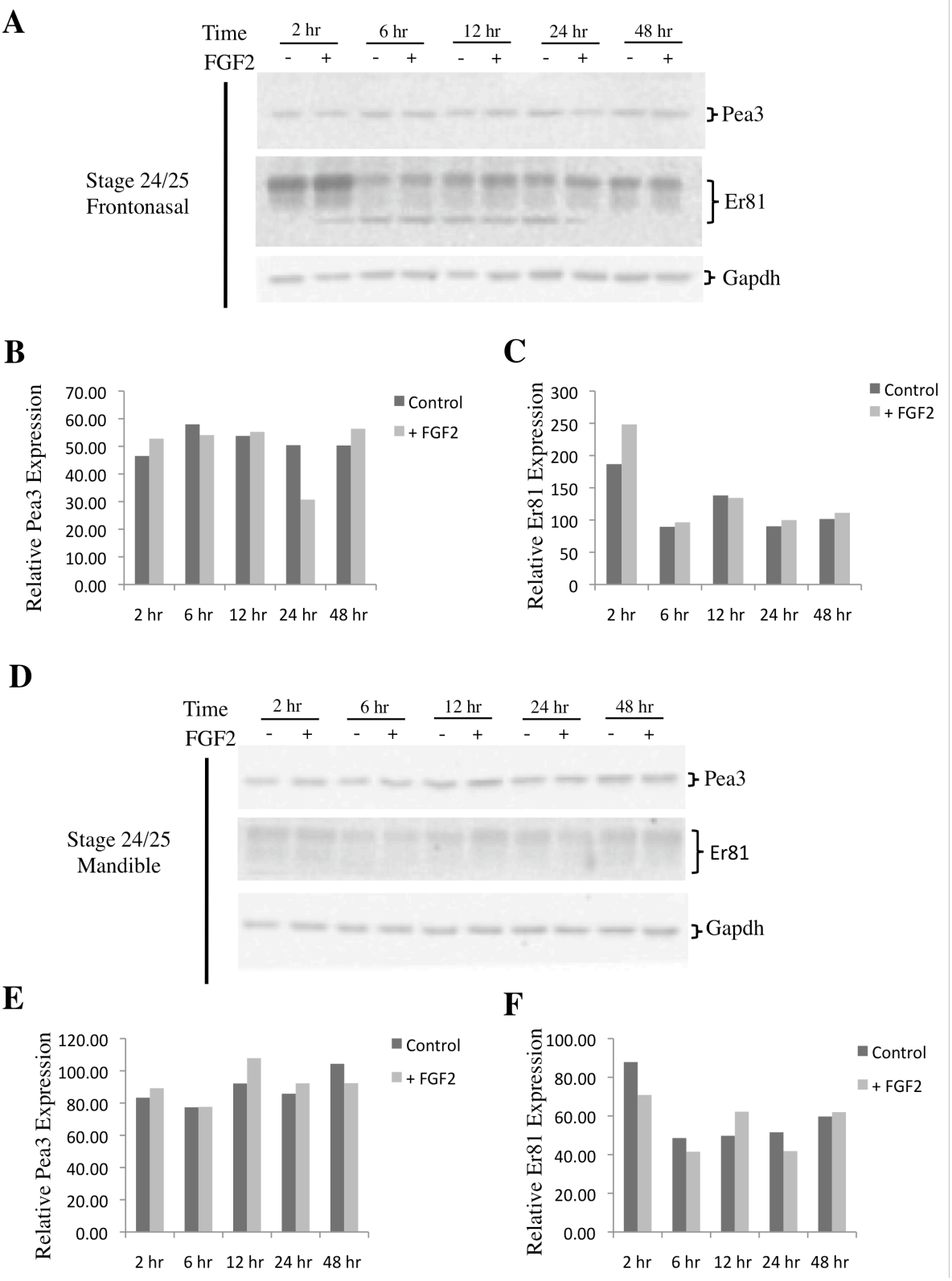
A
Time
2 hr
6 hr
12 hr
24 hr
48 hr
FGF2
- + - + - + - + - +
Pea3
Er81
Gapdh
Stage 24/25
Frontonasal
B
Relative Pea3 Expression
70.00
60.00
50.00
40.00
30.00
20.00
10.00
0.00
2 hr 6 hr 12 hr 24 hr 48 hr
Control
+ FGF2
C
Relative Er81 Expression
300
250
200
150
100
50
0
2 hr 6 hr 12 hr 24 hr 48 hr
Control
+ FGF2
D
Time
2 hr
6 hr
12 hr
24 hr
48 hr
FGF2
- + - + - + - + - +
Pea3
Er81
Gapdh
Stage 24/25
Mandible
E
Relative Pea3 Expression
120.00
100.00
80.00
60.00
40.00
20.00
0.00
2 hr 6 hr 12 hr 24 hr 48 hr
Control
+ FGF2
F
Relative Er81 Expression
100.00
80.00
60.00
40.00
20.00
0.00
2 hr 6 hr 12 hr 24 hr 48 hr
Control
+ FGF2

In stage 24/25 frontonasal mesenchyme micromass cultures, FGF2 treatment had no marked effect on Pea3 protein levels relative to parallel control cultures at any of the time points examined (± 20% of control values) (Figure 19A and B). Western blots for Er81 protein of stage 24/25 frontonasal mesenchyme micromass cultures treated with FGF2 for 2 hours showed a slight increase in Er81 protein levels (33%) relative to untreated controls (Figure 19A). At all other time points, Er81 protein expression values in FGF2 treated cultures were within ± 10% of control cultures (Figure 19C).

Similarly, in stage 24/25 mandibular micromass cultures, FGF2 treatment had minimal effect on Pea3 protein expression at all time points examined (±20% of control cultures) (Figure 19D and E). Er81 protein levels also appeared to be unaffected by FGF2 treatment in stage 24/25 mandibular mesenchyme micromass cultures (±20% of control values) (Figure 19D and E).

4.6.2 Western blotting of explant cultures

Western blotting was also used to examine if observed changes in levels of Pea3, Erm, and Er81 mRNA transcripts in explant cultures were accompanied by similar changes in levels of the corresponding proteins. Stage 24/25 frontonasal and mandibular mesenchyme tissue explant cultures were established and treated with 20 ng/ml FGF2 for 6 hours. Cell lysates containing equal amounts of total protein were separated on SDS-polyacrylamide gels, transferred to nitrocellulose, and probed with Pea3 and Er81 antibodies. Levels of constitutively expressed Gapdh were used to normalize signal intensities for Pea3, Erm, and Er81 proteins. Antibodies were successful at detection of appropriately sized Pea3 and Er81 proteins on Western blots of explant cell lysates (Figure 20A).

Pea3 protein expression was not markedly different in 6 hour FGF treated stage 24/25 frontonasal mesenchyme explant cultures relative to untreated controls (±20%) (Figure 20A and B). In contrast, Western blots of stage 24/25 mandibular mesenchyme explants treated with FGF for 6 hours showed elevated levels of Pea3 protein expression (~2.5 fold) relative to untreated controls (Figure 20A and B). FGF2 had no notable affect on Er81 protein expression in either stage 24/25 frontonasal or mandibular mesenchyme explants relative to untreated controls (±20%) (Figure 20A and C).

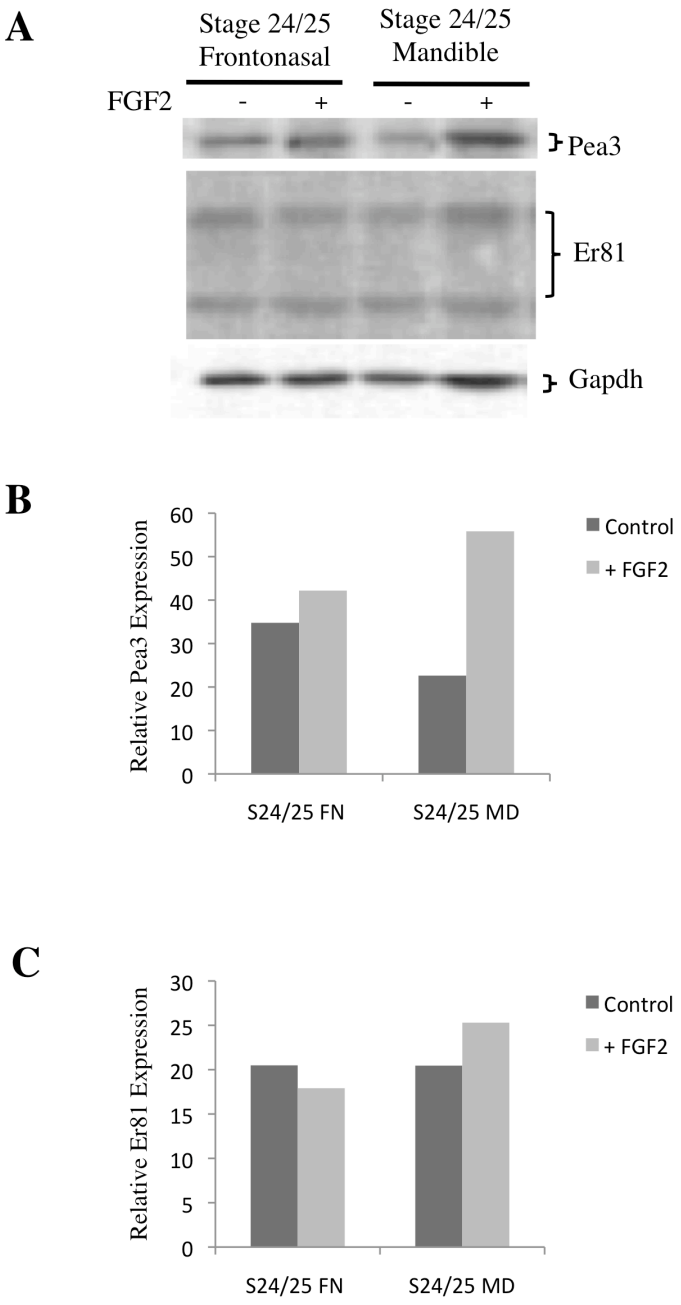

Figure 20 Western blot analysis demonstrating the effects of FGF2 treatment on Pea3 and Er81 protein level in stage 24/25 frontonasal and mandibular mesenchyme explant cultures. Stage 24/25 frontonasal and mandibular mesenchyme explant cultures were treated with 20 ng/ml FGF2 for a period of 6 hours. Relative levels of Pea3 and Er81 proteins were determined by Western blot analysis of using specific antibodies. Equivalent amounts of total protein were loaded in each lane. Values shown on graphs were obtained by NIH image analysis of relative band intensities on the Western blots, and were normalized to levels of constitutively expressed Gapdh. (A) Western blot of protein samples from frontonasal explant cultures, together with histograms depicting relative levels of (B) Pea3 and (C) Er81

proteins. (D) Western blot of protein samples from mandibular explant cultures, with corresponding histograms depicting relative levels of (E) Pea3 and (F) Er81 proteins.

5 Discussion

It is well established that FGF signalling plays essential roles in development and patterning of the vertebrate embryo (Ornitz and Itoh, 2001). For example, FGFR mutations are responsible for a number of congenital craniofacial skeletal defects (Winter, 1996). However, despite extensive literature documenting the diverse roles of FGF signalling during craniofacial development, comparatively little is known about the specific downstream effectors through which FGFs influence gene expression.

A previous study in our laboratory had reported that FGF treatment inhibits chondrogenesis in micromass cultures of frontonasal mesenchyme cells, whereas it stimulates chondrogenesis in mandibular mesenchyme cultures (Bobick et al., 2007). Nevertheless, FGF treatment increased ERK activation in both the frontonasal and mandibular mesenchyme cultures, and ERK inhibition blocked the effects of FGFs on both cell populations. This suggested that the mechanism responsible for the differential effects of FGFs on frontonasal and mandibular mesenchyme cells lies downstream of ERK activation (Bobick et al., 2007).

Transcription factors of the Pea3 subfamily (*pea3*, *erm*, and *er81*) are potential targets of ERK phosphorylation (O'Hagan et al., 1996) and are crucial components of the downstream effector pathway through which FGFs influence gene expression (Raible and Brand, 2001). Accordingly, the objective of my thesis was to examine whether cultures of embryonic chick frontonasal and mandibular mesenchyme cells exhibited differential expression patterns of the *pea3*, *erm*, and *er81* genes, and whether FGF treatment has distinct effects on *pea3* expression profiles in the two facial mesenchyme cell populations.

Collectively, my findings demonstrate that *pea3*, *erm*, and *er81* gene expression levels are differentially altered in frontonasal and mandibular mesenchyme cells in response to FGF signalling. In addition, my data show that *pea3*, *erm*, and *er81* exhibit subtly different, although overlapping, expression patterns in the frontonasal and mandibular cell populations, as well as stage-dependent changes in the expression profile of *pea3* in mandibular mesenchyme. A summary of the *pea3*,

erm, and *er81* mRNA expression data is provided in Table 3. The evidence supporting these conclusions is discussed below.

5.1 The mRNA Expression Profiles of *pea3*, *erm*, and *er81* Are Similiar Between Stage 24/25 Frontonasal and Mandibular Mesenchyme in the Absence of Exogenous FGF

A previous study, using *in situ* hybridization, had demonstrated that *pea3*, *erm*, and *er81* gene transcripts are expressed within the head processes of chick embryos from stage 5 to stage 10 of development (Lunn et al., 2007). However, it was not yet known whether they were expressed specifically within the developing facial primordia. The RT-qPCR and RNA dot blot data in the current study clearly demonstrates that *pea3*, *erm*, and *er81* are spontaneously expressed at both stage 24/25 and stage 28/29 of development within chick frontonasal and mandibular mesenchyme (Figures 4, 10, 11, 12 and 13). To our knowledge, this investigation marks the first attempt to quantitatively analyse Pea3 transcription factor gene expression levels within the developing facial primordia of chick embryos.

In the absence of exogenous FGF2, the expression profiles of *pea3*, *erm*, and *er81* between stage 24/25 frontonasal and mandibular explant control cultures were not significantly different. Similarly, no significant differences were observed in the expression profiles of *pea3*, *erm*, and *er81* between stage 24/25 frontonasal and mandibular mesenchyme cells in micromass cultures (Figure 11). Collectively, this data strongly suggests that the endogenous expression profiles of *pea3*, *erm*, and *er81* are similar between chick frontonasal and mandibular mesenchyme prior to addition of exogenous FGF2. Thus, it is unlikely that pre-existing differences in *pea3*, *erm*, and *er81* expression are responsible for differential responses of frontonasal and mandibular mesenchyme to FGF stimuli.

Transcripts for the Pea3 genes were still present in untreated frontonasal and mandibular mesenchyme explants 6 hours after tissue isolation, and at 12 to 32 h of incubation in control micromass cultures. Endogenous Pea3 transcription factor expression was sustained for approximately 32 h after establishment of micromass cultures (Figure 4). Notably, the overlying epithelia (endoderm and ectoderm) had been removed from the frontonasal and mandibular mesenchyme prior to establishment of both explant and micromass cultures. This indicates that expression of *pea3*, *erm*, and *er81* in facial mesenchyme may occur independently of the

Table 3 A data summary of relative differences *pea3*, *erm*, and *er81* mRNA expression based on RT-qPCR analyses.

Micromass	***pea3***	***erm***	***er81***
S24/25 MD relative to S24/25 FN	nsd	nsd	nsd
S28/29 FN relative to S24/25 FN	nsd	nsd	nsd
S28/29 MD relative to S24/25 MD	↓	nsd	nsd
S24/25 FN + FGF2 relative to S24/25 FN Control	↑	nsd	↑
S24/25 MD + FGF2 relative to S24/25 MD Control	↑	↑	nsd
Explants	***pea3***	***erm***	***er81***
S24/25 FN relative to S24/25 MD	nsd	nsd	nsd
S24/25 FN + FGF2 relative to S24/25 FN Control	↑	nsd	nsd
S24/25 MD + FGF2 relative to S24/25 MD Control	nsd	↑ ?	nsd

The REST™ *pea3*, *erm*, and *er81* mRNA expression data analysis from all RT-qPCR experiments is summarized above. A 'nsd' indicates no significant difference. Significant changes in levels of *pea3*, *erm*, and *er81* gene transcripts are indicated by arrows, while a '?' indicates a trend nearing significance. S24/25 = stage 24/25; S28/29 = stage 28/29; FN = frontonasal mesenchyme; MD = mandibular mesenchyme; ↑ = significant upregulation; ↓ = significant down regulation.

sustained influence of adjacent epithelia, which are a significant source of FGF production *in vivo* (Stanier and Pauws, 2012). This contrasts with a previous report by Firnberg et al. (2007) suggesting FGF signalling is both necessary and sufficient for Pea3 transcription factor expression in facial development of chick embryos (Firnberg and Neubuser, 2002). However, the facial mesenchyme explants and micromass cultures in my experiments were maintained in medium supplemented with fetal bovine serum, which contains a variety of growth stimulatory factors (Zheng et al., 2006). It is possible therefore, that certain serum factors might substitute for epithelia-derived FGFs in sustaining expression of Pea3 genes in isolated facial mesenchyme.

5.1.1 Exogenous FGF differentially alters expression profiles of *pea3*, *erm*, and *er81* in stage 24/25 frontonasal and mandibular mesenchyme

The data indicates that the mRNA levels of *pea3*, *erm*, and/or *er81* are increased in response to FGF2 treatment in frontonasal and mandibular mesenchyme explants and micromass cultures of chick embryos (Figures 4, 8, 9, 12, and 13). This is consistent with previous accounts in both chick and zebrafish embryos that the mRNA levels of Pea3 transcription factors are frequently upregulated in response to FGF signalling (Lunn et al., 2007; Roehl and Nusslein-Volhard, 2001).

As discussed earlier, *pea3*, *erm* and *er81* expression levels were found to be similar in stage 24/25 frontonasal and mandibular mesenchyme in the absence of exogenous FGF. However, RT-qPCR analysis revealed differences in the relative extents to which FGF2 treatment altered expression of Pea3 genes in frontonasal and mandibular mesenchyme. A 6 h treatment with FGF2 increased *pea3* mRNA expression in stage 24/25 frontonasal explants, but had no significant effect on *pea3* expression in mandibular explants (Figure 9).

Differential responses to FGF2 were also seen between stage 24/25 frontonasal and mandibular mesenchyme cells in micromass cultures. A 2 h treatment with FGF2 elevated levels of *pea3* gene transcripts in both frontonasal and mandibular mesenchyme (Figure 8). In frontonasal mesenchyme exogenous FGF2 also elevated levels of *er81* mRNA but had no effect on *erm* expression. In contrast, exogenous FGF2 significantly increased levels of *erm* mRNA but had no effect on *er81* expression in stage 24/25 mandibular mesenchyme.

Collectively, these findings indicate that the expression profiles of *pea3*, *erm*, and *er81* in frontonasal and mandibular mesenchyme become distinct only after

exposure to exogenous FGF. This raises the possibility that the differences in Pea3 transcription factor expression patterns that arise in response to FGF stimuli might subsequently lead to distinct chondrogenic outcomes in the two facial mesenchyme populations.

5.1.2 Mandibular mesenchyme, but not frontonasal mesenchyme, exhibits a stage-dependent change in the expression profile of *pea3*

Bobick and Kulyk (2007) reported that the development of the chick frontonasal process was accompanied by a stage-dependent shift in the intracellular pathway responsible for transducing FGF signals (Bobick et al., 2007). Specifically, the effects of FGF on chondrogenesis in stage 24/25 frontonasal mesenchyme micromass cultures were dependent on ERK1/2 activation, whereas ERK inhibition was unable to block the chondro-inhibitory effects of FGFs on stage 28/29 frontonasal mesenchyme (Bobick et al., 2007). Therefore, I examined whether developmental maturation of the facial mesenchyme was correlated with stage-associated changes in the patterns of *pea3*, *erm*, and *er81* expression.

Comparisons between micromass cultures of stage 24/25 and stage 28/29 frontonasal mesenchyme revealed no statistically significant differences in the intrinsic profiles of *pea3*, *erm*, or *er81* expression. Therefore, developmental maturation of the frontonasal primordium does not appear to involve a stage-dependent change in its expression profile of Pea3 transcription factors. It would be important to examine whether FGF exposure differentially alters *pea3*, *erm*, and/or *er81* expression between stage 28/29 and stage 24/25 frontonasal mesenchyme. However due to time constraints, FGF2 treatment experiments were only performed on cultures of stage 24/25 chick mesenchyme.

Interestingly, *pea3* mRNA was expressed at significantly lower levels in stage 28/29 mandibular micromass cultures compared to stage 24/25 mandibular cultures (Figure 10). As previously reported (Hoffman and Kulyk, 1999), my data confirmed that stage 28/29 mandibular mesenchyme displays a much lower capacity for spontaneous chondrogenesis *in vitro* than mandibular mesenchyme from stage 24/25 chick embryos (Figures 14, 16, 17 and 18). Additional experiments would be required to determine whether reduced *pea3* expression in stage 28/29 mandibular mesenchyme may contribute to the relatively lower capacity of these cells for spontaneous chondrogenesis in micromass culture.

5.1.3 Pea3 and Er81 proteins are expressed in micromass cultures of both frontonasal and mandibular mesenchyme

Western blot analysis demonstrated that both the Pea3 and Er81 proteins are endogenously expressed within the frontonasal and mandibular facial primordia of stage 24/25 chick embryos (Figures 19 and 20). Although antibodies specific for chicken Pea3 are not commercially available, I showed that antibodies against the mouse specific Pea3 protein could also be used for avian Pea3 detection. An examination of the pattern of Erm protein expression in chick facial mesenchyme was not possible, as a suitable antibody was not found.

Although *pea3*, *erm*, and/or *er81* mRNA levels were differentially altered in response to FGF2 treatment in explant and micromass cultures of frontonasal and mandibular mesenchyme, the levels of Pea3 and Er81 protein were similar in control and FGF2-treated cultures. A statistical analysis of the Western blot data for Pea3 and Er81 protein expression was not possible as experiments were performed only once due to time constraints. As such, any interpretation of the Pea3 and Er81 protein expression is currently very tentative. It remains possible that exogenous FGF2 might have modest effects on Pea3 and Er81 protein levels in stage 24/25 frontonasal and mandibular mesenchyme. Additional experiments are necessary to determine if the changes in *pea3* and *er81* mRNA expression profiles correspond to similar subtle changes in their respective proteins. Furthermore, the overall protein abundance in a tissue does not necessarily parallel its corresponding gene transcript levels, due to post-transcriptional controls at the levels of RNA processing and RNA stability.

Previous studies have demonstrated that Pea3 transcription factor proteins are affected by phosphorylation and other post-translational modifications. Thus, while no visible differences were observed in total Pea3 or Er81 protein levels in stage 24/25 frontonasal and mandibular mesenchyme in response to exogenous FGF2, there may be effects on phosphorylation or other post-translational modifications that affect their transcriptional activities. Additional analyses to address these possibilities would be worthwhile.

5.1.4 FGF inhibits chondrogenesis in micromass cultures of stage 24/25 frontonasal mesenchyme, but has no effect on mandibular mesenchyme cultures

In an earlier study, Bobick et al. reported that FGF2, -4, and -8 exhibited opposite effects on chondrogenesis of chick frontonasal and mandibular mesenchyme cells in micromass cultures (Bobick et al., 2007). Specifically, whereas addition of FGF to frontonasal mesenchyme micromass cultures of both stage 24/25 and stage 28/29 chick embryos inhibited chondrogenesis, FGFs stimulated chondrogenesis in mandibular mesenchyme micromass cultures of stage 24/25 and stage 28/29 chick embryos.

The data I obtained were only partially consistent with these results. As previously reported (Bobick et al., 2007), FGF2 treatment inhibited chondrogenesis in stage 24/25 and stage 28/29 frontonasal mesenchyme as evidenced by decreased Alcian blue stainable cartilage matrix deposition (Figure 14), reduced sulphated GAG accumulation in the cell layer and medium fractions (Figure 16 and 17), and decreased type II collagen production (Figure 18). In addition, I observed that stage 28/29 mandibular mesenchyme exhibited a lower capacity for spontaneous chondrogenesis in micromass cultures compared to stage 24/25 mandibular mesenchyme cells (Figures 14, 16, 17, and 18), observations that are consistent with a previous report (Hoffman and Kulyk, 1999).

A notable difference in my data was observed in regard to the previously reported chondro-stimulatory effects of FGFs on mandibular mesenchyme micromass cultures (Bobick et al., 2007). Under the specific conditions of my experiments, FGF2 exhibited no discernible effect (i.e. neither stimulatory nor inhibitory) on mandibular mesenchyme chondrogenesis as determined by Alcian blue stainable cartilage matrix deposition (Figure 14), sulphated GAG in the cell layer or culture medium (Figure 16 and 17), or type II collagen accumulation (Figure 18). Although opposite responses of frontonasal and mandibular mesenchyme were not observed, the cells within these two populations responded differently to exogenous FGF2. Specifically, while FGF inhibited chondrogenesis in stage 24/25 frontonasal mesenchyme, it had no effect on chondrogenic differentiation of stage 24/25 mandibular mesenchyme.

Bobick and Kulyk demonstrated that a higher dose of FGF2 (40 ng/ml) reduced the average DNA content of stage 24/25 frontonasal and mandibular mesenchyme cultures to approximately 65 and 82% of the levels in untreated cultures (Bobick, 2006a). No similar reduction was observed at the same FGF2 dose in my experiments. Interestingly, while Bobick and Kulyk found no significant difference in the total DNA content of stage 28/29 mandibular micromass cultures in response to 20 ng/ml FGF2, the same dose of FGF2 significantly increased the DNA content of these cultures in my experiments (Figure 15). This further indicates that under the experimental conditions employed in the current study, mandibular mesenchyme behaved differently in response to FGF signalling than was previously reported.

To investigate the potential causes of this discrepancy, several experimental parameters were examined. Bobick et al. (2007) observed the chondro-stimulatory effects of FGF on mandibular mesenchyme chondrogenesis using several different FGF concentrations (10, 20, and 40 ng/ml) and three different types of FGF (FGF2, -4, and -8) (Bobick et al., 2007). My RT-qPCR and RNA dot blot experiments had consistently utilized FGF2, at a single dose of 20 ng/ml FGF2. As such, I performed additional experiments to examine if mandibular mesenchyme micromass cultures showed stimulatory responses when treated with FGF8 rather than FGF2 (data not shown). However, as with the FGF2 experiments, FGF8 treatment had no effect on chondrogenic differentiation of stage 24/25 and stage 28/29 mandibular mesenchyme micromass cultures. I further speculated that the discrepancy could relate to a lower sensitivity of stage 24/25 mandibular mesenchyme to respond to exogenous FGF2. If so, elevating the concentration of either FGF in the cell culture media would be expected to increase the magnitude of the response, perhaps revealing a chondro-stimulatory effect. However, doubling the concentration of either FGF2 or FGF8 to a concentration of 40 ng/ml in the culture media still had no stimulatory effects on Alcian blue stainable cartilage matrix accumulation in stage 24/25 mandibular mesenchyme cells (data not shown).

Loss of activity during storage or lot-specific variability in the FGF2 stock might also have potentially affected its observed effects on facial mesenchyme micromass cultures. Therefore experiments were performed using aliquots of the same FGF2 stock used in the Bobick et al. (2007) study, as well as a fresh FGF2 stock purchased from a different supplier. In neither case did the FGF2 invoke a stimulatory

effect on mandibular chondrogenesis. Use of an alternate Alcian blue staining protocol also showed the same results as my previous experiments, as did experiments utilizing different stocks of FBS as the medium supplementation. Nevertheless, my results consistently demonstrated that FGF2 inhibited chondrogenesis in frontonasal mesenchyme micromass cultures but had no effect on chondrogenic differentiation of mandibular mesenchyme micromass cultures. This evidence strongly suggests that mandibular mesenchyme cells used in my experiments had an inherently different response to exogenous FGF2 than was previously reported. Since these results were observed throughout multiple independent assays, it is unlikely the discrepancy is related to systematic experimental error.

Interestingly, FGF2 treatment resulted in increased levels of type II collagen immunostaining in stage 28/29 mandibular mesenchyme micromass cultures (Figure 18), which was consistent with the findings of Bobick et al. (Bobick et al., 2007). However, neither Alcian blue staining nor the DMMB assay showed any parallel stimulatory effect on matrix proteoglycan accumulation as was previously reported. The majority of the sulphated GAG produced by stage 28/29 mandibular mesenchyme micromass cultures was secreted into the surrounding culture media, rather than being retained in close proximity to the chondrocytes as primarily occurs with type II collagens. Thus, the disparity between patterns of pericellular sulphated GAG accumulation and type II collagen deposition in stage 28/29 mandibular mesenchyme micromass cultures may relate to differences in localization of the two chondrogenic markers.

5.2 Advantages and Limitations of Methodology

Although not a specific objective of my thesis project, during the course of my experiments it became evident that critical precautionary measures are necessary to ensure the reliability and reproducibility of RT-qPCR data. Considerable time and effort was directed towards implementing a set of standard operating procedures in our laboratory for RT-qPCR experiments. These precautionary measures will be briefly discussed below.

5.2.1 Experimental considerations for RT-qPCR

The very high sensitivity of RT-qPCR is particularly advantageous for gene expression analysis in developmental studies where the amount of embryonic tissue

available is extremely limited. This high sensitivity, however, also presents significant challenges within the laboratory environment. Contamination from non-template DNA within the laboratory (i.e. bacteria, human DNA, crossover contamination) can greatly influence RT-qPCR gene expression data. Numerous methods and procedures to minimize this risk are well-documented within the literature, however many laboratories fail to follow the rigorous precautions recommended by the MIQE guidelines (Bustin et al., 2009). Considerable time and effort was directed towards meeting the stringent requirements outlined by these guidelines.

In preliminary RT-qPCR trials, I relied solely on NCBI Primer Blast software to automatically design primers for amplification of *pea3*, *erm*, and *er81*. However, although these primers amplified a single amplicon of the appropriate size using conventional PCR, they proved to be unsuitable for RT-qPCR analysis as numerous gene transcripts were amplified in the presence of the SYBR green master mix. This was most likely the result of residual genomic DNA present after RNA isolation or contamination of PCR reagents with trace amounts of genomic DNA. As such, new *pea3*, *erm*, and *er81* primers were designed to span putative intron/exon junctions, thus minimizing the risk of amplification of genomic DNA. In addition, while the cDNA synthesis and qPCR reaction mixtures were initially prepared on a standard laboratory bench, it subsequently proved to be important to prepare all RT-qPCR reaction mixtures in a biosafety cabinet that had been first decontaminated with bleach and UV irradiation.

Despite these initial precautionary measures, my early RT-qPCR reactions remained contaminated with non-template DNA as evidenced by multiple melt peaks and the presence of multiple amplicons when products were analyzed by acrylamide gel electrophoresis. Thus, it was deemed necessary to purchase new pipetters designated solely for RT-qPCR use in conjunction with barrier filter pipette tips. It was also necessary to include an on-column DNAse I digestion during the RNA isolation procedure and an additional DNase I digestion step during the reverse transcription reaction to maximally reduce levels of genomic DNA present prior to cDNA amplification by RT-qPCR. Validation of the RNA isolation procedure (Figure 5) using a Biorad Experion microfluidic electrophoresis station further increased our confidence in our RT-qPCR data by ensuring RNA samples were of high integrity and purity.

Uracil-DNA-glycosylase (UDG) catalyzes the N-glycosylic bond between uracil and the phosphodiester backbone of single- or double-stranded DNA, leaving a pyrimidinic site which blocks replication by DNA polymerase. Since the SYBR green master mix includes dUTP instead of dTTP, inclusion of UDG within the RT-qPCR reaction can effectively control crossover contamination (i.e. the products from previous reactions) (Longo et al., 1990). As such, our laboratory now includes UDG in all RT-qPCR reactions. The use of no-template controls (NTCs) in each RT-qPCR experiment is also essential to ensure the absence of primer-dimers and that reagents do not become contaminated over the course of experiments. Similarly, no reverse transcription reaction controls (NRTs) should also be performed to ensure sufficient removal of genomic DNA during the RNA isolation procedure. It is still possible, even when all the aforementioned precautionary measures have been taken, to occasionally observe amplification within NTC and NRT control reactions. In such instances, if amplification in the NTC or NRT controls occurred more than 5 cycles later than the least expressed transcript in experimental samples or beyond total 40 amplification cycles, it was considered negligible as proposed by the authors of the MIQE guidelines (Bustin et al., 2009).

When a sufficient amount of experimental RNA sample is available, it is highly advantageous to utilize an alternative method of RNA expression analysis (e.g., northern blots, RNA dot blots, or RNAse protection assay) to validate the data obtained from RT-qPCR methodologies. Issues pertaining to non-template contamination of RT-qPCR reactions have much less of an impact upon these traditional RNA analysis techniques. In the present study, independent validation of some RT-qPCR data using the RNA dot blot method greatly increased our confidence in our RT-qPCR protocol.

All primers used in this study were optimized for annealing temperatures and were shown to specifically recognize a single target transcript (Figure 6). The MIQE guidelines recommend amplification efficiencies should range between 90 to 110% (Bustin et al., 2009). Lack of sufficient precautionary measures to minimize the risk of non-template contamination typically results in amplification efficiencies above this range. The amplification efficiencies for most primer pairs used in my experiments were within the range of those recommended by the MIQE guidelines, with the exception of those for *pea3* and *er81*. Although the amplification efficiencies

of our *pea3* and *er81* primer sets fell slightly below the stringent MIQE threshold (85.5% and 86% respectively), they were within the efficiency range recommended by the manufacturer of the specific RT-qPCR instrument employed in this study. (BioRad online support: www3.biorad.com/gexp/html/support/amp_central).

There are substantial financial implications when choosing RT-qPCR over traditional methods of RNA expression analysis. The fluorescently labelled dyes or probes required for real-time monitoring of the qPCR reaction are typically much more expensive than conventional PCR reagents. The initial financial investment in probe based RT-qPCR methods (e.g., Taqman probes) is greater than that of fluorescently labelled dyes (i.e. SYBR green). However, the costs associated with the extensive optimization/validation procedures required for reliable RT-qPCR data using SYBR green dye may diminish this financial benefit. The additional costs associated with RT-qPCR analyses may also limit the feasibility of temporal RNA expression profile analyses.

It is also interesting to note that while the preliminary RNA dot blot was unable to detect the presence of *erm* within micromass cultures of stage 24/25 frontonasal and mandibular mesenchyme (Figure 4), subsequent RNA dot blots successfully detected *erm* mRNA (Figures 12 and 13). Failure to detect e*rm* transcripts within these early experiments most likely related to cDNA probe synthesis and/or primer/template design, as subsequent experiments utilized an alternate primer-template combination. It may have been possible to utilize traditional RNA dot blot methodologies to examine *pea3*, *erm*, and *er81* expression profiles. Although RNA dot blots lack the sensitivity of RT-qPCR, they are simple, inexpensive and relatively quick. As such, with additional embryonic tissue, RNA dot blots may have been beneficial for preliminary experiments into temporal changes in the expression patterns of the Pea3 subfamily of transcription factors.

5.2.2 Variability in RT-qPCR data

The data from several individual experiments was pooled for final REST™ analysis. While the gene expression trends observed in RT-qPCR experiments were generally comparable between individual experiments, variation between the data obtained from individual experiments did exist. Notably, this type of variation was much less evident in experiments involving the micromass culture model than in

explants. The establishment of micromass cultures involves tissue dissociation to create a homogeneous high-density cell suspension, which is then spotted in replicate aliquots onto cell cultures plates. Thus, the greater homogeneity of the micromass culture system may explain the reduced variability observed in the resulting REST™ data, in comparison to the data obtained from explant experiments. Since the latter procedure does not involve a tissue dissociation step, it is necessary to use facial primordia excised from different individual embryos when establishing replicate explant cultures. Although all embryos were staged according to the methods of Hamburger and Hamilton (Hamburger and Hamilton, 1951), differences in external dimensions are evident between facial processes excised from separate embryos. Due to the greater thickness of facial explants in comparison to micromass cultures it is possible that exposure of mesenchyme cells to exogenous FGF2 in explant cultures was less uniform than in micromass cultures. Mesenchyme cells located within the innermost region of the facial explants may have been partially insulated from the effects of exogenous FGF2, further increasing the variability in *pea3*, *erm*, and *er81* mRNA expression values obtained from replicate explant cultures.

5.2.3 Differences between *pea3*, *er81*, and *erm* expression profiles between micromass and explant cultures of stage 24/25 frontonasal and mandibular mesenchyme in response to exogenous FGF2

The effects of FGF2 on the expression profiles of *pea3*, *erm*, and *er81* in stage 24/25 frontonasal and mandibular mesenchyme as determined by RT-qPCR differed between explant and micromass cultures (Figures 8 and 9). Specifically, whereas FGF2 increased *pea3* expression in stage 24/25 frontonasal explants alone, it elevated *pea3* expression in both stage 24/25 frontonasal and stage 24/25 mandibular mesenchyme micromass cultures. Furthermore, while FGF2 treatment affected neither *erm* or *er81* expression in explant cultures of frontonasal or mandibular mesenchyme, FGF2 exposure increased *er81* expression in frontonasal mesenchyme micromass cultures and elevated *erm* expression in mandibular mesenchyme micromass cultures.

There are several possible explanations for the differences observed in the effects of FGFs on *pea3*, *erm*, and *er81* mRNA expression profiles between micromass and explant cultures. While micromass cultures were treated with FGF2 for 2 h, explant cultures were treated for 6 h. As mentioned previously, unlike

micromass cultures, explant cultures retain their native cell-cell contacts, and explants from individual embryos display slight differences in size and thickness. The native cell-cell contacts may directly contribute to the differences in Pea3 transcription factor expression profiles between micromass and explant cultures. Our experimental design had also assumed a longer FGF2 incubation period would be necessary to obtain comparable effects to those observed with 2 h FGF2 treatment of frontonasal and mandibular mesenchyme micromass cultures. The increased exposure of explant cultures to exogenous FGF2 may have contributed to the difference in *pea3*, *erm*, and *er81* expression profiles in comparison to those for micromass cultures.

5.2.4 Considerations for the use of commercially purchased fertilized eggs for research purposes

My study has raised a number of possible concerns in relation to the use of eggs from commercially bred chickens as a source of embryos for research purposes. First is the difficulty to control all factors that might be sources of biological variability. The rate of chick development is readily influenced by environmental factors, such as temperature and maternal nutritional status. Changes to either of these factors can imprint upon early stages of embryonic development and potentially impact cellular behaviour or tissue responses. Secondly, there may be gradual genetic drift in the population due to selective breeding aimed at generating chickens with more rapid postnatal growth and a correspondingly shorter time to market. Within my own experiments, the rates of chondrogenic differentiation in micromass cultures of both stage 24/25 frontonasal and mandibular mesenchyme cells appeared to be accelerated in comparison to earlier studies performed in our lab (W. Kulyk, personal communication).

The local commercial hatchery from which our fertilized eggs are purchased had previously distributed eggs from several different chicken breeds, including White Leghorn, Red Sussex, and Cornish Cross. However, all the eggs used for my experiments were from Giant Cornish Cross chickens, a breed deliberately developed for an exceptionally rapid rate of development.

It is possible that any of these factors, or a combination thereof, may account for the lack of chondro-stimulatory response of mandibular mesenchyme to FGF2 signalling observed within the current study in comparison to that previously reported by Bobick and Kulyk (Bobick et al., 2007).

5.3 Conclusions

In summary, my research findings support the following main conclusions:

- Mesenchyme cells from both the frontonasal and mandibular facial primordia of stage 24/25 and stage 28/29 chick embryos express mRNA transcripts for all three genes of the Pea3 transcription factor family (*pea3*, *erm*, and *er81)*.
- Western blot analysis indicates that frontonasal and mandibular mesenchyme cells also express at least two of these transcription factors (Pea3 and Er81) at the protein level.
- Prior to stimulation with exogenous FGF2, the expression profiles of *pea3*, *erm*, and *er81* mRNA transcripts are not significantly different between frontonasal and mandibular mesenchyme cells of the stage 24/25 chick embryo. This is true for facial mesenchyme explants and micromass cell cultures
- Exposure to FGF2 alters *pea3*, *erm*, and/or *er81* gene transcript levels in a differential manner in explant and micromass cultures of frontonasal versus mandibular mesenchyme of the stage 24/25 chick embryo. Specifically, in frontonasal explant cultures, *pea3* gene transcripts were upregulated in response to FGF2, while *erm* and *er81* were unaffected. Mandibular explants exhibited no changes in any of the Pea3 transcription factors following treatment with FGF2. In micromass cultures, *pea3* was elevated in both frontonasal and mandibular mesenchyme following FGF2 exposure. In addition, *er81* was upregulated in frontonasal mesenchyme, while *erm* was upregulated in mandibular mesenchyme following FGF2 treatment.
- There is a stage-associated change in *pea3* mRNA expression during developmental maturation of the mandibular primordium. Specifically, stage 28/29 mandibular mesenchyme exhibited significantly lower levels of *pea3* expression than stage 24/25 mandibular mesenchyme. However, no stage-dependent changes in Pea3 transcription factor expression were observed in frontonasal mesenchyme micromass cultures.
- Contrary to a previously published study, my data indicate that stage 24/25 chick frontonasal and mandibular mesenchyme cells exhibit distinct, although not opposite, chondrogenic responses to exogenous FGF2. Specifically, whereas exogenous FGF2 inhibited chondrogenesis in frontonasal

mesenchyme, it had neither an inhibitory nor stimulatory effect on mandibualr mesenchyme.

5.4 Future Directions

My thesis research represents a first step toward examining the role of Pea3 transcription factors in embryonic facial development. The results of this study have demonstrated that exposure to exogenous FGF differentially alters *pea3*, *erm*, and/or *er81* gene expression profiles in mesenchyme derived from the frontonasal and mandibular primordia of the chick embryo. It is not yet apparent, however, whether there is any functional relationship between the distinct chondrogenic responses of stage 24/25 frontonasal and mandibular mesenchyme cells to FGF signalling and the differential effects of FGF on *pea3*, *erm*, and *er81* mRNA expression levels *in vitro*.

In 2007, Bobick et al. reported that stage 24/25 and stage 28/29 frontonasal and mandibular mesenchyme exhibit opposing chondrogenic responses to exogenous FGF2, -4, and -8 (Bobick et al., 2007). Specifically, whereas exogenous FGF inhibited chondrogenesis of frontonasal mesenchyme, it stimulated chondrogenesis in mandibular mesenchyme. The current examination, however, found that while exogenous FGF2 inhibited chondrogenesis in frontonasal mesenchyme, it had no chondrogenic effect on mandibular mesenchyme. While attempts were made to determine the cause of this discrepancy, thus far, no specific factor has been identified. Future experiments to examine the effects of FGF on facial tissues from another breed of chicken to determine if genetic differences are responsible for this disparity would be useful.

In the current examination, statistical analysis of the Western blot data was not possible due to an insufficient number of replicates. While I observed no obvious differences in the levels of total Pea3 or Er81 proteins, it is possible exogenous FGF2 may exhibit more subtle effects on Pea3 transcription factor expression in frontonasal and mandibular mesenchyme. Additional Western blot experiments are necessary to more thoroughly examine the effects of FGFs on Pea3 and Er81 protein expression.

The specific Erm antibody we tested for species cross-reactivity was not able to detect Erm in chicken lysates. However, there are a number of other Erm antibodies commercially available which could be tested for cross-reactivity to enable analysis of Erm protein expression in chick embryos. In addition, previous studies have demonstrated that Pea3 transcription factor proteins are affected by

phosphorylation and other post-translational modifications. Thus, there may be effects on phosphorylation or other post-translational modifications that affect their physiological activities. Additional analyses to address these possibilities would be worthwhile.

Znosko et al. (2010) demonstrated that simultaneous knockdown of Pea3, Erm, and Er81 in zebrafish embryos using antisense morpholinos resulted in phenotypes resembling embryos deficient in FGF signalling (Znosko et al., 2010). Future experiments should be performed using RNA silencing methods (e.g., siRNA of shRNA treatments) to determine whether knockdown of *pea3*, *erm*, and *er81 genes* affects the ability of embryonic chick frontonasal and mandibular mesenchyme to undergo chondrogenic differentiation or to respond to exogenous FGFs. Znosko et al. (2010) had found that it was necessary to simultaneously knockdown expression of all three Pea3 genes in order to effectively block FGF signalling in zebrafish embryos. As such, it will be important to not only test the effects of *pea3*, *erm* and *er81* gene knockdown individually, but to also examine how the simultaneous combinatorial knockdown of two or more of these transcription factors influences skeletal tissue differentiation in chick embryo facial primordia.

Another worthwhile area to investigate is whether there exists micro-heterogeneity in patterns of *pea3*, *erm*, and *er81* between specific sub-regions of each facial primordium, such as the mandibular process. Mina et al. (2002) demonstrated that within the developing mandibular process of chick embryos at least two functionally distinct regions exist (Mina et al., 2002). Morphogenesis within the lateral mandibular regions is dependent upon FGF8 signalling, while morphogenesis within the medial portion of the mandibular process occurs independently of FGF8 signalling. Moreover, these two regions of mandibular mesenchyme were found to differentially respond to FGF signalling (Mina et al., 2002). If the Pea3 transcription factors play functional roles in mediating FGF responses in the developing mandible development, it may be possible to demonstrate regional differences in *pea3*, *erm*, and *er81* expression profiles between the lateral and medial portions of the mandibular primordium. A combination of *in situ* hybridization methods and RT-qPCR analyses could be used to address this possibility.

It will ultimately be important to perform *in vivo* experiments to investigate the role of Pea3 transcription factors in chondrogenesis of facial mesenchyme, as the

current study relied solely on *in vitro* experiments. For example, localized infection with retroviral viruses that express *pea3*, *erm*, and/or *er81* coding sequences could be used to examine the effects of overexpression of these genes in specific facial regions of the chick embryo developing *in ovo*. Alternatively, conditional knockouts of the Pea3 transcription factors in individual facial regions of mouse embryos could help elucidate the roles of pea, erm, and er81 *in vivo*.

Such studies would provide greater insight into the molecular mechanisms through which FGFs affect chondrogenic differentiation *in vitro,* and may help elucidate the mechanisms responsible for the cellular signalling cascades regulating facial development *in vivo*.

6 REFERENCES

Adachi, M., Fukuda, M., Nishida, E., 1999. Two co-existing mechanisms for nuclear import of MAP kinase: passive diffusion of a monomer and active transport of a dimer. EMBO J. 18**,** 5347-58.

Ahrens, P. B., Solursh, M., Reiter, R. S., 1977. Stage-related capacity for limb chondrogenesis in cell culture. Dev Biol. 60**,** 69-82.

Akiyama, H., Lefebvre, V., 2011. Unraveling the transcriptional regulatory machinery in chondrogenesis. J Bone Miner Metab. 29**,** 390-5.

Ala-Kokko, L., Kvist, A. P., Metsaranta, M., Kivirikko, K. I., de Crombrugghe, B., Prockop, D. J., Vuorio, E., 1995. Conservation of the sizes of 53 introns and over 100 intronic sequences for the binding of common transcription factors in the human and mouse genes for type II procollagen (COL2A1). Biochem J. 308 (Pt 3)**,** 923-9.

Ausubel, F. M., 1987. Current protocols in molecular biology. Greene Pub. Associates ; J. Wiley, order fulfillment, Brooklyn, N.Y. Media, Pa.

Barbosa, I., Garcia, S., Barbier-Chassefiere, V., Caruelle, J. P., Martelly, I., Papy-Garcia, D., 2003. Improved and simple micro assay for sulfated glycosaminoglycans quantification in biological extracts and its use in skin and muscle tissue studies. Glycobiology. 13**,** 647-53.

Bastow, E. R., Byers, S., Golub, S. B., Clarkin, C. E., Pitsillides, A. A., Fosang, A. J., 2008. Hyaluronan synthesis and degradation in cartilage and bone. Cell Mol Life Sci. 65**,** 395-413.

Bi, W., Deng, J. M., Zhang, Z., Behringer, R. R., de Crombrugghe, B., 1999. Sox9 is required for cartilage formation. Nat Genet. 22**,** 85-9.

Bobick, B. E., Regulation of in vitro chondrogenesis by mitogen-activated protein kinases. University of Saskatchewan, 2006., 2006a, pp. xxii, 281 leaves.

Bobick, B. E., Chen, F. H., Le, A. M., Tuan, R. S., 2009. Regulation of the chondrogenic phenotype in culture. Birth Defects Res C Embryo Today. 87**,** 351-71.

Bobick, B. E., Kulyk, W. M., 2004. The MEK-ERK signaling pathway is a negative regulator of cartilage-specific gene expression in embryonic limb mesenchyme. J Biol Chem. 279**,** 4588-95.

Bobick, B. E., Kulyk, W. M., 2008. Regulation of cartilage formation and maturation by mitogen-activated protein kinase signaling. Birth Defects Res C Embryo Today. 84**,** 131-54.

Bobick, B. E., Kulyk, W. M., 2006b. MEK-ERK signaling plays diverse roles in the regulation of facial chondrogenesis. Exp Cell Res. 312**,** 1079-92.

Bobick, B. E., Thornhill, T. M., Kulyk, W. M., 2007. Fibroblast growth factors 2, 4, and 8 exert both negative and positive effects on limb, frontonasal, and mandibular chondrogenesis via MEK-ERK activation. J Cell Physiol. 211**,** 233-43.

Bottcher, R. T., Niehrs, C., 2005. Fibroblast growth factor signaling during early vertebrate development. Endocr Rev. 26**,** 63-77.

Bradford, M. M., 1976. A rapid and sensitive method for the quantitation of microgram quantities of protein utilizing the principle of protein-dye binding. Anal Biochem. 72**,** 248-54.

Brugmann, S. A., Tapadia, M. D., Helms, J. A., 2006. The molecular origins of species-specific facial pattern. Curr Top Dev Biol. 73, 1-42.

Bustin, S. A., 2005. Real-time, fluorescence-based quantitative PCR: a snapshot of current procedures and preferences. Expert Rev Mol Diagn. 5, 493-8.

Bustin, S. A., 2010. Why the need for qPCR publication guidelines?--The case for MIQE. Methods. 50, 217-26.

Bustin, S. A., Benes, V., Garson, J. A., Hellemans, J., Huggett, J., Kubista, M., Mueller, R., Nolan, T., Pfaffl, M. W., Shipley, G. L., Vandesompele, J., Wittwer, C. T., 2009. The MIQE guidelines: minimum information for publication of quantitative real-time PCR experiments. Clin Chem. 55, 611-22.

Cancedda, R., Descalzi Cancedda, F., Castagnola, P., 1995. Chondrocyte differentiation. Int Rev Cytol. 159, 265-358.

Chandler, H. L., Colitz, C. M., 2006. Molecular biology for the clinician: understanding current methods. J Am Anim Hosp Assoc. 42, 326-35.

Chang, S. H., Oh, C. D., Yang, M. S., Kang, S. S., Lee, Y. S., Sonn, J. K., Chun, J. S., 1998. Protein kinase C regulates chondrogenesis of mesenchymes via mitogen-activated protein kinase signaling. J Biol Chem. 273, 19213-9.

Chotteau-Lelievre, A., Desbiens, X., Pelczar, H., Defossez, P. A., de Launoit, Y., 1997. Differential expression patterns of the PEA3 group transcription factors through murine embryonic development. Oncogene. 15, 937-52.

Cobourne, M. T., 2000. Construction for the modern head: current concepts in craniofacial development. J Orthod. 27, 307-14.

Corson, L. B., Yamanaka, Y., Lai, K. M., Rossant, J., 2003. Spatial and temporal patterns of ERK signaling during mouse embryogenesis. Development. 130, 4527-37.

Coutte, L., Monte, D., Imai, K., Pouilly, L., Dewitte, F., Vidaud, M., Adamski, J., Baert, J. L., de Launoit, Y., 1999. Characterization of the human and mouse ETV1/ER81 transcription factor genes: role of the two alternatively spliced isoforms in the human. Oncogene. 18, 6278-86.

Daniels, K., Reiter, R., Solursh, M., 1996. Micromass cultures of limb and other mesenchyme. Methods Cell Biol. 51, 237-47.

de Launoit, Y., Baert, J. L., Chotteau, A., Monte, D., Defossez, P. A., Coutte, L., Pelczar, H., Leenders, F., 1997. Structure-function relationships of the PEA3 group of Ets-related transcription factors. Biochem Mol Med. 61, 127-35.

Debiais, F., Lemonnier, J., Hay, E., Delannoy, P., Caverzasio, J., Marie, P. J., 2001. Fibroblast growth factor-2 (FGF-2) increases N-cadherin expression through protein kinase C and Src-kinase pathways in human calvaria osteoblasts. J Cell Biochem. 81, 68-81.

DeLise, A. M., Fischer, L., Tuan, R. S., 2000. Cellular interactions and signaling in cartilage development. Osteoarthritis Cartilage. 8, 309-34.

Dessau, W., von der Mark, H., von der Mark, K., Fischer, S., 1980. Changes in the patterns of collagens and fibronectin during limb-bud chondrogenesis. J Embryol Exp Morphol. 57, 51-60.

Dhillon, A. S., Kolch, W., 2002. Untying the regulation of the Raf-1 kinase. Arch Biochem Biophys. 404, 3-9.

Erlebacher, A., Filvaroff, E. H., Gitelman, S. E., Derynck, R., 1995. Toward a molecular understanding of skeletal development. Cell. 80, 371-8.

Eswarakumar, V. P., Lax, I., Schlessinger, J., 2005. Cellular signaling by fibroblast growth factor receptors. Cytokine Growth Factor Rev. 16, 139-49.

Farndale, R. W., Sayers, C. A., Barrett, A. J., 1982. A direct spectrophotometric microassay for sulfated glycosaminoglycans in cartilage cultures. Connect Tissue Res. 9, 247-8.

Firnberg, N., Neubuser, A., 2002. FGF signaling regulates expression of Tbx2, Erm, Pea3, and Pax3 in the early nasal region. Dev Biol. 247, 237-50.

Fleige, S., Pfaffl, M. W., 2006. RNA integrity and the effect on the real-time qRT-PCR performance. Mol Aspects Med. 27, 126-39.

Francis-West, P., Ladher, R., Barlow, A., Graveson, A., 1998. Signalling interactions during facial development. Mech Dev. 75, 3-28.

Gehris, A. L., Stringa, E., Spina, J., Desmond, M. E., Tuan, R. S., Bennett, V. D., 1997. The region encoded by the alternatively spliced exon IIIA in mesenchymal fibronectin appears essential for chondrogenesis at the level of cellular condensation. Dev Biol. 190, 191-205.

Goldring, M. B., Goldring, S. R., 1990. Skeletal tissue response to cytokines. Clin Orthop Relat Res. 245-78.

Goldring, M. B., Tsuchimochi, K., Ijiri, K., 2006. The control of chondrogenesis. J Cell Biochem. 97, 33-44.

Gould, S. E., Upholt, W. B., Kosher, R. A., 1995. Characterization of chicken syndecan-3 as a heparan sulfate proteoglycan and its expression during embryogenesis. Dev Biol. 168, 438-51.

Graves, B. J., Petersen, J. M., 1998. Specificity within the ets family of transcription factors. Adv Cancer Res. 75, 1-55.

Greene, R. M., Pisano, M. M., 2004. Perspectives on growth factors and orofacial development. Curr Pharm Des. 10, 2701-17.

Hall, B. K., Miyake, T., 2000. All for one and one for all: condensations and the initiation of skeletal development. Bioessays. 22, 138-47.

Hamburger, V., Hamilton, H. L., 1951. A series of normal stages in the development of the chick embryo. 1951. J Morphol. 88, 49-92.

Han, Y., Lefebvre, V., 2008. L-Sox5 and Sox6 drive expression of the aggrecan gene in cartilage by securing binding of Sox9 to a far-upstream enhancer. Mol Cell Biol. 28, 4999-5013.

Hartmann, C., 2009. Transcriptional networks controlling skeletal development. Curr Opin Genet Dev. 19, 437-43.

Hassell, J. R., Horigan, E. A., 1982. Chondrogenesis: a model developmental system for measuring teratogenic potential of compounds. Teratog Carcinog Mutagen. 2, 325-31.

Havens, B. A., Rodgers, B., Mina, M., 2006. Tissue-specific expression of Fgfr2b and Fgfr2c isoforms, Fgf10 and Fgf9 in the developing chick mandible. Arch Oral Biol. 51, 134-45.

Helms, J. A., Kim, C. H., Hu, D., Minkoff, R., Thaller, C., Eichele, G., 1997. Sonic hedgehog participates in craniofacial morphogenesis and is down-regulated by teratogenic doses of retinoic acid. Dev Biol. 187, 25-35.

Hoffman, L. M., Kulyk, W. M., 1999. Alcohol promotes in vitro chondrogenesis in embryonic facial mesenchyme. Int J Dev Biol. 43, 167-74.

Hoffman, L. M., Weston, A. D., Underhill, T. M., 2003. Molecular mechanisms regulating chondroblast differentiation. J Bone Joint Surg Am. 85-A Suppl 2, 124-32.

Itoh, N., Ornitz, D. M., 2004. Evolution of the Fgf and Fgfr gene families. Trends Genet. 20, 563-9.

Itoh, N., Ornitz, D. M., 2011. Fibroblast growth factors: from molecular evolution to roles in development, metabolism and disease. J Biochem. 149, 121-30.

Jaye, M., Schlessinger, J., Dionne, C. A., 1992. Fibroblast growth factor receptor tyrosine kinases: molecular analysis and signal transduction. Biochim Biophys Acta. 1135, 185-99.

Jiang, T. X., Yi, J. R., Ying, S. Y., Chuong, C. M., 1993. Activin enhances chondrogenesis of limb bud cells: stimulation of precartilaginous mesenchymal condensations and expression of NCAM. Dev Biol. 155, 545-57.

Johnson, G. L., Lapadat, R., 2002. Mitogen-activated protein kinase pathways mediated by ERK, JNK, and p38 protein kinases. Science. 298, 1911-2.

Katz, M., Amit, I., Yarden, Y., 2007. Regulation of MAPKs by growth factors and receptor tyrosine kinases. Biochim Biophys Acta. 1773, 1161-76.

Knudson, C. B., Knudson, W., 1993. Hyaluronan-binding proteins in development, tissue homeostasis, and disease. FASEB J. 7, 1233-41.

Konat, G. W., 1996. Generation of high efficiency ssDNA hybridization probes by linear polymerase chain reaction (LPCR). Scanning Microsc Suppl. 10, 57-60.

Kosher, R. A., Gay, S. W., Kamanitz, J. R., Kulyk, W. M., Rodgers, B. J., Sai, S., Tanaka, T., Tanzer, M. L., 1986a. Cartilage proteoglycan core protein gene expression during limb cartilage differentiation. Dev Biol. 118, 112-7.

Kosher, R. A., Kulyk, W. M., Gay, S. W., 1986b. Collagen gene expression during limb cartilage differentiation. J Cell Biol. 102, 1151-6.

Koyama, E., Leatherman, J. L., Shimazu, A., Nah, H. D., Pacifici, M., 1995. Syndecan-3, tenascin-C, and the development of cartilaginous skeletal elements and joints in chick limbs. Dev Dyn. 203, 152-62.

Kulyk, W. M., Coelho, C. N., Kosher, R. A., 1991. Type IX collagen gene expression during limb cartilage differentiation. Matrix. 11, 282-8.

Kulyk, W. M., Franklin, J. L., Hoffman, L. M., 2000. Sox9 expression during chondrogenesis in micromass cultures of embryonic limb mesenchyme. Exp Cell Res. 255, 327-32.

Kulyk, W. M., Kosher, R. A., 1987. Temporal and spatial analysis of hyaluronidase activity during development of the embryonic chick limb bud. Dev Biol. 120, 535-41.

Kulyk, W. M., Reichert, C., 1992. Staurosporine, a protein kinase inhibitor, stimulates cartilage differentiation by embryonic facial mesenchyme. J Craniofac Genet Dev Biol. 12, 90-7.

Kulyk, W. M., Rodgers, B. J., Greer, K., Kosher, R. A., 1989. Promotion of embryonic chick limb cartilage differentiation by transforming growth factor-beta. Dev Biol. 135, 424-30.

Labarca, C., Paigen, K., 1980. A simple, rapid, and sensitive DNA assay procedure. Anal Biochem. 102, 344-52.

Laurent, T. C., Fraser, J. R., 1992. Hyaluronan. FASEB J. 6, 2397-404.

Lefebvre, V., Behringer, R. R., de Crombrugghe, B., 2001. L-Sox5, Sox6 and Sox9 control essential steps of the chondrocyte differentiation pathway. Osteoarthritis Cartilage. 9 Suppl A, S69-75.

Lefebvre, V., Li, P., de Crombrugghe, B., 1998. A new long form of Sox5 (L-Sox5), Sox6 and Sox9 are coexpressed in chondrogenesis and cooperatively activate the type II collagen gene. EMBO J. 17, 5718-33.

Leonard, C. M., Fuld, H. M., Frenz, D. A., Downie, S. A., Massague, J., Newman, S. A., 1991. Role of transforming growth factor-beta in chondrogenic pattern

formation in the embryonic limb: stimulation of mesenchymal condensation and fibronectin gene expression by exogenenous TGF-beta and evidence for endogenous TGF-beta-like activity. Dev Biol. 145, 99-109.

Lin, J. H., Saito, T., Anderson, D. J., Lance-Jones, C., Jessell, T. M., Arber, S., 1998. Functionally related motor neuron pool and muscle sensory afferent subtypes defined by coordinate ETS gene expression. Cell. 95, 393-407.

Liu, B., Rooker, S. M., Helms, J. A., 2010. Molecular control of facial morphology. Semin Cell Dev Biol. 21, 309-13.

Livak, K. J., Schmittgen, T. D., 2001. Analysis of relative gene expression data using real-time quantitative PCR and the 2(-Delta Delta C(T)) Method. Methods. 25, 402-8.

Longo, M. C., Berninger, M. S., Hartley, J. L., 1990. Use of uracil DNA glycosylase to control carry-over contamination in polymerase chain reactions. Gene. 93, 125-8.

Loo, B. B., Darwish, K. K., Vainikka, S. S., Saarikettu, J. J., Vihko, P. P., Hermonen, J. J., Goldman, A. A., Alitalo, K. K., Jalkanen, M. M., 2000. Production and characterization of the extracellular domain of recombinant human fibroblast growth factor receptor 4. Int J Biochem Cell Biol. 32, 489-97.

Lunn, J. S., Fishwick, K. J., Halley, P. A., Storey, K. G., 2007. A spatial and temporal map of FGF/Erk1/2 activity and response repertoires in the early chick embryo. Dev Biol. 302, 536-52.

Maccabe, A. B., Gasseling, M. T., Saunders, J. W., Jr., 1973. Spatiotemporal distribution of mechanisms that control outgrowth and anteroposterior polarization of the limb bud in the chick embryo. Mech Ageing Dev. 2, 1-12.

MacCabe, J. A., Errick, J., Saunders, J. W., Jr., 1974. Ectodermal control of the dorsoventral axis in the leg bud of the chick embryo. Dev Biol. 39, 69-82.

Mackie, E. J., Ahmed, Y. A., Tatarczuch, L., Chen, K. S., Mirams, M., 2008. Endochondral ossification: how cartilage is converted into bone in the developing skeleton. Int J Biochem Cell Biol. 40, 46-62.

Mackie, E. J., Murphy, L. I., 1998. The role of tenascin-C and related glycoproteins in early chondrogenesis. Microsc Res Tech. 43, 102-10.

Mackie, E. J., Tatarczuch, L., Mirams, M., 2011. The skeleton: a multi-functional complex organ: the growth plate chondrocyte and endochondral ossification. J Endocrinol. 211, 109-21.

McAlinden, A., Havlioglu, N., Liang, L., Davies, S. R., Sandell, L. J., 2005. Alternative splicing of type II procollagen exon 2 is regulated by the combination of a weak 5' splice site and an adjacent intronic stem-loop cis element. J Biol Chem. 280, 32700-11.

McIntosh, I., Bellus, G. A., Jab, E. W., 2000. The pleiotropic effects of fibroblast growth factor receptors in mammalian development. Cell Struct Funct. 25, 85-96.

Milner, R. J., Brow, M. D., Cleveland, D. W., Shinnick, T. M., Sutcliffe, J. G., 1983. Glyceraldehyde 3-phosphate dehydrogenase protein and mRNA are both differentially expressed in adult chickens but not chick embryos. Nucleic Acids Res. 11, 3301-15.

Mina, M., Upholt, W. B., Kollar, E. J., 1994. Enhancement of avian mandibular chondrogenesis in vitro in the absence of epithelium. Arch Oral Biol. 39, 551-62.

Mina, M., Wang, Y. H., Ivanisevic, A. M., Upholt, W. B., Rodgers, B., 2002. Region- and stage-specific effects of FGFs and BMPs in chick mandibular morphogenesis. Dev Dyn. 223, 333-52.

Minamide, L. S., Bamburg, J. R., 1990. A filter paper dye-binding assay for quantitative determination of protein without interference from reducing agents or detergents. Anal Biochem. 190, 66-70.

Miraoui, H., Marie, P. J., 2010. Fibroblast growth factor receptor signaling crosstalk in skeletogenesis. Sci Signal. 3, re9.

Nah, H. D., Rodgers, B. J., Kulyk, W. M., Kream, B. E., Kosher, R. A., Upholt, W. B., 1988. In situ hybridization analysis of the expression of the type II collagen gene in the developing chicken limb bud. Coll Relat Res. 8, 277-94.

Nickel, W., 2010. Pathways of unconventional protein secretion. Curr Opin Biotechnol. 21, 621-6.

Nishimura, R., Hata, K., Matsubara, T., Wakabayashi, M., Yoneda, T., 2012. Regulation of bone and cartilage development by network between BMP signalling and transcription factors. J Biochem. 151, 247-54.

Noden, D. M., 1991. Cell movements and control of patterned tissue assembly during craniofacial development. J Craniofac Genet Dev Biol. 11, 192-213.

Nolan, T., Hands, R. E., Bustin, S. A., 2006. Quantification of mRNA using real-time RT-PCR. Nat Protoc. 1, 1559-82.

O'Hagan, R. C., Tozer, R. G., Symons, M., McCormick, F., Hassell, J. A., 1996. The activity of the Ets transcription factor PEA3 is regulated by two distinct MAPK cascades. Oncogene. 13, 1323-33.

Oberlender, S. A., Tuan, R. S., 1994. Expression and functional involvement of N-cadherin in embryonic limb chondrogenesis. Development. 120, 177-87.

Oettgen, P., Alani, R. M., Barcinski, M. A., Brown, L., Akbarali, Y., Boltax, J., Kunsch, C., Munger, K., Libermann, T. A., 1997. Isolation and characterization of a novel epithelium-specific transcription factor, ESE-1, a member of the ets family. Mol Cell Biol. 17, 4419-33.

Oh, C. D., Chang, S. H., Yoon, Y. M., Lee, S. J., Lee, Y. S., Kang, S. S., Chun, J. S., 2000. Opposing role of mitogen-activated protein kinase subtypes, erk-1/2 and p38, in the regulation of chondrogenesis of mesenchymes. J Biol Chem. 275, 5613-9.

Oikawa, T., Yamada, T., 2003. Molecular biology of the Ets family of transcription factors. Gene. 303, 11-34.

Olsen, B. R., Reginato, A. M., Wang, W., 2000. Bone development. Annu Rev Cell Dev Biol. 16, 191-220.

Ornitz, D. M., Itoh, N., 2001. Fibroblast growth factors. Genome Biol. 2, REVIEWS 3005.

Ornitz, D. M., Marie, P. J., 2002. FGF signaling pathways in endochondral and intramembranous bone development and human genetic disease. Genes Dev. 16, 1446-65.

Patil, A. S., Sable, R. B., Kothari, R. M., 2012. Role of insulin-like growth factors (IGFs), their receptors and genetic regulation in the chondrogenesis and growth of the mandibular condylar cartilage. J Cell Physiol. 227, 1796-804.

Pfaffl, M. W., 2001. A new mathematical model for relative quantification in real-time RT-PCR. Nucleic Acids Res. 29, e45.

Pfaffl, M. W., 2010. The ongoing evolution of qPCR. Methods. 50, 215-6.

Pfaffl, M. W., Horgan, G. W., Dempfle, L., 2002. Relative expression software tool (REST) for group-wise comparison and statistical analysis of relative expression results in real-time PCR. Nucleic Acids Res. 30, e36.
Poole, A., 2000. Cartilage in Health and Disease. In: Arthritis and Allied Conditions: A Textbook of Rheumatology., 226-284.
Raible, F., Brand, M., 2001. Tight transcriptional control of the ETS domain factors Erm and Pea3 by Fgf signaling during early zebrafish development. Mech Dev. 107, 105-17.
Ramos, J. W., 2008. The regulation of extracellular signal-regulated kinase (ERK) in mammalian cells. Int J Biochem Cell Biol. 40, 2707-19.
Richman, J. M., Herbert, M., Matovinovic, E., Walin, J., 1997. Effect of fibroblast growth factors on outgrowth of facial mesenchyme. Dev Biol. 189, 135-47.
Richman, J. M., Lee, S. H., 2003. About face: signals and genes controlling jaw patterning and identity in vertebrates. Bioessays. 25, 554-68.
Roehl, H., Nusslein-Volhard, C., 2001. Zebrafish pea3 and erm are general targets of FGF8 signaling. Curr Biol. 11, 503-7.
Ross, M. H., Pawlina, W., 2006. Histology : a text and atlas with correlated cell and molecular biology. Lippincott Williams & Wilkins, Baltimore.
Rousche, K. T., Knudson, C. B., 2002. Temporal expression of CD44 during embryonic chick limb development and modulation of its expression with retinoic acid. Matrix Biol. 21, 53-62.
Ruijter, J. M., Ramakers, C., Hoogaars, W. M., Karlen, Y., Bakker, O., van den Hoff, M. J., Moorman, A. F., 2009. Amplification efficiency: linking baseline and bias in the analysis of quantitative PCR data. Nucleic Acids Res. 37, e45.
Ryan, M. C., Sandell, L. J., 1990. Differential expression of a cysteine-rich domain in the amino-terminal propeptide of type II (cartilage) procollagen by alternative splicing of mRNA. J Biol Chem. 265, 10334-9.
Saga, Y., Yagi, T., Ikawa, Y., Sakakura, T., Aizawa, S., 1992. Mice develop normally without tenascin. Genes Dev. 6, 1821-31.
Sahni, M., Raz, R., Coffin, J. D., Levy, D., Basilico, C., 2001. STAT1 mediates the increased apoptosis and reduced chondrocyte proliferation in mice overexpressing FGF2. Development. 128, 2119-29.
Sai, S., Tanaka, T., Kosher, R. A., Tanzer, M. L., 1986. Cloning and sequence analysis of a partial cDNA for chicken cartilage proteoglycan core protein. Proc Natl Acad Sci U S A. 83, 5081-5.
Santagati, F., Rijli, F. M., 2003. Cranial neural crest and the building of the vertebrate head. Nat Rev Neurosci. 4, 806-18.
Seth, A., Ascione, R., Fisher, R. J., Mavrothalassitis, G. J., Bhat, N. K., Papas, T. S., 1992. The ets gene family. Cell Growth Differ. 3, 327-34.
Shapiro, I. M., Adams, C. S., Freeman, T., Srinivas, V., 2005. Fate of the hypertrophic chondrocyte: microenvironmental perspectives on apoptosis and survival in the epiphyseal growth plate. Birth Defects Res C Embryo Today. 75, 330-9.
Sharrocks, A. D., 2001. The ETS-domain transcription factor family. Nat Rev Mol Cell Biol. 2, 827-37.
Sharrocks, A. D., Brown, A. L., Ling, Y., Yates, P. R., 1997. The ETS-domain transcription factor family. Int J Biochem Cell Biol. 29, 1371-87.
Smits, P., Li, P., Mandel, J., Zhang, Z., Deng, J. M., Behringer, R. R., de Crombrugghe, B., Lefebvre, V., 2001. The transcription factors L-Sox5 and Sox6 are essential for cartilage formation. Dev Cell. 1, 277-90.

Stahlberg, A., Hakansson, J., Xian, X., Semb, H., Kubista, M., 2004. Properties of the reverse transcription reaction in mRNA quantification. Clin Chem. 50**,** 509-15.
Stanier, P., Pauws, E., 2012. Development of the lip and palate: FGF signalling. Front Oral Biol. 16**,** 71-80.
Stanton, L. A., Underhill, T. M., Beier, F., 2003. MAP kinases in chondrocyte differentiation. Dev Biol. 263**,** 165-75.
Summerbell, D., 1974. A quantitative analysis of the effect of excision of the AER from the chick limb-bud. J Embryol Exp Morphol. 32**,** 651-60.
Szebenyi, G., Savage, M. P., Olwin, B. B., Fallon, J. F., 1995. Changes in the expression of fibroblast growth factor receptors mark distinct stages of chondrogenesis in vitro and during chick limb skeletal patterning. Dev Dyn. 204**,** 446-56.
Tsang, M., Dawid, I. B., 2004. Promotion and attenuation of FGF signaling through the Ras-MAPK pathway. Sci STKE. 2004**,** pe17.
VanGuilder, H. D., Vrana, K. E., Freeman, W. M., 2008. Twenty-five years of quantitative PCR for gene expression analysis. Biotechniques. 44**,** 619-26.
Wagner, T., Wirth, J., Meyer, J., Zabel, B., Held, M., Zimmer, J., Pasantes, J., Bricarelli, F. D., Keutel, J., Hustert, E., Wolf, U., Tommerup, N., Schempp, W., Scherer, G., 1994. Autosomal sex reversal and campomelic dysplasia are caused by mutations in and around the SRY-related gene SOX9. Cell. 79**,** 1111-20.
Wasylyk, B., Hagman, J., Gutierrez-Hartmann, A., 1998. Ets transcription factors: nuclear effectors of the Ras-MAP-kinase signaling pathway. Trends Biochem Sci. 23**,** 213-6.
Wedden, S. E., Ralphs, J. R., Tickle, C., 1988. Pattern formation in the facial primordia. Development. 103 Suppl**,** 31-40.
Whitley, C. B., Ridnour, M. D., Draper, K. A., Dutton, C. M., Neglia, J. P., 1989. Diagnostic test for mucopolysaccharidosis. I. Direct method for quantifying excessive urinary glycosaminoglycan excretion. Clin Chem. 35**,** 374-9.
Widelitz, R. B., Jiang, T. X., Murray, B. A., Chuong, C. M., 1993. Adhesion molecules in skeletogenesis: II. Neural cell adhesion molecules mediate precartilaginous mesenchymal condensations and enhance chondrogenesis. J Cell Physiol. 156**,** 399-411.
Widmann, C., Gibson, S., Jarpe, M. B., Johnson, G. L., 1999. Mitogen-activated protein kinase: conservation of a three-kinase module from yeast to human. Physiol Rev. 79**,** 143-80.
Wilke, T. A., Gubbels, S., Schwartz, J., Richman, J. M., 1997. Expression of fibroblast growth factor receptors (FGFR1, FGFR2, FGFR3) in the developing head and face. Dev Dyn. 210**,** 41-52.
Wilkie, A. O., Patey, S. J., Kan, S. H., van den Ouweland, A. M., Hamel, B. C., 2002. FGFs, their receptors, and human limb malformations: clinical and molecular correlations. Am J Med Genet. 112**,** 266-78.
Winter, R. M., 1996. What's in a face? Nat Genet. 12**,** 124-9.
Wong, M. L., Medrano, J. F., 2005. Real-time PCR for mRNA quantitation. Biotechniques. 39**,** 75-85.
Yoon, Y. M., Oh, C. D., Kim, D. Y., Lee, Y. S., Park, J. W., Huh, T. L., Kang, S. S., Chun, J. S., 2000. Epidermal growth factor negatively regulates chondrogenesis of mesenchymal cells by modulating the protein kinase C-alpha, Erk-1, and p38 MAPK signaling pathways. J Biol Chem. 275**,** 12353-9.

Zehentner, B. K., Dony, C., Burtscher, H., 1999. The transcription factor Sox9 is involved in BMP-2 signaling. J Bone Miner Res. 14**,** 1734-41.

Zheng, X., Baker, H., Hancock, W. S., Fawaz, F., McCaman, M., Pungor, E., Jr., 2006. Proteomic analysis for the assessment of different lots of fetal bovine serum as a raw material for cell culture. Part IV. Application of proteomics to the manufacture of biological drugs. Biotechnol Prog. 22**,** 1294-300.

Znosko, W. A., Yu, S., Thomas, K., Molina, G. A., Li, C., Tsang, W., Dawid, I. B., Moon, A. M., Tsang, M., 2010. Overlapping functions of Pea3 ETS transcription factors in FGF signaling during zebrafish development. Dev Biol. 342**,** 11-25.